A DECISION-MAKING STRATEGY FOR THE OPERATION OF MANUFACTURING PROCESSES

by

Michael Kenneth Domroese

B.S. Mechanical Engineering, Valparaiso University (1984)

S.M. Mechanical Engineering, M.I.T. (1986)

Submitted to the Department of
Mechanical Engineering
in Partial Fulfillment of the Requirements
for the Degree of

DOCTOR OF PHILOSOPHY
in Mechanical Engineering

at the

Massachusetts Institute of Technology

June 1992

© 1992 Massachusetts Institute of Technology
All rights reserved

Signature of Author_____
Department of Mechanical Engineering
May 1,1992

Certified by_____ May 1 1992
George Chryssolouris
Associate Professor of Mechanical Engineering
Thesis Supervisor

Accepted by_____
Ain A. Sonin
Chairman, Department Graduate Committee

ARCHIVES
MASSACHUSETTS INSTITUTE OF TECHNOLOGY
DEC 19 1995
LIBRARIES

A DECISION-MAKING STRATEGY FOR THE OPERATION OF MANUFACTURING PROCESSES

by

Michael Kenneth Domroese

Submitted to the Department of Mechanical Engineering on May 1, 1992
in partial fulfillment of the requirements for the degree of Doctor of Philosophy
in Mechanical Engineering

Abstract

This thesis considers a sequential decision-making approach to the operation of manufacturing processes. In this approach decisions are made with the help of functions which explicitly relate performance objectives. such as cost or production rate, with the process input parameters and with sensor signals used to monitor the process. In order to minimize the difficulties caused by a lack of reliable sensing devices and inadequate process models the decision-making approach uses multiple sensors and multiple process models for monitoring the process. Synthesizing information from several sensors may provide an estimate of the process behavior which is more accurate, more reliable and less sensitive to random sensor noise than an estimate based on information from a single sensor.

In this thesis two basic approaches to the synthesis of multiple sensor information are considered and compared. The first approach is to synthesize the state variable estimates determined by the different sensors and corresponding process models through a mechanism based on training such as a neural network. The second approach utilizes statistical criteria to estimate the best synthesized state variable from the state variable estimates provided by the process models. As a "test bed" for studying the effectiveness of the above sensor synthesis approaches the turning process was considered, as turning processes are heavily used throughout industry. The approaches were evaluated and compared for providing estimates of the state variable tool wear based on multiple sensor information. The robustness of each scheme with respect to noisy and inaccurate sensor information was investigated in a simulated environment and also based on turning experiments.

Through simulation of a turning process, the decision-making approach was compared with other control schemes. In the decision-making approach the input settings for the process are selected by evaluating, on-line, a set of feasible alternatives with respect to several criteria. Relevant performance measures such as process cost and production rate can be directly influenced in this approach by establishing appropriate definitions for the decision criteria.

Thesis Supervisor:	Professor George Chryssolouris
Title:	Associate Professor of Mechanical Engineering
Thesis Committee:	Professor Stephen Graves
	Professor Thomas Sheridan
	Professor Karl Ulrich
	Professor Patrick Winston

Acknowledgements

I would like to thank Professor George Chryssolouris for supporting my research and teaching me to "think and produce". I learned a lot about engineering and about life during many meetings in his office. My thinking and presentation skills have improved tremendously through his critiques and encouragement. I also want to thank Professor Ulrich for his extensive review of this document. Many of his suggestions were helpful in improving the presentation of the material. Professors Graves, Sheridan and Winston provided key insights and valuable feedback while performing the research for this thesis.

This work was partially funded by the National Science Foundation's Strategic Manufacturing Research Initiative project "Decision Making in Manufacturing Systems."

I owe my thanks to many of the "buddies" who worked with me in the lab, I benefitted intellectually through my discussions with them, they often provided a needed release of pressure, and they let me be their buddy even when I went to lunch with my "other buddies": Velusamy Subramaniam (let's beat the competition), Moshin Lee, Paul Sheng, Ken Wright, Nick Anastasia, Nick Nassuphis, Stan Kyi, and Don Lee. Many others who worked in the lab also contributed to the research presented in this thesis: Michel Guillot, Mike Benco, Orlando Martinez, Hui Nam, Laszlo Zsoldos, Pierre Beaulieu, Laura Pitone and Jeffrey Hwang.

I would have not have benefitted nearly as much from my time at M.I.T., nor would I have been nearly as happy during this period of my life were it not for my brothers and sisters in the Boston Church of Christ. Many of them made a great impact on my life during the time I worked on this thesis. Among others, Howard Loree, John "Blooter" Oates, Dan "Spike" Zachary, Cedric Logan (Yes Cedric, Pharaoh finally let Mike go), Bryan Klassen, Pete Rothschild, Charlie White and Keith Tabor encouraged me during critical times and were vital to the completion of this work.

I am very grateful for the support and encouragement of my family. Mom and Dad, thanks for the late night phone calls which were so critical in keeping my spirits up. Thanks to my brother Mark for sending me "wild and funky stuff" over the e-mail, I am proud that you are becoming an educational dude just like me - I just hope your years in graduate school are fewer than mine. To my sister Meg, thanks for your letters and for your visits to Boston while I was here.

Finally, but most importantly I thank God for showing me his love through Jesus Christ and for giving me the talents, the right circumstances and the right people in my life for me to complete this work. All I have is through his grace.

You may say to yourself, "My power and the strength of my hands have produced this wealth for me." But remember the Lord your God, for it is he who gives you the ability to produce wealth, and so confirms his covenant, which he swore to your forefathers, as it is today.

Deuteronomy 8:17-18

TABLE OF CONTENTS

LIST OF FIGURES

LIST OF TABLES

1 INTRODUCTION

1.1 APPROACHES TO MANUFACTURING PROCESS OPERATION

A considerable amount of work regarding the operation of manufacturing equipment and processes has been done over the past two to three decades. A major effort has been focussed on the application of the scientific principles of control theory to manufacturing processes. Despite the high quality of work in this area, it appears that the vast majority of manufacturing processes remain uncontrolled or empirically controlled due to the lack of two necessary elements for applying control theory principles to the control of manufacturing processes:

- a comprehensive model which sufficiently reflects the complexity of the manufacturing process

- sensing devices that will be robust and reliable enough to provide the necessary signals from the manufacturing process and/or equipment

Lack of progress in these two areas seems inevitably related to uncontrolled manufacturing processes.

In the context of this thesis, manufacturing processes are processes which transform a material's shape, form and/or physical properties in order to produce a prespecified part according to the design and process planning. In discrete parts

manufacturing, there are probably more than 200 different processes which are practiced in the industrial environment. Among these, material removal processes, particularly machining, have great significance because of their flexibility and the achievable accuracy of a part. Material removal processes and particularly machining have been widespread in industry for a considerable time and therefore improvements and better control of these processes would have a great economical impact on the entire manufacturing industry. Although the decision-making concepts and control aspects of manufacturing processes considered in this thesis are of general importance and can be applied to a variety of processes, the work presented here will particularly be concentrated on machining because of the reasons mentioned above.

Large amounts of research in manufacturing have been dedicated to control concepts for machine tools. Numerically controlled machine tools generally use predetermined parameters such as feed and speed as well as an open-loop control system, which has as inputs machining parameters which are normally determined off line during the process planning stage [1,47,99]. These parameters are often determined with the aid of tables, machinability standards and previous experience. Due to the fact that these parameters are determined well before the actual manufacturing process occurs, there is no way that automatic adaptation to the actual process can be achieved. Since factors disrupting the process are, for the most part, unpredictable, the choice of machining parameters must be made in such a manner that production is executed without breakdowns, even under the worst possible circumstances. Consequently, the capabilities of the machine are not fully utilized, and the manufacturing process does not operate efficiently. Whenever adaptation to the actual situation or requirements of the process is needed, human intervention is required, often arriving inefficiently or too late.

Adaptive control concepts for machining processes have been researched over the past twenty-five years [2, 7-9, 15, 23, 31, 35, 36, 38, 39, 41-45, 49, 54, 55, 57, 60, 61, 63-65, 68-70, 72, 74, 76, 81-85, 88, 91, 94, 101-103, 105, 108-111, 113, 116, 117, 119-124]. In the control literature the term "adaptive control" refers to a control approach where some parameters of the controller are modified on-line using some adaptation scheme in order to obtain more adequate operation of the controller. However, in the context of this thesis the term "adaptive control" is used in the sense that it is used in the manufacturing literature which refers to any process operation approach which has the objective of automatically adjusting input parameters such as the speed and feed in response to the actual process conditions. In Adaptive Control Constraint (ACC), the goal of the control approach is generally to adjust the machine tool's setting parameters in order to maintain a measured quantity, such as the cutting force, at a specified value. ACC control schemes are primarily based on closed-loop control theory. In its most basic form, an ACC control approach has a single input and single output and employs fixed proportional and integral control gains (Figure 1.1). For the machining process, the input may be the feed rate or cutting speed and the output may be the cutting force. More complex schemes adjust the controller gains on-line in order to improve the control performance. Regardless of the complexity of the scheme, the goal is usually to drive a measured or estimated state or set of states to a desired set point. The general drawback of any ACC system is that maintaining a variable such as the cutting force at a given set point will generally not optimize the process. Indeed, the significant optimization objectives for machining are generally a function of the tool wear and wear rate as well as the process input parameters rather than direct functions of measured process variables such as the cutting force or tool temperature. Functions relating these objectives with a measured variable, such as the cutting force, would undoubtedly be very complex and nonlinear, since the cutting process is highly nonlinear. The optimization objectives may not even be a monotonically increasing or decreasing function of the process input parameters. This characteristic is in

sharp contrast with standard transfer functions used in linear control design, where provided the system is stable, the quasi-static output of the plant is assumed to be a linear function of the input. In addition, linear control design is primarily effective for time-invariant systems, while the machining process is a complex time-varying system. Furthermore, linear control theory was primarily developed to maintain an objective at a specified set point; however, the goal of a process optimization scheme is not to maintain an objective at a present value, but rather to obtain the maximum (or minimum) of the objective over the feasible range of process input parameters. For these reasons, classical and modern control theory can be rendered inadequate for operating not only the machining process but manufacturing processes in general.

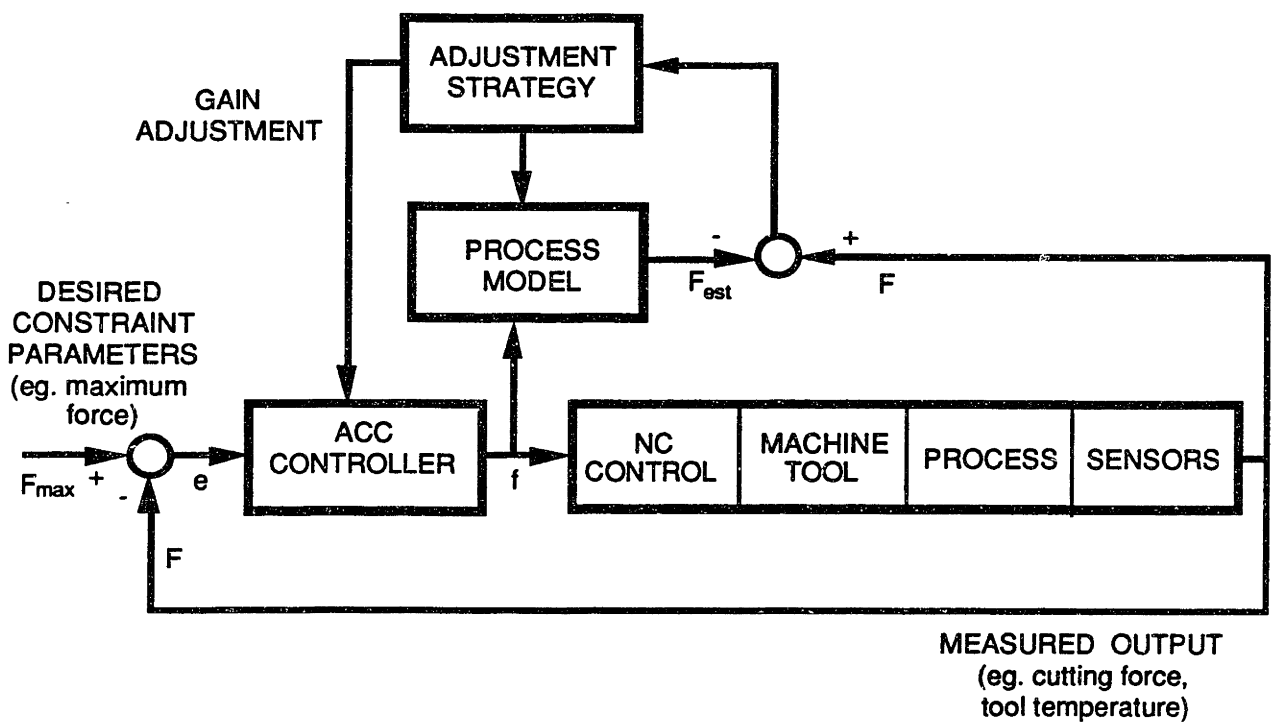

Figure 1.1 Machining Control Using an Adaptive Control Constraint (ACC) Scheme

Artificial intelligence techniques [120] are most effective for relatively complicated problems with a substantial degree of uncertainty, and thus offer an alternate approach to the treatment of the control problem of a manufacturing process. However, a "simplistic" adaptation of AI technology to the control problem of a manufacturing process would be inadequate [123]. Typical knowledge-based systems utilized in areas such as diagnostics in medicine assume the existence of an expert that can be interviewed and provide adequate knowledge that is later codified by so-called knowledge engineers. In the case of machining, however, such a simplified approach will be prone to failure because, despite the common perception of an expert machinist, the scientific principles utilized by a machinist are either absent or fully inadequate. Furthermore, an approach based on interviewing different machinists would find subjective points of view that would be extremely difficult to codify in an objective and sufficiently general knowledge based that would be useful under many different conditions. The execution of this type of expert system under current and foreseeable computer technology will require a substantial amount of time; this characteristic is inappropriate in an environment where real-time or near real-time responses are needed. Simply building a system of IF-THEN rules would be too slow for the reaction times of a machine tool. In addition, the empirical manner in which the knowledge of such systems is stored would make it difficult to interface an AI controller with the scheduling and control schemes of the rest the manufacturing system.

Adaptive Control Optimization (ACO) schemes have been researched in an effort to optimize the machining process (Figure 1.2). The major obstacles to successful in-process optimization of machining operations have been the lack of sensing devices that can reliably monitor the process an the lack of a single process model which can comprehensively reflect the complexity of the machining process. Past research has shown that accurate process models are difficult to build and are generally unreliable for machining control over a wide variety of operating conditions. When using sensing devices to monitor a process,

the values these devices deliver as input to the model may include errors due to the physical phenomena the sensor uses to measure the particular process variable. Furthermore, for many processes several of the process variables cannot be directly measured due to the physics or geometry of the process. Most manufacturing processes involve a complex interaction between a number of physical phenomena; the nature of these interactions and the relative significance of the physical phenomena can change with respect to time. It is difficult for one model to adequately reflect all of these these phenomena and the complexity of the interaction between them. In addition, the constants, particularly material-related constants, used in a process model are uncertain. Material properties cannot always be accurately determined and can vary considerably for each batch of material; they can also be sensitive to different physical conditions such as temperature.

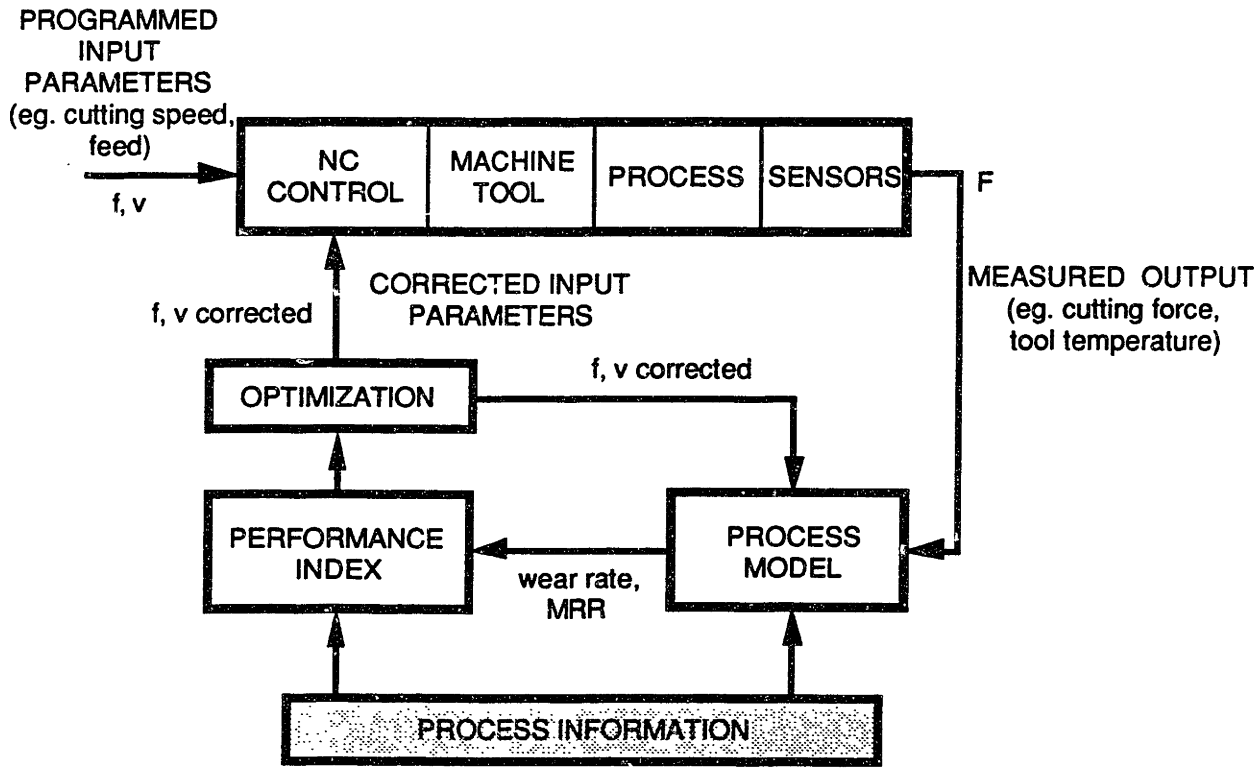

Figure 1.2 Machining Control Using an Adaptive Control Optimization (ACO) Scheme

1.2 DECISION-MAKING APPROACH TO PROCESS OPERATION

As an alternative to the above efforts, this thesis considers an approach to the operation of manufacturing processes where the process input parameters are selected with the help of functions which explicitly relate performance objectives with the input parameters and sensor signals which are used to monitor the process. Most manufacturing processes must be operated in accordance with multiple performance objectives such as cost per part, production rate and quality. The goal of the process operation approach considered in this thesis is to select the input parameters in-process in an attempt to operate the process in accordance with multiple performance objectives.

With few exceptions [2,93], most machining control schemes use a single sensor to monitor the process and therefore consider a single process model. Because of the lack of reliable sensors for manufacturing processes and the difficulty in developing one model which comprehensively reflects the complexity of the process, the approach to be investigated in this thesis considers the use of multiple sensors and process models for monitoring the behavior of the process. Although each of the models may not adequately reflect the process behavior when considered individually, in combination they may provide sufficient information to adequately monitor the process. If information from a variety of sensors and sensor-based models is synthesized, the maximum amount of information would be considered in selecting the values for the process input parameters and thus the quality of the process operation would likely be better than when operated based on information from only a single sensor. In addition, if one sensor fails during the process, a process operation scheme utilizing multiple sensors could probably continue to operate, while an approach based on a single sensor would be forced to stop the process.

An objective which realistically reflects the conditions during a manufacturing process may contain several local maxima over the feasible range of process inputs. In addition, the location of the overall maximum for an objective may shift significantly in the feasible input space during the process. Such a space would have to be searched periodically during the process in order to locate the changing set of optimal input parameters. The method used to search the space must not be susceptible to convergence problems and should not get stuck at a local maximum.

A number of different methods could be considered for searching the feasible input space for the best input parameters. This thesis considers a decision-making approach to the operation of a manufacturing process which provides a robust and flexible methodology for searching the space of input parameters [24, 27-29]. This approach proceeds by executing a number of logical steps:

1. The feasible alternatives are determined whenever a decision must be made; in general, these alternatives will be a set of input parameters such as feed rate and/or cutting speed.

2. Appropriate criteria, which must be considered when evaluating the feasible alternatives established previously, are determined. These criteria may include the cost or time of remaining machining operations or the part surface quality.

3. The values of the criteria for each of the proposed alternatives are estimated based on sensory information and previously learned principles and relationships. These principles and relationships will frequently be represented in the form of mathematical models.

4. Considering the values of the criteria established previously, one or more decision-making rules are applied to select the best alternative.

The execution of these steps reflects the manner in which a human would proceed to make a decision during the operation of a process. The decision-making process can be concisely expressed in a decision matrix format, where the matrix elements express the values of the criteria for each feasible alternative. The majority of the decisions made by such an operation scheme must be made within a relatively short period of time. The decision-making process can be implemented most quickly by assigning each decision-making step to a separate module. Each module can then be structured specifically to execute each step in the most systematic and efficient way. In addition, it is not necessary that each step be re-executed every time a decision is made. Since each of the modules can be modified or replaced in order to adapt to a new set of processing conditions without changing the overall structure of the system, a wide variety of tool conditions, materials and geometries can easily be considered within the same decision-making framework.

In a general schematic of the decision-making scheme described, the system is structured in a modular and generic manner (Figure 1.3). The significant modules of the system can be briefly described as follows.

Module 1: A rule-base system for determining the criteria provides the connection between the machining operation and the goals and objectives set at higher levels of the manufacturing hierarchy. This module determines the significant criteria which must be considered during the machining operation.

Module 2: An A.I. based system for determining the alternatives provides the decision-making process with a set of feasible alternatives from which the optimal alternative is selected.

Module 3: A set of independent process models, based on sensor information and the physics of the process provides the basis for the estimation of the criteria values for each of the alternatives.

Module 4: The consequences of the different alternatives are estimated via an intelligent synthesis of sensor information. This module provides the values of the criteria to the decision-making process and operates in tandem with the process models (module 3).

Module 5: A set of decision-making rules is applied to the process information gathered thus far to select the best alternative.

The development of module 2 has been addressed previously [22]. In [22] the feasibility of a set of input parameters is based on several state variables, which may include surface roughness, the type of chips produced, machine tool vibrations, and the cutting power required. The objective of this module is to obtain acceptable values for the state variables by selecting an appropriate range of machining input parameters. In order to

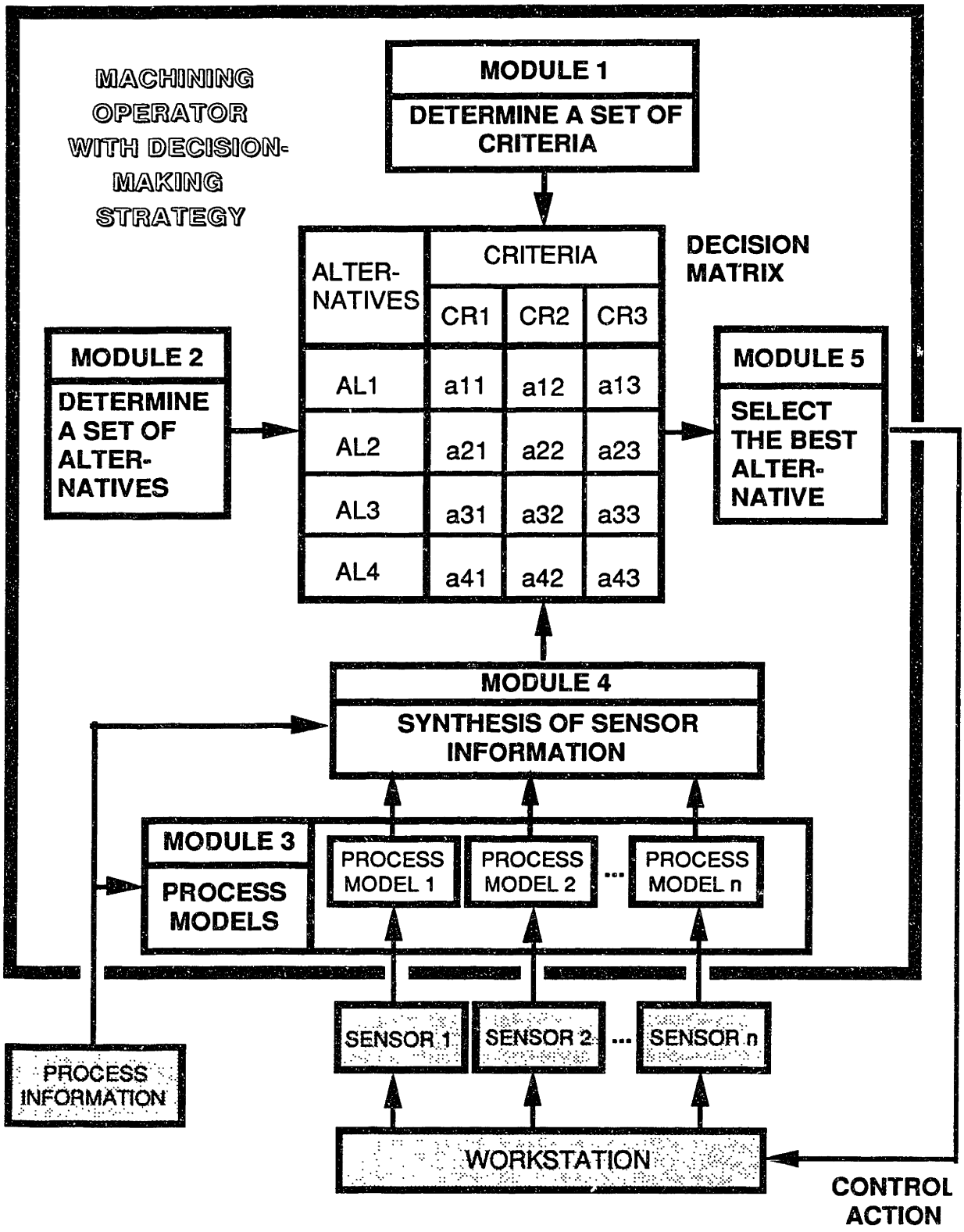

Figure 1.3 Basic Structure of a Decision-Making Approach to Machining Operation

achieve this objective, relationships between the state variables and the process inputs must be established. By applying constraints such as a maximum vibration level or maximum allowable surface roughness to the appropriate state variable these relationships can be used to determine an acceptable range of process inputs. The module for selecting the best alternative (module 5) can subsequently choose the optimal alternative from this feasible set of alternatives. A number of researchers have tried to use analytical or empirical approaches to defining relationships between the process inputs and the state variables. The success of these efforts has been limited because of the complexity of the metal cutting process. As an alternative to the previous approaches the work reported in [22] considered new A.I. and self-organizing empirical modelling techniques. Modelling techniques which were considered and evaluated included: the group method of data handling (GMDH) and neural networks.

1.3 THESIS FOCUS AND STRUCTURE

This thesis will concentrate on the development of modules 3, 4 and 5 (Figure 1.3). In general, the significant optimization criteria during a machining process will be dependent on the tool wear and the process input parameters. Chapter 2 considers the fundamental relationships between the acoustic emission produced during machining and the parameters of the machining process. These relationships are necessary in order to develop an acoustic-emission based model adequate for tool wear monitoring. Such a model would be used in module 3 of the decision-making approach to machining process operation. This investigation was based on turning experiments performed using both steel and aluminum workpiece materials.

Chapter 3 discusses and evaluates methods for the synthesis module (module 4). This module operates in tandem with the process models and provides the final estimates of process state variables used in determining the values of the optimization criteria. In a machining application, each process model would be used to provide independent estimates of the tool wear to the sensor synthesis scheme based on the sensor signals. Additional machining parameters, such as the feed and cutting speed, could also be used as inputs in order to provide the sensor synthesis scheme with additional information about the machining process. The scope of the synthesis scheme is to determine the best final estimate for the wear based on information provided by multiple sensors. It must consider information about the particular machining operation as well as the reliability and accuracy of the sensors and the related process models. Chapter 3 considers two basic approaches to the synthesis of sensor information. The first approach is to use a mechanism based on training. Methods in this category include neural networks, least-squares regression and the group method of data handling (GMDH). The second approach utilizes statistical criteria to determine the best synthesized estimate from the independent estimates provided by the process models. In Chapter 3 these methods are first evaluated and compared in a simulated environment and then based on tool wear experiments performed on a lathe.

Chapter 4 focuses primarily on module 5 in which the best alternative is selected based on a set of decision-making criteria. The feasibility and limitations of a decision-making approach to machining operation are discussed. In addition the decision-making approach is compared with typical Adaptive Control Constraint (ACC) and Adaptive Control Optimization (ACO) approaches to process control. These comparisons were based on applying each of these control approaches to a simulated turning process. Performance measures of cost per part, production rate and surface roughness were used for the purpose of the comparisons.

2 ASPECTS OF ACOUSTIC EMISSION BASED MODELLING FOR MACHINING OPERATION

2.1 INTRODUCTION

During the machining process, the decision-making approach or an adaptive control approach operates the process by changing machine tool setting parameters such as the speed and feed. Often it is desirable for the process operation scheme to monitor the progressive tool wear during the process. In addition, for most machining operations, the important optimization criteria are dependent upon the magnitude of the tool wear. Therefore, it is essential that the process models used within an operation scheme are capable of providing an estimate of the tool wear during the process even as the machine tool settings are changed.

In general, both tool wear and changes in the machine tool setting parameters affect process monitoring signals such as tool vibration, cutting forces, and tool temperature. In order to be useful for wear monitoring during process operation, the model must account for changes in the sensor signal due to changes in the machine tool settings. For example, as shown in Figure 2.1, the cutting force increases during machining both due to an increase in feed rate and due to an increase in tool wear. In the force-feed plane, the force component due to tool wear remains constant. In the force-time plane, the feed rate remains constant while the force component due to tool wear increases. If the increase in the force component due to the feed rate can be determined independently, then it is

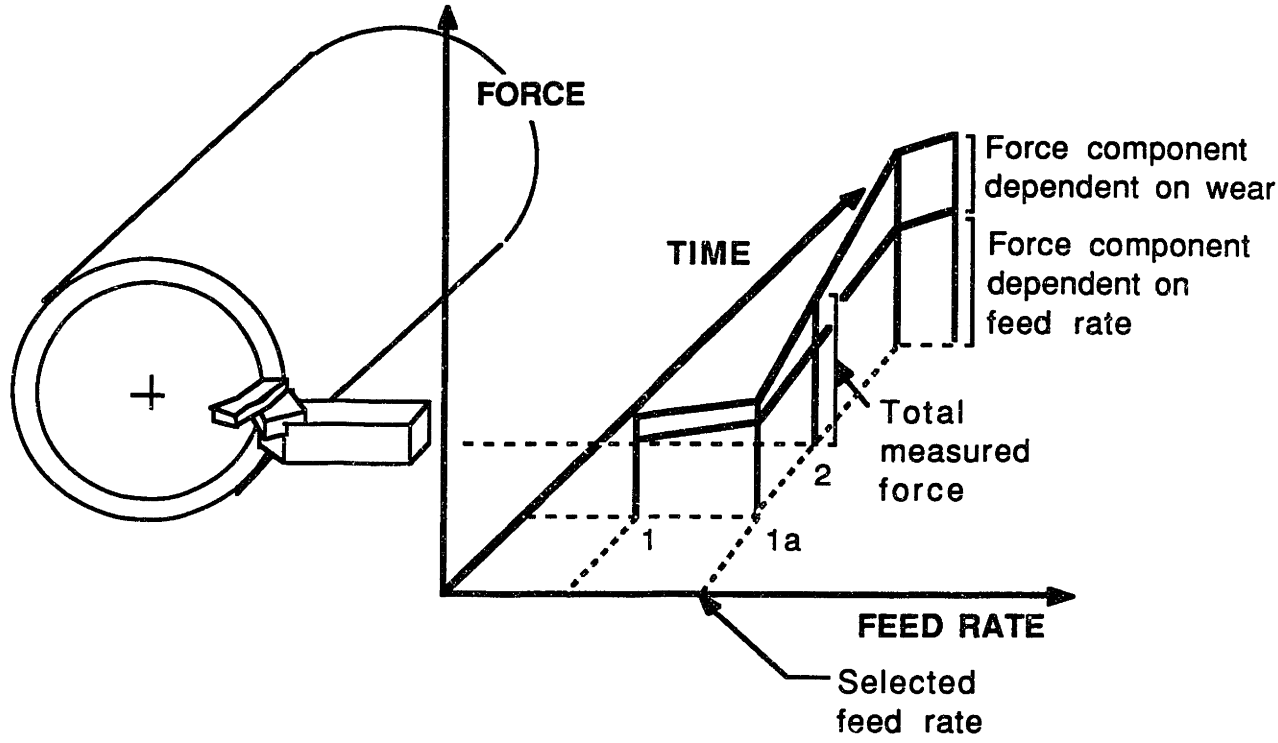

Figure 2.1 Feed Rate and Cutting Time/Tool Wear Effect on Cutting Force

possible to calculate the increase in the cutting force due to tool wear. From the value of this force increase, the tool wear can be determined. Although in this example the measured parameter is force and the control input is feed rate, this example illustrates that a process model used to monitor tool wear must account for changes in the sensor signal due to changes in the machine tool settings regardless of the sensor signal and machine tool setting parameters used.

The work presented in this chapter considers the development of an acoustic emission-based model adequate for tool wear monitoring within a scheme such as the decision-making approach to process operation.

Acoustic emission (AE) is developed by the rapid release of strain energy within a

material [89]. Some of the energy released radiates from the source in the form of elastic waves to the surface of the material. These waves can be detected by a piezoelectric transducer mounted on the surface of the material. AE activity can originate from numerous sources. Any changes in the internal structure of the material will generate AE. Possible AE sources include twinning and grain boundary movement, point defects or dislocations, plastic deformation, creation and collapsing of voids, initiation and propagation of cracks, phase transformations, and fracture.

In metal cutting, plastic deformation associated with shearing of the workpiece material is the primary source of AE. In the case of discontinuous chips, fracture associated with chip breaking is also a significant source of AE activity.

Several different techniques have been considered for analyzing AE signals. Some common methods include [89]:

- **Frequency spectral analysis**--a recorded AE signal is Fourier analyzed to determine the frequency components in the signal.

- **Autocorrelation analysis**--a signal is compared with a delayed version of the same signal in order to identify periodic components within the signal.

- **Count rate**--a threshold voltage, usually above the noise level, is established, and the number of threshold crossings per unit of time is counted.

- **Amplitude distribution analysis**--several discrete threshold values are chosen, and the relative number of emission events that occur within each threshold interval are recorded.

- **RMS value of the signal**--this can be determined using a true RMS to DC converter and is an indicator of the energy level of the signal.

Advantages of acoustic emission for in-process detection of tool wear are:

- The signal frequency range is far above that of machine tool vibrations and other sources of noise. Therefore, undesirable noise components can easily be removed from the signal using a low-pass filter.

- The AE transducer can be mounted easily on the tool or tool holder and does not interfere with the cutting process. Recently, a process has also been developed for placing a thin film transducer directly on cutting inserts [92]. These thin film transducers allow for detection of the AE signal with a minimal distance and a minimal number of mechanical interfaces between the signal sources and the transducer and yet do not interfere with the cutting process

Several different AE signal analysis approaches for in-process detection of tool wear have been investigated:

- Iwata and Moriwaki [53] found that the count rate for the AE signal tends to increase as the flank wear increases.

- Dornfeld [32], Iwata and Moriwaki [53], and Uehara and Kanda [112] noted that certain components in the frequency spectrum of the AE signal increase dramatically with increased flank wear.

- Statistical analysis of the RMS AE signal was considered by Dornfeld and Kannatey-Asibu [58]. The skew and kurtosis of an assumed β distribution for the RMS signal were found to be sensitive to progressive flank wear.

- A time series analysis of the dynamic components in the RMS AE signal was implemented by Dornfeld and Liang [71]. The parameters in an adaptive time series model were found to be sensitive to increasing flank wear.

- Dornfeld and Rangwala [93] used characteristics of the AE and cutting force frequency spectra as inputs to a neural network. The network was trained to identify the tool wear state. Recognition accuracies of up to 95% were reported for classification of a tool as fresh or worn.

- An analytical relationship between the RMS AE signal and the parameters of the cutting process was developed by Dornfeld and Kannatey-Asibu [59]. This relationship was later extended by Lan and Dornfeld [66] to include the effect of flank wear on the RMS AE signal.

Work has not been done to quantify the effect of changing the machine tool setting parameters such as speed and feed rate on the count rate, frequency spectrum, or distribution moments for the AE signal. Therefore, it is uncertain whether the count rate, frequency spectrum, or statistical analysis techniques would be applicable to process monitoring for machining control. The frequency spectrum of the AE signal can be greatly colored by many factors such as damping of the medium, transducer response, and, above all, the resonance of the waveguide [89]. These effects may cause inaccuracies in tool wear estimates and may also make the methods dependent on the analysis of the frequency spectrum difficult to calibrate.

For unmanned machining operations, it is desirable to have short broken chips rather than long continuous chips. For this reason, it is critical that the AE signal analysis method used for detection of tool wear be as insensitive as possible to chip breaking. For the adaptive time series analysis approach implemented by Dornfeld and Liang [71], the method is dependent on the dynamics of the RMS AE signal (the D.C. component of the signal was filtered out). Chip breaking introduces high frequency components into the RMS AE signal. It would be difficult to filter out the components due to chip breaking, as the method is dependent on the dynamics of the signal. Thus, the time series method may be inappropriate for unmanned monitoring and control of the machining process. In a similar way, the frequency spectrum-based methods may be overly sensitive to chip breaking. For the neural network approach, which utilizes features of the frequency spectrum, Dornfeld and Rangwala [93] noted that chip breaking caused most of the errors in the tool state classification. In contrast to other methods, the analytical AE model is primarily dependent on the D.C. component of the AE RMS signal. Consequently, the analytical model can be made less sensitive to chip breaking by filtering high-frequency components out of the RMS signal.

The most sophisticated analytical AE machining model was developed by Dornfeld et al. [59, 66]. This model correlates the power expended in the orthogonal cutting process with the RMS AE signal. During machining, power is expended primarily in four regions, as illustrated in Figure 2.2:

- the shear zone, where the chip is sheared from the workpiece.

- the chip-tool interface on the rake face, where both bulk shear and sliding may occur.

- the chip-workpiece interface on the flank face, where both bulk shear and sliding may occur.

- the chip after leaving the tool rake face, where fracture of the chip may occur.

In this model developed by Dornfeld, the power dissipated due to chip fracture was not accounted for. Chip breaking, however, generally generates high-frequency components in the RMS signal while shear and friction in the other zones primarily generates lower frequency components. A low-pass filter, therefore, can be used to remove the components of the RMS signal due to chip breaking.

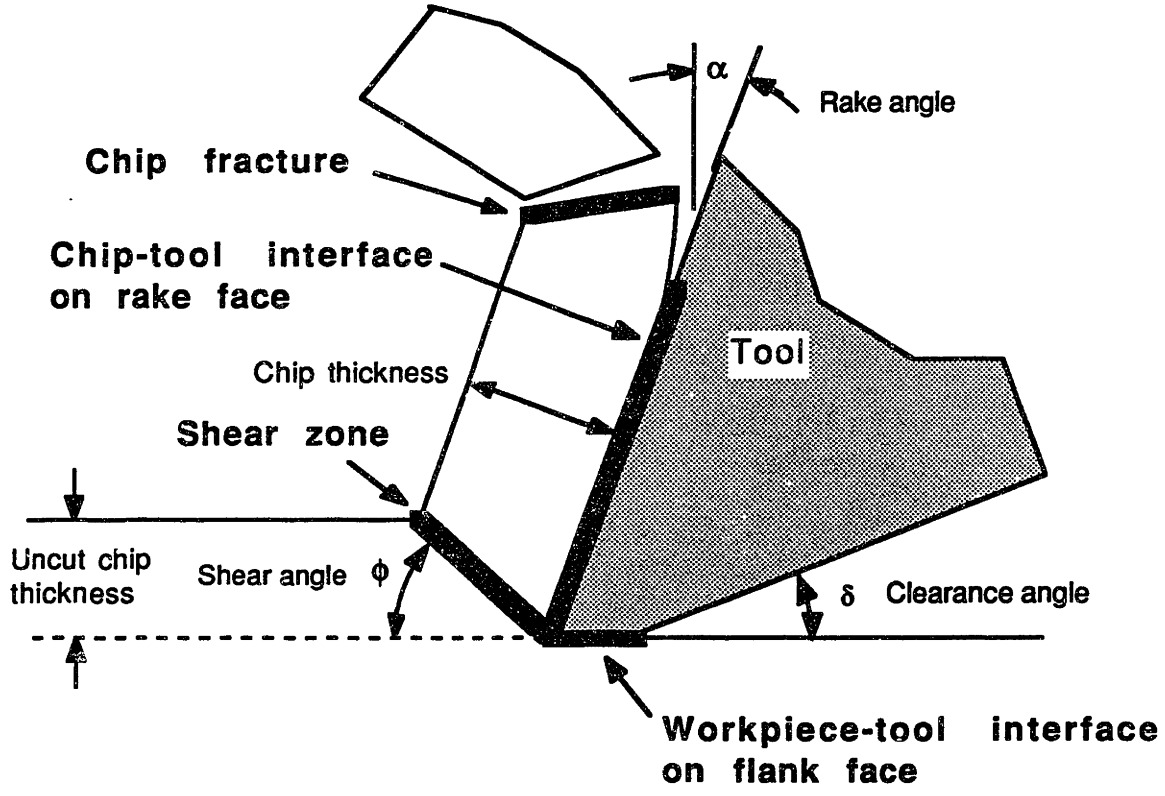

Figure 2.2 Locations of Acoustic Emission Generation in the Cutting Process

The estimates provided by the analytical model for the change in the RMS AE signal due to changes in the cutting velocity correspond very well with experimental data. However, experimental data shows results quite different from the model predictions for changes in the RMS signal due to changes in feed rate or width of cut [66]. In addition, the sensitivity of the RMS AE signal to rake angle changes has not been adequately investigated.

2.2 MODELLING THE MACHINING PROCESS VIA ACOUSTIC EMISSION

The objective of the work presented in this chapter is to develop a model which adequately relates the AE signal to changes in the machine tool setting parameters. As explained above, the model must meet this objective in order to provide a process operation scheme with an estimate of the progressive tool wear during the process. As a first step in the model development, it was necessary to determine whether the RMS AE signal is proportional to the power expended in the process, as assumed in previous analytical AE models.

In the AE model developed by Dornfeld et al. [59, 66], it was assumed that the ratio of the power used to produce AE divided by the total power expended in the cutting process, P_{AE}/P_T, is always constant. Previous studies [66, 50] have shown that the RMS AE signal is more sensitive to changes in cutting velocity than changes in feed rate or width of cut. Changes in cutting velocity primarily change the shear velocity in the shear zone, the chip velocity on the rake face, and the workpiece velocity on the flank face. On the other hand, changes in the feed rate and width of cut primarily influence the size of the shear zone and the area of contact between workpiece and tool on the tool faces. Thus,

changes in width of cut and feed rate primarily influence the cutting forces rather than the shear and friction velocities. These observations indicate that the fraction of the total cutting power which goes into producing acoustic emission is dependent upon the cutting speed, feed rate, and width of cut. Specifically, the fraction of the cutting power dissipated as acoustic emission is greater if the power increases due to an increase in cutting velocity than if the power increases due to an increase in cutting force.

The basis of the model developed by Dornfeld et al. [59,66] is that the RMS of the AE signal is an exponential function of the power expended in the cutting process.

$$RMS = C_1 \left[P_t \right]^m \tag{2-1}$$

where:

C_1 is a proportionality constant that takes into account factors such as amplifier gains.

P_t = total power expended in the cutting process (excluding power dissipated due to chip fracture).

m is an exponent (originally considered by Dornfeld to be 1/2).

For the machining process, the sum of the power expended in the shear zone, tool-chip interface on the rake face, and tool-workpiece interface on the flank face can be written as:

$$P_t = v_s F_{ts} + v_r F_{tr} + v\, F_{tf} \tag{2-2}$$

where:

v_s = shear velocity

F_{ts} = tangential shear force

v_r = chip velocity on the rake face

F_{tr} = tangential force of the chip on the rake face

v = cutting velocity

F_{tf} = tangential force of the workpiece on the flank face

The shear velocity, v_s, and the chip velocity on the rake face, v_r, can be written in terms of the cutting surface velocity, v, and the cutting geometry.

$$v_s = \frac{\cos[\alpha]}{\cos[\phi-\alpha]} v \tag{2-3}$$

$$v_r = \frac{\sin[\phi]}{\cos[\phi-\alpha]} v \tag{2-4}$$

where:

α = rake angle

ϕ = shear angle

Substituting the above expressions for power and velocity into the RMS relationship yields

$$RMS = C_1 \left[v \left[F_{ts} \frac{\cos[\alpha]}{\cos[\phi-\alpha]} + C_2 F_{tr} \frac{\sin[\phi]}{\cos[\phi-\alpha]} + C_3 F_{tf} \right] \right]^m \tag{2-5a}$$

where:

C_2, C_3 = relative signal attenuation coefficients for the AE generated on the the rake and flank faces with respect to that generated in the shear plane.

Taking the logarithm of both sides of equation (2-5a) allows the exponent, m, and the constant of proportionality, C_1, to be determined from measured RMS AE signal vs.

cutting force data using least-squares regression:

$$\log\left[RMS\right] = \log\left[C_1\right] + m \log\left[v\left[F_{ts}\frac{\cos\left[\alpha\right]}{\cos\left[\phi-\alpha\right]} + C_2F_{tr}\frac{\sin\left[\phi\right]}{\cos\left[\phi-\alpha\right]} + C_3F_{tf}\right]\right] \tag{2-5b}$$

In equation (2-5) the RMS signal is expressed as an exponential function of the power expended in the process. Experimental data indicates that the RMS signal is more sensitive to variations in the cutting velocity than the cutting forces. Allowing the velocity term in equation (2-5) to have a different exponent than the force term permits the sensitivity of the RMS AE signal to the cutting velocity to be modelled as different than the sensitivity of the RMS signal to the cutting force components.

$$RMS = C_1v^m\left[F_{ts}\frac{\cos\left[\alpha\right]}{\cos\left[\phi-\alpha\right]} + C_2F_{tr}\frac{\sin\left[\phi\right]}{\cos\left[\phi-\alpha\right]} + C_3F_{tf}\right]^n \tag{2-6a}$$

Taking the logarithm of both sides of the above RMS equation allows the exponents, m and n, and the constant of proportionality, C_1, to be determined from RMS AE signal vs. cutting force data using least-squares regression:

$$\log\left[RMS\right] = \log\left[C_1\right] + m\log\left[v\right] + n \log\left[F_{ts}\frac{\cos\left[\alpha\right]}{\cos\left[\phi-\alpha\right]} + C_2F_{tr}\frac{\sin\left[\phi\right]}{\cos\left[\phi-\alpha\right]} + C_3F_{tf}\right] \tag{2-6b}$$

2.3 EXPERIMENTAL PROCEDURE

The experimental apparatus shown in Figure 2.3 was used to conduct cutting tests for verification and analysis of the AE model presented in equation (2-6). Tests were performed on a Daewoo Puma10 CNC lathe, with 20 HP maximum spindle power. The tool holder was equipped for measuring the cutting forces along three orthogonal axes. A Physical Acoustics WD wideband transducer mounted on the tool holder was used to detect the AE signal. The signal from the AE transducer was preamplified using a Physical Acoustics 1220A preamplifier and then amplified by a Physical Acoustics AE1A postamplifier for a total gain of 40db. The AE signal was highpass filtered with a 50 kHz cutoff frequency in order to remove components due to machine vibrations and other low-frequency noise from the signal. An Analog Devices AD636 true RMS to D.C. converter chip was used to determine the RMS of the AE signal. The RMS signal was then lowpass filtered with a cutoff frequency of 1.59 Hz in order to remove components of the AE signal associated with chip breaking. Data from the tests were recorded using a Compaq Deskpro 286 computer equipped with a Data Translation DT2801 data acquisition board. After each cutting test, the chip thickness was measured in order to determine the cutting ratio and the shear angle.

In order to perform the orthogonal cutting tests, 6061-T6 aluminum tubes, 2.25 in. (57.2 mm) inside diameter with thicknesses of 0.125 in. and 0.063 in. (3.18 and 1.60 mm), and ASTM A53, 6 in. (152 mm) steel pipe with a thickness of 0.125 in. (3.18 mm), were used for the workpiece material. For the aluminum cutting tests, WKE 45 HSS orthogonal cutting tools, by Seco Tools, with 8° clearance angles and 15° and 30° rake angles were used. In the steel cutting tests, M2 HSS orthogonal tools, by Enco Mfg., with 6° clearance angles and 15° and 30° rake angles were used. The tools were reconditioned periodically between tests by honing.

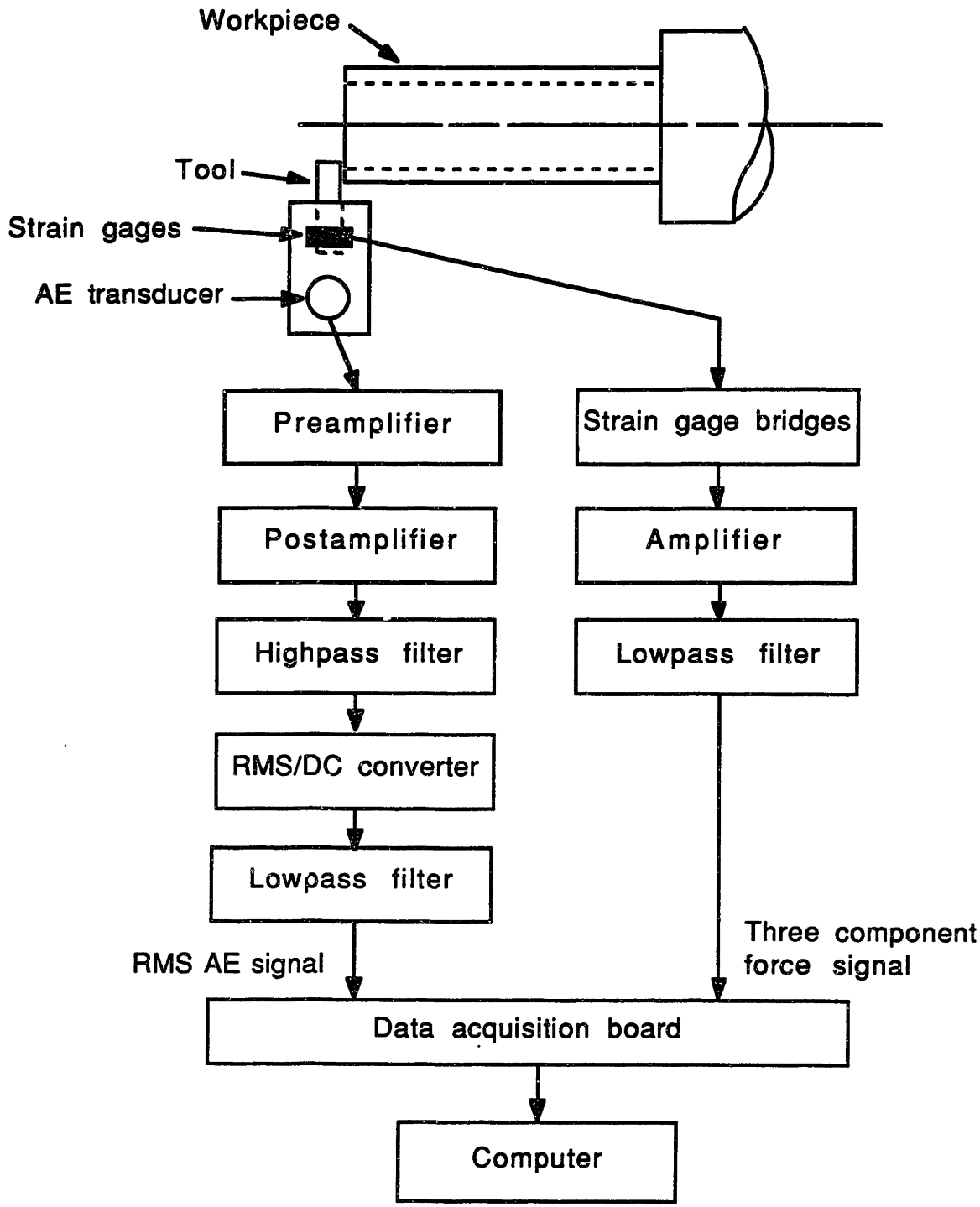

Figure 2.3 Experimental Apparatus

For each of the cutting tests, the tangential forces along the shear plane and the rake face were determined from the measured cutting and feed forces based on the cutting geometry (Figure 2.4).

$$F_{tr} = F_c \sin(\alpha) - F_f \cos(\alpha) \tag{2-7}$$

$$F_{ts} = F_c \cos(\phi) + F_f \sin(\phi) \tag{2-8}$$

These forces, as well as the cutting velocity and cutting geometry, were used in the RMS equations (2-5) and (2-6). Least-squares regression of the log of the measured RMS AE signal on the log of the power expended in the process was used to determine the constant of proportionality, C_1, and the exponent, m, in expression (2-5). Multiple least-squares regression of the log of the measured RMS AE signal on the log of the cutting velocity and the log of the cutting force term, as shown in expression (2-6b), was used to determine the constant of proportionality, C_1, and the exponents, m and n, in equation (2-6a).

Surface velocities of 50, 100, 200 and 400 fpm (0.254, 0.508, 1.02 and 2.03 m/sec) were used in the aluminum cutting tests. At each of these velocities, tests for feed rates of 0.002, 0.005, 0.010 and 0.015 ipr (0.051, 0.127, 0.254 and 0.381 mm/rev) and widths of cut of 0.125 in. and 0.063 in. (3.18 and 1.60 mm) were performed. For the steel cutting tests, surface velocities of 50, 100, 200 and 300 fpm (0.254, 0.508, 1.02 and 1.52 m/sec) were used. At each of these velocities, tests for feed rates of 0.0020, 0.0035 and 0.0050 ipr (0.051, 0.089 and 0.127 mm/rev) with a 0.125 in. (3.18 mm) width of cut were performed.

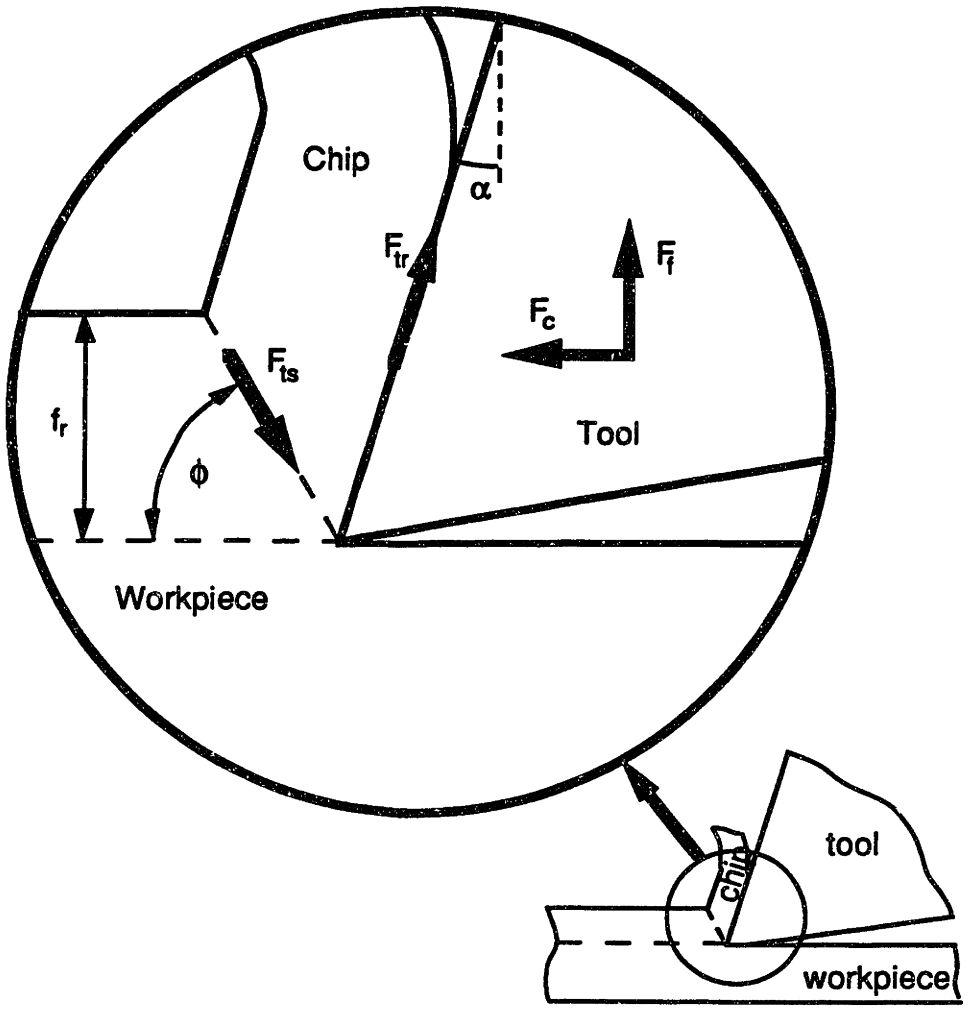

Figure 2.4 Forces in Orthogonal Cutting
(F_{tr} = tangential force of chip on rake face, F_{ts} = tangential shear force,
F_c = measured cutting force, F_f = measured feed force,
f_r = feed, α = rake angle, ϕ = shear angle)

Because the constant of proportionality, C_1, in expressions (2-5) and (2-6) can be significantly changed simply by removing and replacing the same tool in the tool holder, all tests with a given cutting tool were completed before removing the tool. This procedure ensured that data from the aluminum cutting tests with different widths of cut (tube thicknesses) could be meaningfully evaluated. However, in order to change the rake angle, the tool had to be removed and replaced with a tool of a different rake angle; therefore, an

investigation of the effect of different rake angles on the RMS signal was not possible from the data collected in these tests.

2.4 RESULTS AND DISCUSSION

2.4.1 Aluminum Cutting Tests

From experimental data for tests with aluminum workpiece material with a 30° rake angle tool, the constants in expression (2-5) were found to be C_1 = 1.04E-2 and m = 0.496. The constants in expression (2-6) were determined as C_1 = 4.44E-2, m = 0.806 and n = 0.092. Data from the tests for 0.002 and 0.005 ipr feed rates with a 0.063 in. width of cut and 400 fpm cutting velocity were omitted in the analysis because of chatter that occurred during these tests which significantly influenced the RMS AE signal. Plots of the RMS AE as determined from expression (2-5), using the constants determined above, versus the measured RMS signal for 0.125 in. and 0.063 in. widths of cut are shown in Figures 2.5a and 2.6a, respectively. Plots of the RMS AE as determined from equation (2-6) versus the measured RMS signal for 0.125 in. and 0.063 in. widths of cut are shown in Figures 2.5b and 2.6b, respectively. The lines with zero y-intercept and 1/1 slope shown in these figures and in all of the following figures illustrate the ideal relationship between the estimated RMS, as determined from measured cutting forces and cutting conditions, and the measured RMS AE signal. The coefficient of correlation between the measured RMS signals and the RMS values provided by expression (2-5) is 0.793. The correlation coefficient between the measured RMS and the RMS provided by expression (2-6) is 0.968.

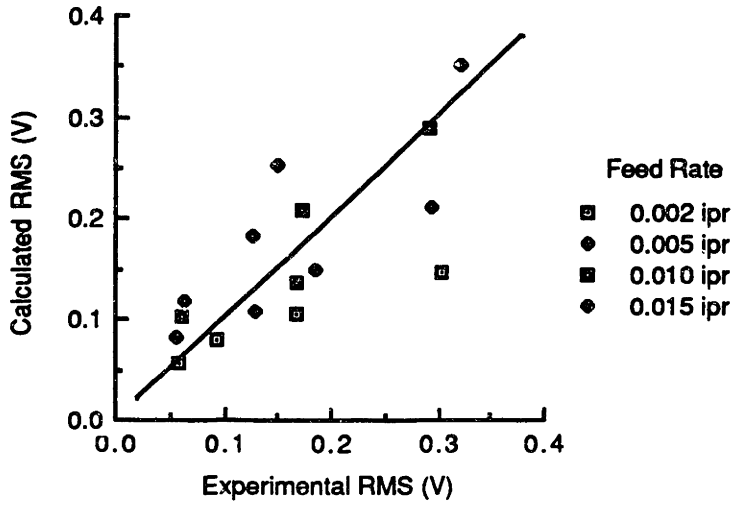

Figure 2.5a Calculated RMS from Equation (2-5)

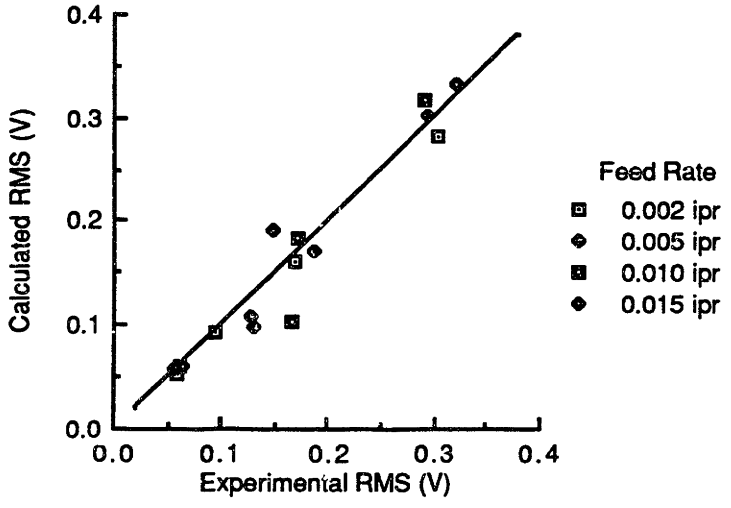

Figure 2.5b Calculated RMS from Equation (2-6)

Figure 2.5 Calculated RMS Versus Experimental RMS for Aluminum Cutting Tests with 30° Rake Angle Tool, 0.125 in. Width of Cut, and Cutting Speeds v=50, 100, 200, and 400 fpm

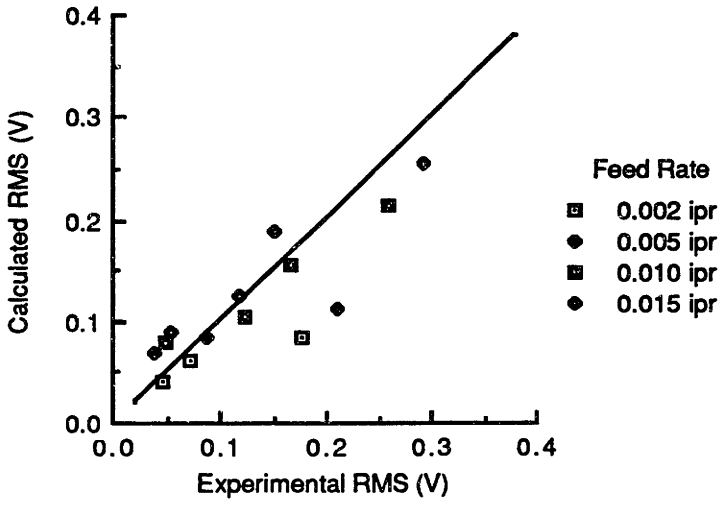

Figure 2.6a Calculated RMS from Equation (2-5)

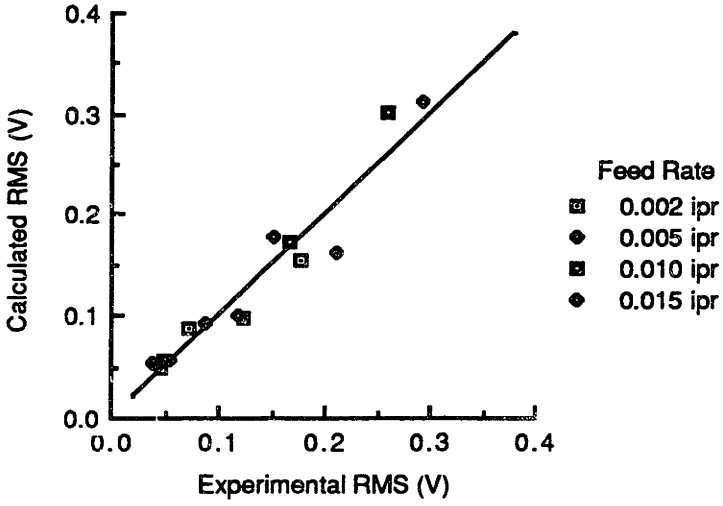

Figure 2.6b Calculated RMS from Equation (2-6)

Figure 2.6 Calculated RMS Versus Experimental RMS for Aluminum Cutting Tests with 30° Rake Angle Tool, 0.063 in. Width of Cut, and Cutting Speeds v=50, 100, 200, and 400 fpm

It was found that the results in the above and in all following analyses were not very sensitive to the attenuation coefficients C_2 and C_3 in expressions (2-5) through (2-6); this was particularly true for equation (2-6). These coefficients would be quite difficult to identify, and, in the work presented here, C_2 and C_3 were assumed to be one.

Using experimental data from tests with aluminum workpiece material with a 15° rake angle, the constants in relationship (2-5) were determined as C_1 = 9.68E-3 and m = 0.406. The constants in equation (2-6) were found to be C_1 = 3.61E-2, m = 0.714 and n = 0.049. The RMS AE determined from expression (2-5), using the above constants, versus the measured RMS signals for 0.125 in. and 0.063 in. widths of cut are shown in Figures 2.7a and 2.8a, respectively. Figures 2.7b and 2.8b show the RMS signals found using expression (2-6) versus the measured signal for 0.125 in. and 0.063 in. widths of cut, respectively. The correlation coefficient between the RMS values provided by expression (2-5) and the measured RMS signal is 0.724. The correlation coefficient between the measured RMS signal and the values determined using equation (2-6) is 0.939.

2.4.2 Steel Cutting Tests

The constants in equation (2-5), using data from tests with steel workpiece material and a tool with a 30° rake angle, were determined to be C_1 = 1.22E-3 and m = 0.771. In equation (2-6), the constants were found to be C_1 = 2.37E-2, m = 0.808 and n = 0.140. A plot of the RMS values determined using equation (2-5) versus the measured RMS signals is shown in Figure 2.9a. Figure 2.9b shows the RMS estimates determined using equation (2-6) versus the measured RMS signals. The coefficient of correlation between the measured RMS signals and the estimated RMS provided by expression (2-5) is 0.898. The

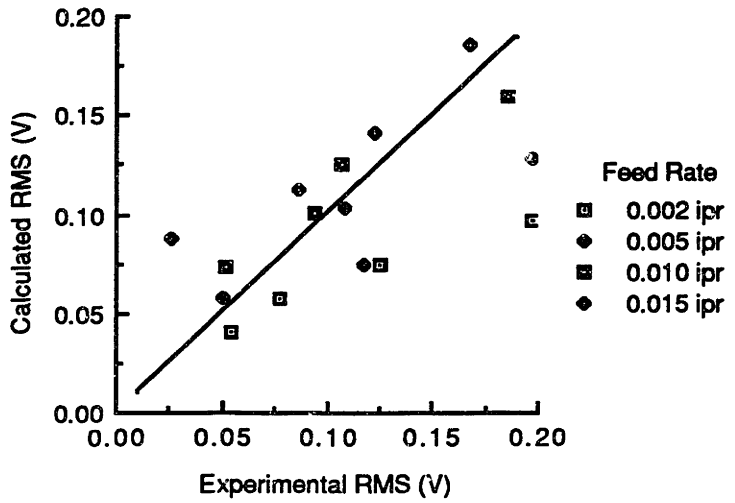

Figure 2.7a Calculated RMS from Equation (2-5)

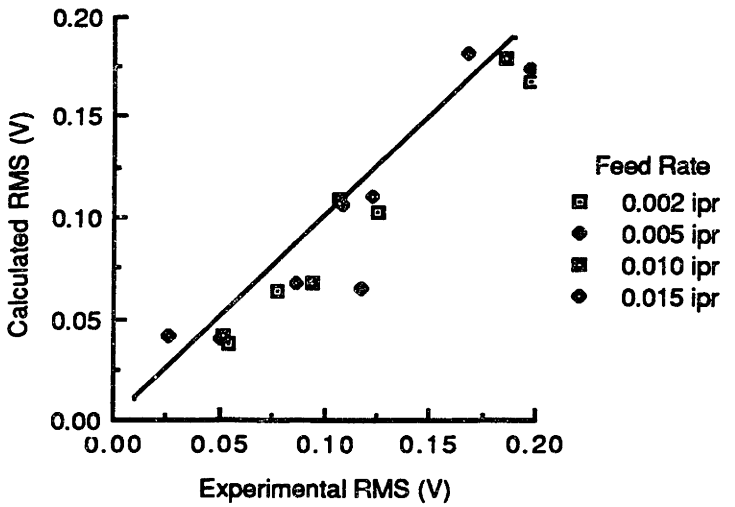

Figure 2.7b Calculated RMS from Equation (2-6)

Figure 2.7 Calculated RMS Versus Experimental RMS for Aluminum Cutting Tests with 15° Rake Angle Tool, 0.125 in. Width of Cut, and Cutting Speeds v=50, 100, 200, and 400 fpm

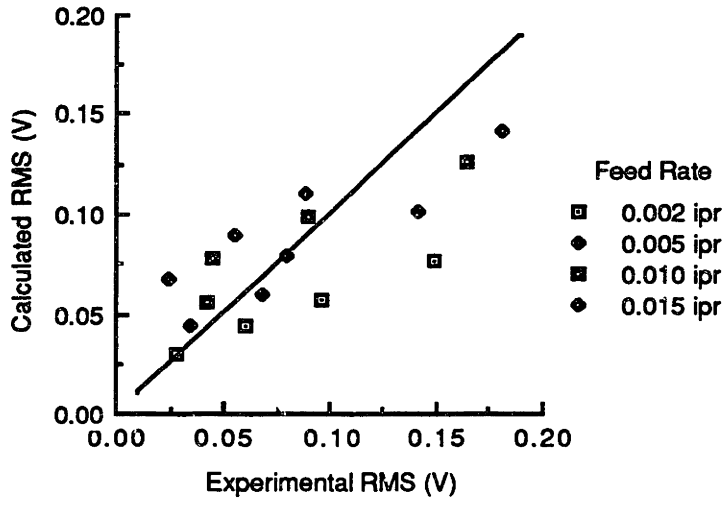

Figure 2.8a Calculated RMS from Equation (2-5)

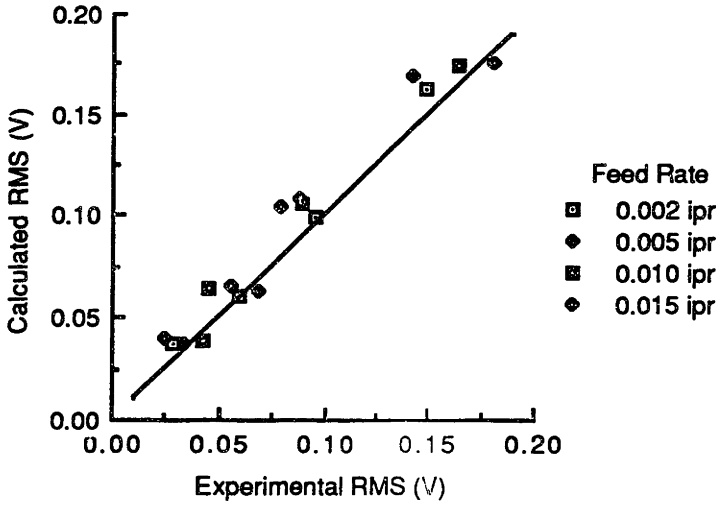

Figure 2.8b Calculated RMS from Equation (2-6)

Figure 2.8 Calculated RMS Versus Experimental RMS for Aluminum Cutting Tests with 15° Rake Angle Tool, 0.063 in. Width of Cut, and Cutting Speeds v=50, 100, 200, and 400 fpm

correlation coefficient between the measured RMS signal and the estimates supplied by relationship (2-6) is 0.988.

Using experimental data from tests with steel workpiece material and a 15° rake angle tool, the constants in expression (2-5) were found to be C_1 = 5.91E-3 and m = 0.425. For expression (2-6), the constants were determined as C_1 = 2.50E-2 , m = 0.500 and n = 0.135. Data from the test with a 50 fpm surface velocity and a 0.005 ipr feed rate were not included in the analysis, as the test could not be completed due to excessively high cutting forces developed during the test. Chatter significantly influenced the AE RMS signal in the tests with 300 fpm cutting velocity and 0.0035 and 0.0050 ipr feed rates; therefore, data from these tests were omitted from the analysis. Figure 2.10a shows the RMS values determined using equation (2-5) versus the measured RMS signals. The RMS signals estimated using equation (2-6) versus the measured RMS signal are shown in Figure 2.10b. The correlation coefficients between the measured and estimated RMS values is 0.819 for the estimates provided by equation (2-5), and it is 0.867 for the estimates determined using equation (2-6).

The above numerical and graphical results indicate that over a wide variety of cutting conditions equation (2-6) more adequately models the relationship between the RMS AE and the cutting forces and velocity than equation (2-5). This conclusion indicates that the fraction of the total cutting power used to produce acoustic emission is not constant. Rather it seems that the proportion of the power expended in the cutting process used to produce AE is greater when the power increases due to an increase in cutting velocity than when the power increases due to an increase in cutting forces.

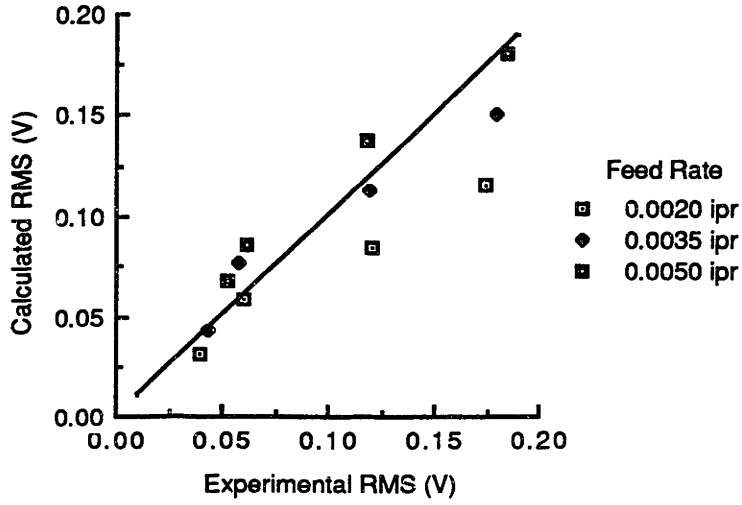

Figure 2.9a Calculated RMS from Equation (2-5)

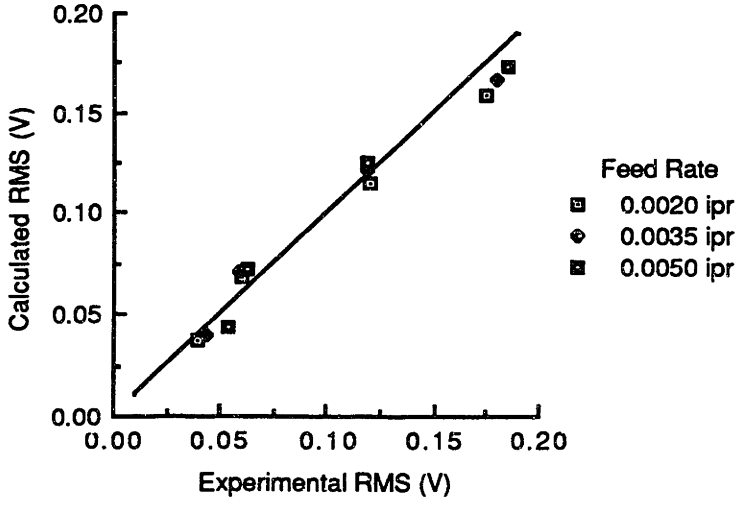

Figure 2.9b Calculated RMS from Equation (2-6)

Figure 2.9 Calculated RMS Versus Experimental RMS for Steel Cutting Tests with 30° Rake Angle Tool, 0.125 in. Width of Cut, and Cutting Speeds v=50, 100, 200, and 300 fpm

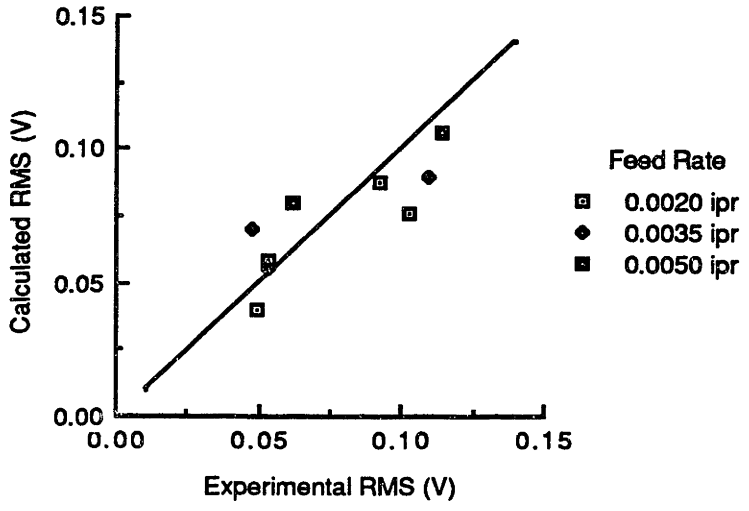

Figure 2.10a Calculated RMS from Equation (2-5)

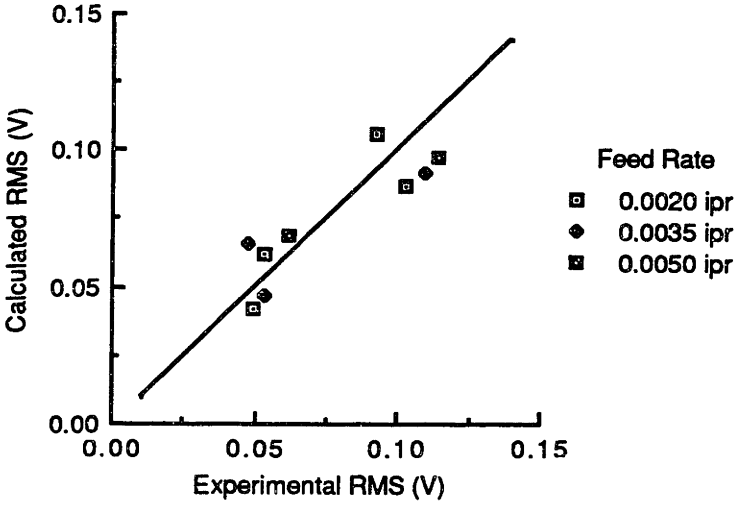

Figure 2.10b Calculated RMS from Equation (2-6)

Figure 2.10 Calculated RMS Versus Experimental RMS for Steel Cutting Tests with 15° Rake Angle Tool, 0.125 in. Width of Cut, and Cutting Speeds v=50, 100, 200, and 300 fpm

In general, relationships (2-5) and (2-6) did not relate the RMS AE signal with the cutting forces and velocity as well for a 15° rake angle tool as for a 30° rake angle tool. This result may be explained by the fact that, in general, assumptions made in the orthogonal cutting model more realistically reflect the actual cutting process for the 30° than the 15° rake angle. For example, it was obvious from examination of the cross section of the chips formed that the chip shearing process occurred in a less uniform zone for the 15° than the 30° rake angle tests. An increase in the rake angle provides a general improvement in the chip formation process [126].

2.5 CONCLUSIONS

The development of an acoustic emission-based model appropriate for in-process monitoring of tool wear within a scheme such as the decision-making approach to process operation has been considered. In order to be adequate for this application, the model must account for changes in the AE signal due to changes in the machine tool setting parameters. It was concluded that a model based on fundamental cutting principles and parameters would be best for monitoring the tool wear.

A model was developed that, over a wide range of cutting conditions, more adequately relates the cutting forces and velocity with the RMS signal than previous models. This model indicates that the proportion of the total power expended in the cutting process that goes into producing acoustic emission is not constant. Instead, the proportion is greater if the power increases due to an increase in cutting velocity than if the power increases due to an increase in cutting forces.

3 SENSOR SYNTHESIS

3.1 INTRODUCTION

With few exceptions, control schemes for manufacturing processes use a single sensor to monitor the process (Figure 3.1). In many cases this approach is inadequate primarily due to inaccurate sensor information and the lack of a single process model which can sufficiently reflect the complexity of the process. The signals that sensing devices deliver as inputs to a process model may include errors. In addition, the physics or geometry of many processes do not allow several of the process variables to be directly measured. A complex interaction between a number of physical phenomena occurs in many manufacturing processes; the characteristics of these interactions and the relative significance of the physical phenomena can change during the process. It is difficult to develop one model which adequately reflects these phenomena and the complexity of the interaction between them. Furthermore, some parameters, particularly material-related parameters, used in a process model are often somewhat uncertain. Material properties can be sensitive to conditions such as temperature and can vary considerably for each batch of material.

As an alternative to the typical approach to process monitoring, this chapter considers a multiple sensor approach which is similar to the method a human uses to monitor a manufacturing process. The human's approach is characterized by a lack of accurate sensors and process models; however, the human considers a number of different sensors (his/her own senses), and processes information about a variety of process variables such as temperature and force. Similarly, one can consider a system for the

monitoring of manufacturing processes (Figure 3.1) whereby measurement of process variables is performed by several sensing devices which in turn feed their signals into different process models which contain mathematical expressions based on the physics of the process; they relate the measured variables to process state variables, namely process variables which cannot be directly measured [20,21,25,26]. The approach proceeds with a synthesis of the state variable estimates provided by the different process models.

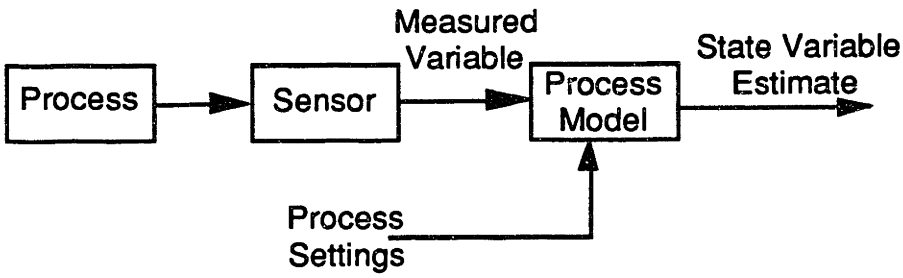

(a) Typical Process Monitoring Scheme

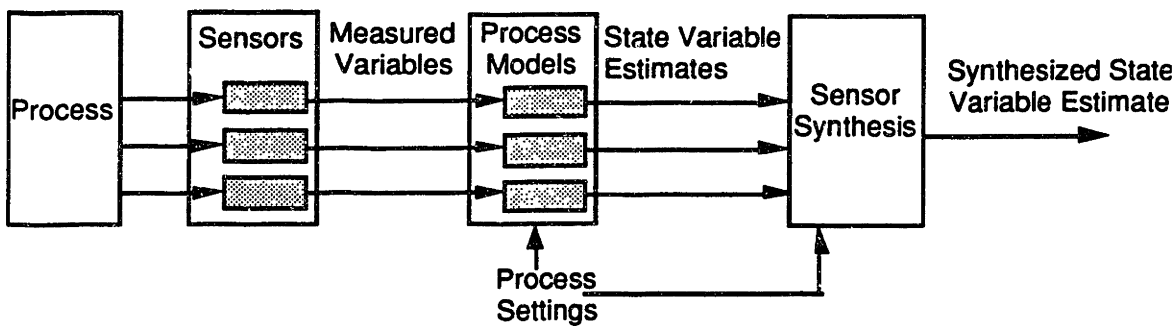

(b) Sensor Synthesis Approach to Process Monitoring

Figure 3.1 Comparison of Typical Process Monitoring Scheme (a) with Sensor Synthesis Approach (b)

The term "synthesis" indicates in the context of this thesis that the estimates of the state variable are combined or "synthesized" to provide a final estimate of the same variable. If e.g. the state variable of a process is the tool wear and three different sensors and process models provide three different estimates of the tool wear at the time of measurement, then the synthesis scheme combines these three estimates in order to provide a final estimate of the wear.

Synthesis of sensor information can provide a number of benefits for process monitoring, particularly for processes and systems which are difficult to model and monitor [19,34]:

- By using a variety of sensors, the maximum amount of information is used for making control decisions; the quality of the decisions will likely be better than decisions based on information from a single sensor.

- Utilizing independent estimates of the same state variable from several sensor-based models can be considered analogous to taking several samples from a random distribution. Statistically, as more samples are taken, the confidence interval for the mean becomes narrower. In the same way, as more sensor-based information is considered, the certainty of the estimated parameter values improves and the uncertainty due to randomness in the sensor signals is reduced. This benefit could potentially be achieved not only by using a variety of sensors but also by using multiples of one type of sensor.

- The reliability of different types of sensors may change relative to one another even during a single process. If this change in reliability can be correlated with the process input parameters or other known parameters, a sensor synthesis scheme

can "weight" the appropriate sensor(s) more heavily for each set of conditions, thus providing the controller with information which is more reliable than information from a single sensor.

- Features from several types of sensors may be synthesized in order to provide greater resolution in the sensor-based parameter estimates. One binary signal provides two classifications while two binary signals provide four classifications. Synthesizing signals from several types of sensors can be considered as a more sophisticated extension of the binary case.

A significant element of the decision-making approach to process operation described in Chapter 1 is the ability to synthesize the state variable estimates provided by the process models. The purpose of this chapter is to investigate the feasibility of different sensor synthesis schemes and to provide a basic comparison of their performance.

3.2 APPROACHES TO SENSOR SYNTHESIS

In this chapter two basic approaches to the synthesis of sensor information are considered. The first approach is to use a mechanism based on training. The second approach utilizes statistical criteria to estimate the best synthesized estimate from the variable estimates provided by the process models.

3.2.1 Approach Requiring Training

An approach can be implemented in which the synthesis occurs through a "mechanism" or a "model" which first "learns" through a training phase how the synthesis

should occur (Figure 3.2). This "mechanism" or "model" can learn with the help of available data where both the input and the output of the synthesis scheme is known; input

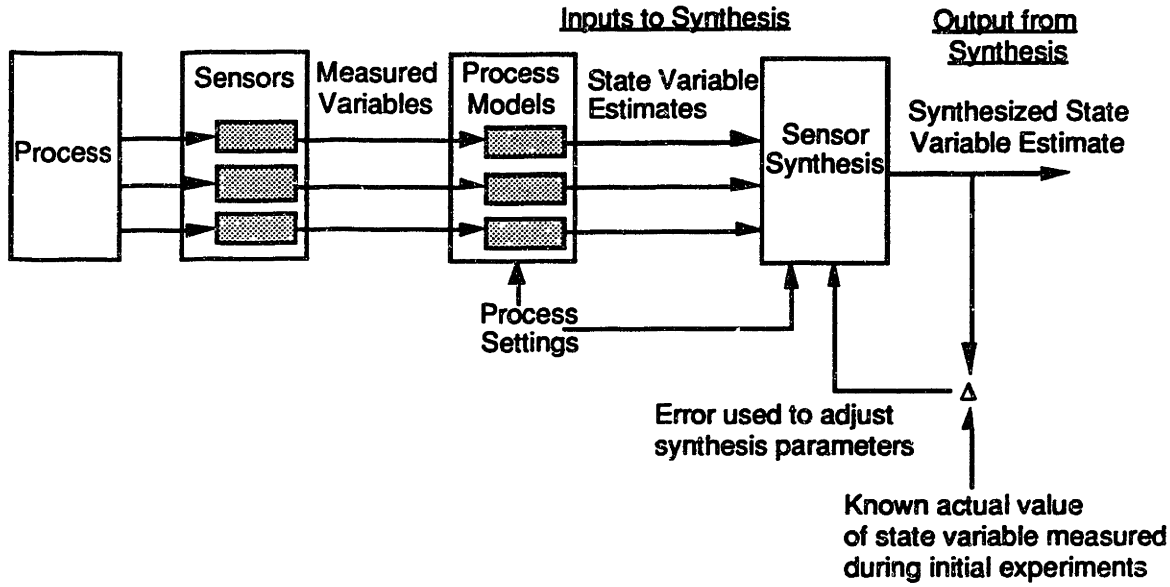

(a) Training Phase

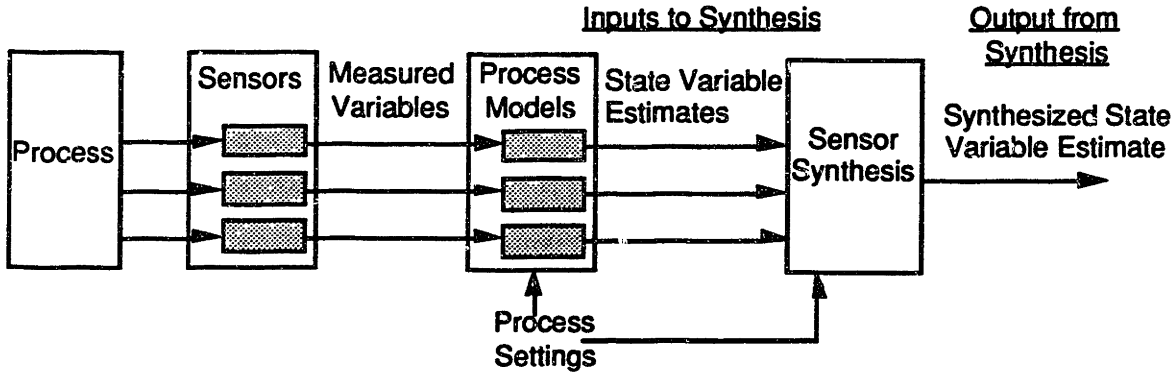

(b) Application Phase

Figure 3.2 Illustration of Training and Application Phases

data in the context of this work consists of state variable estimates provided by the sensors and their corresponding process models and the output is the actual value of the state variable. In order to know the actual value for the state variable, experiments must be performed in which measurements are made of the state variable which is not normally measured during the actual process. In the application phase, the already trained mechanism is used to synthesize the state variable estimates provided by the models in order to obtain a synthesized estimate of the state variable.

Methods of this type include

- least-squares regression
- inverse least-squares regression
- the group method of data handling (GMDH)
- a neural network

In **multiple least-squares regression**, known values for a state variable are regressed on the state variable estimates provided by the process models in order to find appropriate values for the coefficients in a regression model. A typical linear regression model is [86]:

$$y = \beta_0 + \beta_1 x_1 + \beta_2 x_2 + \beta_3 x_3 + ... + \beta_i x_i + \varepsilon \qquad (3\text{-}1)$$

where

y = synthesized state variable estimate

β_i = regression coefficient

x_i = state variable estimates provided by process models

ε = random error

Ideally, the corresponding state estimates provided by the models should be identical to each other. In this ideal case, the strong linear correlation of these estimates will cause numerical difficulties in estimating the regression coefficients, $\hat{\beta}_i$, during multiple regression. In addition, multiple regression of the measurements of the state on the estimates assumes that the measurements of the state contain random error, whereas the model estimates are exact. However, it is more likely that the model estimates will contain far more random error than the measurements of the state variable.

Because of the above shortcomings for standard multiple regression, a different technique using an inverse least-squares approach has been developed for integrating the model estimates. Independent least-squares regressions of the state estimates provided by each process model on measurements of the state will provide functions that relate the estimates provided by each model with the actual state. The regression model is:

$$y_i = \beta_o + \beta_1 x_i + \varepsilon_i \qquad (3\text{-}2)$$

where:

y_i = state variable estimates provided by process models

β_0 = y-intercept of the regression line

β_1 = slope of the regression line

x_i = actual state

ε_i = random error

The regression functions can be used "backwards" to obtain improved estimates for the state variable based on the estimates provided by the models. Associated with the estimates of the state variable are uncertainties which can be quantified as inverse prediction variances. An estimate for the inverse prediction variance is [87]

$$s^2_{inverse} = s^2_{pred.}/\hat{\beta}_1^2 \qquad (3\text{-}3)$$

where:

$s^2_{inverse}$ = estimated inverse prediction variance

$s^2_{pred.}$ = estimated variance for the prediction of a new y_i corresponding to a given x_i

$\hat{\beta}_1$ = least-squares estimate for the slope of the regression line

In general, the average of several samples has a lower variance than the variance for a single sample. Weights can be selected such that a weighted sum of the state estimates provided by several models has a variance at least as low as that for any estimate provided by a single model. Therefore, the inverse prediction of the actual state based on a weighted sum of the estimates provided by several models will have a variance at least as low as that for any inverse prediction based on an estimate from a single model. A weighted sum of the state estimates provided by the sensor-based models can be regressed on measurements of the state. During the actual manufacturing process, the resulting regression function would be used backwards to obtain an integrated estimate from the initial estimates provided by the models.

$$x_{pred,\,i} = \frac{[ay_{1i} + by_{2i} + cy_{3i}] - \hat{B}_0}{\hat{B}_1} \qquad (3\text{-}4)$$

where:

$x_{pred,\,i}$ = inverse prediction of the state variable, used as the synthesized estimate

y_{ji} = state variable estimate provided by jth model

a, b, c are weighting factors

$\hat{B}_0$ and $\hat{B}_1$ are the estimated y-intercept and slope, respectively, obtained from the regression of the weighted sum of model estimates on the measured state variable

Associated with this prediction is an inverse prediction variance which can be estimated as:

$$S^2_{inverse} = S^2_{pred.}/\hat{B}_1^2 \qquad (3\text{-}5)$$

where:

$S^2_{inverse}$ = estimated inverse prediction variance

$S^2_{pred.}$ = estimated variance for the prediction of a new value of the weighted sum corresponding to a given x_i

The values of the weights, a, b, c, can be chosen using a numerical optimization technique such that the estimate for the inverse prediction variance is minimized.

The **group method of data handling** or GMDH is a heuristic method of predicting a dependent variable based on a set of independent variables [51,52,97]. By layering several sets of quadratic polynomials such that the output of one set is the input to the next set, the method allows the dependent variable to be predicted by a very complex, higher-order polynomial of the independent variables (Figure 3.3). The GMDH algorithm is self-organizing; variables which are least valuable for prediction of the dependent variable are dropped from further consideration during he construction of each layer of quadratic polynomials. Because of this selectiveness, numerical difficulties caused by factors such as linear dependence among the independent variables encountered during standard high-order regression are reduced with the GMDH approach. When the regression equations begin to provide a poorer prediction of the dependent variable according to a specified training criterion, no more layers of quadratic polynomials are added. For this reason the model is prevented from becoming overspecialized to the training data. In the context of this work, the synthesized state variable estimate would be considered as the dependent variable and the independent variables would include the state variable estimates provided by the process models.

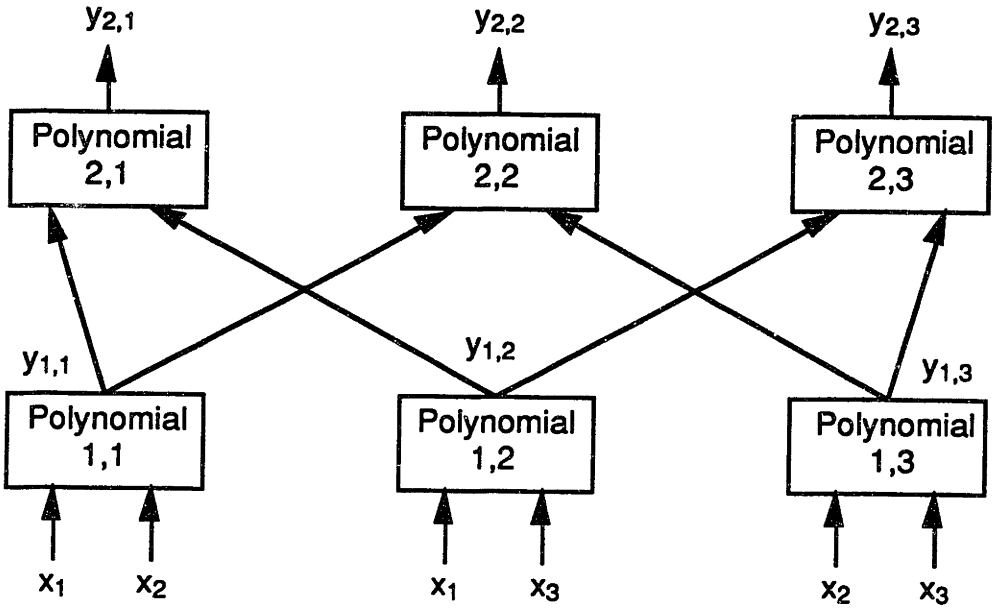

For polynomial 1,1: $y_{1,1} = \beta_0 + \beta_1 x_1 + \beta_2 x_2 + \beta_3 x_1^2 + \beta_4 x_2^2 + \beta_5 x_1 x_2$

x_i = state variable estimates provided by process models

β_i = regression coefficient

$y_{i,j}$ = synthesized state variable estimate provided by jth polynomial in ith layer

Figure 3.3 Structure of GMDH Polynomial

A **neural network** is composed of many nonlinear processors or nodes which operate in parallel. Information is stored in the connection weights between the processors. The weights are adapted during a training phase in order to develop the knowledge stored in the network [11, 46, 73, 96, 118]. Because neural nets have been successfully used to make almost instantaneous decisions based on noisy and incomplete information, this technique appears to have significant potential for real-time monitoring and control of manufacturing processes [16]. For sensor synthesis, the state variable estimates provided by the process models would be used as inputs to the network. The process input variables could also be included as inputs to the network. The network output would be the

synthesized estimate of the state variable. Many different types of neural networks have been developed [46]. In this thesis a multi-layer perceptron and an interpolation network were implemented.

For the multi-layer perceptron, the training algorithm used was the generalized delta rule including a momentum term as described by Rumelhart et al [96]. The sigmoid function [73] was used as the processor at each node. Each node of a given layer was connected with every node in the following layer (Figure 3.4). This type of network has been found to perform well for a variety of problems including speech and image recognition [96]. A multi-layer perceptron neural network has been considered for the problem tool wear monitoring in a turning process [93] whereby the network was used to classify the condition of a tool as "fresh" or "worn". The position of the work reported in this thesis which is related to neural networks differs from [93] in three respects: (a) The use of three sensors, namely force, acoustic emission (AE), and temperature, instead of two [93], namely force and AE. (b) The use of a process model for each of the sensors which provides an initial estimate of the tool wear. In this work the output of these models is synthesized instead of synthesizing the original sensor signals. This is the reason this thesis refers to sensor synthesis instead of sensor fusion or sensor integration since this work considers synthesis of the wear estimates which are based on the different sensor signals and their corresponding process models. (c) The neural network is used to provide a "continuous scale" estimate of the flank wear land. The point is not so much to detect a worn tool but rather to predict when the tool will be worn so that a proper control strategy can be devised in terms of selecting input variables and tool change timing. In addition, this thesis compares the neural network approach with other sensor synthesis approaches. Such comparisons were not made in [93].

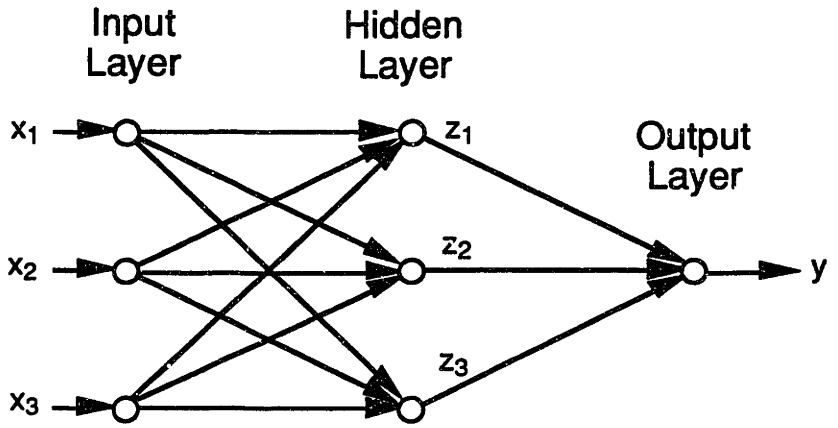

The output of a node in a hidden layer is determined as

$$z_j = \frac{1}{1 + e^{-(\alpha_j - \theta_j)}}$$

similarly, the synthesized state variable estimate, y, is determined as

$$y = \frac{1}{1 + e^{-(\alpha_j - \theta_j)}}$$

where

$$\alpha_j = \sum_{i=1}^{n} w_{ij} z_i$$

x_i = state variable estimates provided by process models

z_i = outputs of nodes in previous layer

n = number of nodes in previous layer

w_{ij} = weight corresponding to connection between nodes i and j

θ_j = threshold corresponding to node j

Figure 3.4 Structure of Multi-Layer Perceptron Neural Network

The interpolation network can be considered as a special two-layer case of the general concept of a neural network. In some cases an interpolation net can perform adequately for tasks which one might think would require a multi-layer network. The

output of the interpolation network in the form in which it was implemented in this thesis is based on a Gaussian function and is determined as [118]:

$$y = \sum_{i=1}^{n} w_i \, e^{-\frac{1}{2\sigma}|x - c_i|^2} \tag{3-6}$$

where

y = network output (synthesized state variable estimate)

w_i = weight corresponding to center i

σ = width of the Gaussian function

x = input vector

c_i = vector center corresponding to weight i

$|x - c_i|^2$ = squared distance between vectors x and c_i

n = number of weights and corresponding centers

The equation above describes a two-layer neural network (Figure 3.5). In an interpolation net the number of nodes in the input layer equals the number of training data points; each of the first layer nodes can be specialized to one particular input-output training point in the sense that it computes the Gaussian function that is centered on that input ($c_1 = x_1$, $c_2 = x_2$,..., $c_n = x_n$ where the x_i are the n vector inputs in the training data set). For small values of the Gaussian function width, σ, each of the first layer nodes will have only a local influence for input data which is similar to the center for that node; for large values of the width, σ, each of the nodes in the first layer will have a global influence for a wider range of input data. In the application of sensor synthesis, the network output is the synthesized state variable estimate. The elements of the input vector include the state variable estimates provided by the process models and may also include known process input variables. Each input-output point in the training data provides a linear equation involving the unknown weights. For an interpolation net, the number of these equations

equals the number of unknown weights. These linear equations can be solved in order to determine the network weights.

$$y_1 = w_1 e^{-\frac{1}{2\sigma}|x_1 - c_1|^2} + w_2 e^{-\frac{1}{2\sigma}|x_1 - c_2|^2} + \ldots + w_n e^{-\frac{1}{2\sigma}|x_1 - c_n|^2}$$

$$y_2 = w_1 e^{-\frac{1}{2\sigma}|x_2 - c_1|^2} + w_2 e^{-\frac{1}{2\sigma}|x_2 - c_2|^2} + \ldots + w_n e^{-\frac{1}{2\sigma}|x_2 - c_n|^2}$$

$$\vdots$$

$$y_n = w_1 e^{-\frac{1}{2\sigma}|x_n - c_1|^2} + w_2 e^{-\frac{1}{2\sigma}|x_n - c_2|^2} + \ldots + w_n e^{-\frac{1}{2\sigma}|x_n - c_n|^2} \qquad (3\text{-}7)$$

3.2.2 Approach Based on Statistical Information

This section considers a different approach to the synthesis of sensor information in which statistical criteria are used to determine the best synthesized state variable estimate from the individual estimates provided by the process models. In order to use this approach, statistical information must be available concerning the correlation between the state variables and their estimates provided by the process models. This statistical information can possibly be obtained by evaluating process models which are based on the process physics. Evaluation of the models can be implemented without extensive experimentation since what is needed is data (in the form of distributions) concerning the physical properties of the materials used in the process. These properties are a primary source of uncertainty in manufacturing process modelling and either can be obtained from handbooks or can be experimentally determined with a limited amount of experimentation. Thus a synthesis approach based on statistical information may have an advantage over techniques requiring extensive "training data."

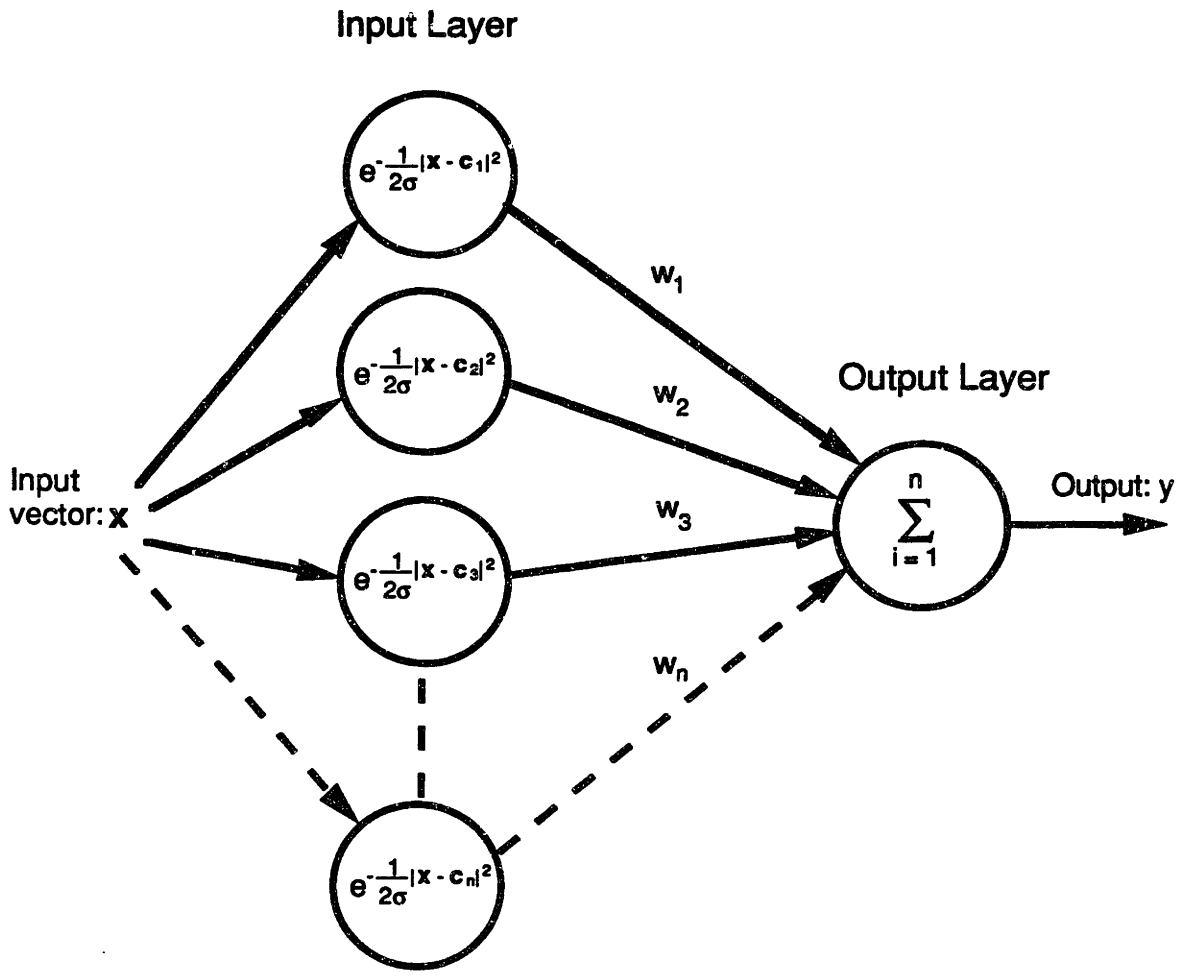

Figure 3.5 Structure of Interpolation Neural Network

The development of synthesis methods based on statistical information has been motivated by the need for reliable identification of targets in military applications [10, 12, 77] and for the identification and measurement of objects in robotic applications [33,77-79]. These applications are generally characterized by a large number of sensors which are in many cases identical. In contrast, the manufacturing environment usually allows only a few sensors to be applied and often each of these sensors measures a different type of variable. The implementation of many of the statistically-based methods developed for military or robotic applications requires a substantial amount of data concerning the correlation of the sensor signals with the measured target or object. In addition, these

statistical methods often assume that there are a limited number of discrete targets or objects and that these types of targets are known beforehand. Accordingly, these methods are motivated from a viewpoint which is different from that of a manufacturing process environment where experimental data is more difficult to obtain and process variables can vary significantly over a continuous range. Therefore, some of the methods used in such applications, such as a Bayesian estimator [33,78] or Shafer-Dempster reasoning [12,98], may be infeasible or impractical for implementation in the manufacturing environment.

In order to implement a Bayesian estimator, statistical information concerning the correlation between the state variables and their estimates provided by the process models must be available. In addition, a probability density function for the estimated state must be established independently of any in-process sensor signals; the requirement for this density function may make this approach infeasible for a manufacturing application. In many manufacturing processes the characteristics of the probability density function for a state variable, such as the mean and variance, can be influenced by the history of many input variables as a function of time. These variables may be changed frequently during the operation of a process. It may be impractical to determine the characteristics of such a probability distribution as a function of the history of the input variables since these variables may be changed in a very large number of ways.

Shafer-Dempster reasoning has been considered as another method for the identification of targets in military applications [12,98]. In this method, the degree of support for a final proposition is determined based on the degree of confidence for the truth of the logical antecedents of the final proposition. The degree of confidence assigned to each antecedent proposition reflects the degree to which the information from a sensor indicates that the proposition is true and also the reliability of the sensor supporting the proposition. In order to implement this method for sensor synthesis in manufacturing

process monitoring, multiple final propositions would have to be considered. Each of these final propositions would suggest that the estimated state variable is within a certain range. The information from each sensor would indicate that the state variable might be within one of several ranges, and logical rules would have to be developed in order to determine the degree of support for each final proposition. Here again, such an approach would be impractical. The assignment of the degree of confidence to each antecedent proposition may be quite subjective. In addition, the implementation of such an approach would require a large number of logical rules to determine the degree of support for the final propositions; it would be difficult to develop these rules in a systematic manner and consequently the rules would depend heavily on the subjective judgement of the person writing the rules based on his/her observations from previous process data.

Other approaches for the synthesis of sensor information have been been utilized in robotic applications [79]. These methods were implemented in this work because they are more appropriate for the concept of sensor synthesis considered in this chapter than a Bayesian estimator or the Shafer-Dempster approach. For both of these methods, the largest consensus group of sensors whose information is considered to be in agreement is first determined. In order to define the sensors in this group, it is first determined for each sensor whether or not the information from each of the other sensors is supportive. *Sensor i* is considered to be supported by *sensor j* if the confidence distance measure d_{ij} is less than a threshold value r_{ij}. Assuming that sensor i measures a variable y_i and that based on this measured variable a model provides an estimate of a state variable, x_i, (for example, in machining y_i may be the cutting force and x_i may be the tool wear) a probability density function, $P_i(x_i)$, can describe the probability that the actual value of the state variable, x, is in a certain range (Figure 3.6). In a similar manner, a probability density function $P_j(x_j)$ can be associated with another estimate for the same state variable, x_j, which is provided by a different model based on a different measured variable y_j. The confidence distance

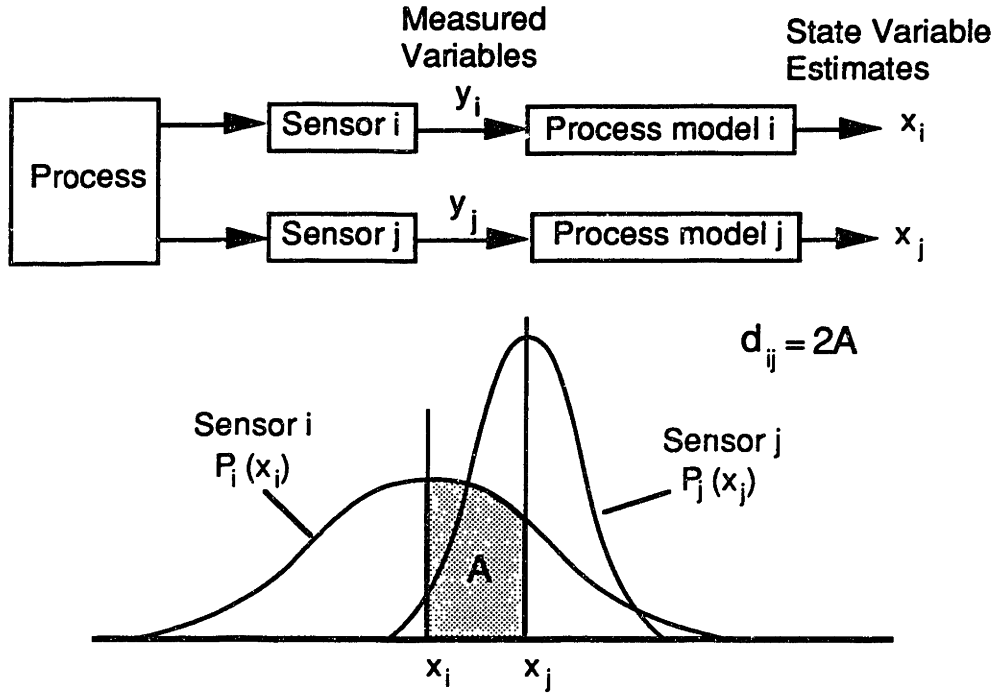

Figure 3.6 Confidence Distance Measure, d_{ij}, for Statistical Sensor Synthesis
$P_i(x_i)$ = probability density function of sensor i
$P_j(x_j)$ = probability density function of sensor j

measure for the support of sensor i by sensor j can be defined as

$$d_{ij} = 2A \tag{3-8}$$

where

A is the area under the probability density curve $P_i(x)$ between x_i and x_j (Figure 3.6)

$P_i(x)$ is the probability density function for the value of state x given that the state estimate provided by sensor i and its corresponding process model is x_i.

The threshold value r_{ij} can be specified e.g. according to prior knowledge of the relative reliability of the sensors or based on particular knowledge about the process. The value of

r_{ij} can range from 0.0 to 1.0. When threshold r_{ij} = 0.0 sensor j will never be found to support sensor i. When threshold r_{ij} = 1.0 sensor j will always be found to support sensor i. The largest group of sensors which is mutually supportive and/or supported by the other sensors can be used to determine the synthesized estimate of the state variable.

In this work as well as in previous applications of these methods the probability density function for each sensor $P_i(x)$ is considered to be Gaussian [79]. The variance for each distribution is considered to be equal to the variance of the sensor-based state estimates about the actual state. This variance can either be determined through experimental data or possibly through evaluating the process models which convert the measured variables to estimates of the state variables based on an understanding of the process.

A synthesized estimate, θ, based on probability density functions for a state variable as estimated by different sensors can be found by maximizing the expression

$$\sum_{i=1}^{l} P_i(\theta / x_i) \qquad (3\text{-}9)$$

where

θ = synthesized estimate

l = number of sensors considered to be in agreement

x_i = state variable estimates provided by each process model

$P_i(\theta / x_i)$ = value of the probability density function at θ given that the distribution is centered at x_i (Figure 3.7)

Such a maximization corresponds to the intuitive approach of maximizing the sum of the probabilities for the synthesized estimate. However, in a different way of finding a

synthesized estimate, θ, can be based on maximizing the expression

$$\prod_{i=1}^{1} P_i(\theta/x_i) \tag{3-10}$$

Such an expression comes from the method of maximum likelihood, which is a very common method of deriving an estimator [14]. For both expression (3-9) and (3-10) the indices are over the set of sensors considered to be in agreement.

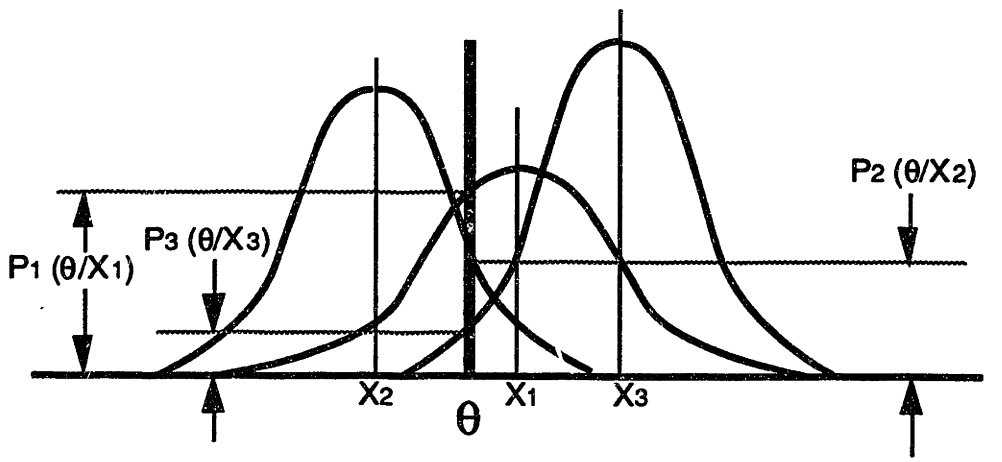

Figure 3.7 Determination of Synthesized Estimate θ Based on Statistical Information

If the process models do not adequately reflect the complexity of the process, the error between the state estimates provided by the models and the actual state may have a deterministic component or bias. Provided that this bias is known, a state estimate from a model can be corrected for the bias before synthesizing the estimate with the state estimates provided by the other models (prior to determining the consensus group of sensors).

Any probability density functions can be used directly in expressions (3-9) or (3-10); however, the solution of the synthesized estimate, θ, may require a significant amount

of computation. On the other hand if the distribution is assumed to be Gaussian the synthesized estimate, θ, in equation (3-9) can be easily determined through an iterative solution: initially, one of the state estimates provided by a model in the consensus group must be assumed to be the synthesized estimate and the values of a variable q_i corresponding to each state variable estimate, x_i, provided by the sensors in the consensus group are determined.

$$q_i = \frac{\exp\left[\frac{-(\theta-(x_i - b_i))^2}{2\sigma_i^2}\right]}{\sqrt{2\pi}\,\sigma_i} \tag{3-11}$$

where

b_i = bias corresponding to the estimate x_i

σ_i = standard deviation of the probability density function $P_i(x)$ corresponding to the estimate x_i

A new value for the synthesized estimate is then determined using the equation

$$\theta = \frac{\sum_{i=1}^{l} \frac{q_i\,(x_i - b_i)}{\sigma_i^2}}{\sum_{i=1}^{l} \frac{q_i}{\sigma_i^2}} \tag{3-12}$$

If the new value of the synthesized estimate is within a specified tolerance of the previous value for the estimate, the solution is considered to have converged on the final value for the estimate. Otherwise the values of q_i are again calculated using equation (3-11) based on the most recent value of θ determined using equation (3-12). Using these values for q_i a new value for the synthesized estimate is determined from equation (3-12).

In the case of expression (3-10) if the probability density function, $P_i(x_i)$, is assumed to be Gaussian one can derive a closed form solution for the synthesized estimate

$$\theta = \frac{\sum_{i=1}^{1} \frac{(x_i - b_i)}{\sigma_i^2}}{\sum_{i=1}^{1} \frac{1}{\sigma_i^2}} \qquad (3\text{-}13)$$

From the above discussion it is clear that for the confidence distance measure and for either of the two expressions to be applied the probability density functions, $P_i(x_i)$ must be determined. These density functions could be established with the aid of data from special experiments where the actual values of the states that are to be estimated have been measured. However, in some cases it may not be possible to measure these states. In addition, it may be impractical to run special experiments to collect such data whenever the process conditions, such as the workpiece material, are changed. As an alternative to such an experimental approach, a method is discussed in Section 3.3.2 of this chapter for obtaining the probability density functions, $P_i(x_i)$, through the evaluation of process models which are based on a physical understanding of the process [25]. Because this method can be implemented without extensive experimentation, it has a significant advantage over synthesis methods requiring training.

3.3 EVALUATION OF METHODS FOR SENSOR SYNTHESIS

Among manufacturing processes, machining is a group of processes where a sensor synthesis approach to process monitoring and control should be tested first since these processes have been extensively researched and a large amount of information is available on their physics and modelling. In addition, machining operations are widely

used throughout industry and improvements in the monitoring and control of these processes would have a great impact on the entire manufacturing industry. In this thesis the synthesis methods are considered for providing estimates of the tool wear during a turning operation based on multiple sensor information.

The sensor synthesis methods were first evaluated and compared in a simulated environment. The purpose of these simulations was to obtain an initial assessment of how these methods perform under different conditions. These simulations reflected a number of potential conditions during a machining operation. To make statistically significant inferences, a relatively large number of tests must be run. The use of simulation allowed many tests to be run while avoiding expensive and time consuming machining experimentation.

Following the simulations, the sensor synthesis methods were evaluated using tool wear data from a turning operation. The experiments were also used to compare the accuracy of the synthesized wear estimates with wear estimates provided directly by sensor-based models. The models considered in this work are based on measurements of force, temperature and acoustic emission (AE). These experiments provided an indication of the relative effectiveness of each sensor synthesis method based on actual machining data.

3.3.1 Simulation

Case 1: Ideal sensor operation and adequate process models

Ideally, all of the sensors should operate properly and the process models should adequately reflect the complexity of the process. In this situation, the wear estimates

provided by the models reasonably reflect the actual wear. However there is some random error between the wear estimates provided by the models and the actual wear. Variations in the workpiece material properties are the primary source of this random error. The purpose of simulating this situation was to determine if sensor synthesis will provide a better estimate for the state variables than information from only one sensor. In addition, this simulation provided a comparison of the synthesis approaches under ideal circumstances and therefore could be used as the basis for comparison under more complex conditions.

In order to simulate the aforementioned conditions, the state variable wear was assumed to start at 0.01 mm and to increase in increments of 0.01 mm to a final wear of 0.30 mm resulting in a total of 30 data points. The wear estimates which would be provided by process models in an actual machining operation were simulated by wear estimates which were calculated as a deterministic function of the actual wear plus a normally distributed random component with mean 0 and standard deviation of 0.05 mm. This random component was added to simulate the random error associated with the state estimates provided by the process models in an actual machining operation.

Three independent wear estimates were input to each sensor synthesis scheme. A set of training data (30 data points) was first determined. The means and variances of the errors between the actual wear and each of the wear estimates in the training data were used as the values of the biases and variances by the statistical methods. The training data was also used to train the methods requiring a training phase. The synthesis approaches were then compared based on the data for 30 simulated machining tests.

The mean squared error between the synthesized wear estimates provided by each scheme and the actual wear was used to quantify the performance of the synthesis approaches. This criterion can be expressed as:

$$MSE = \frac{1}{n}\sum_{i=1}^{n} (y_i - y_{t,i})^2 \qquad (3\text{-}14)$$

where:

MSE = mean squared error

y_i = synthesized wear estimate

$y_{t,i}$ = actual wear (target output)

n = number of data points used for evaluation

Different neural network structures and training tolerances in the case of the multi-layer perceptron neural network, different values of sigma, σ, in the case of the interpolation network, different training criteria in the case of the GMDH method, and different threshold values used to determine the consensus group of sensor in the case of the statistical approach, will all result in different values of the MSE for the data used to evaluate the sensor synthesis approaches. One data set can be used to select the best structure and/or synthesis parameters and also to compare the performance of the synthesis approaches. However, to ensure that the particular structure or parameters used in the synthesis methods have not been unfairly tailored to the particular data set, this data set must be sufficiently large and must adequately reflect all of the data that will be encountered in the application of the approaches. An alternative approach to the comparison of the synthesis methods which requires less data is to divide the data into three parts: one for training, a second data set for selecting the best structure or parameters for the synthesis methods and a third data set for comparing the performance of the synthesis methods [46]. This second approach was implemented in the simulations for comparing the sensor synthesis methods.

To simulate the first case, a set of training data (30 data points), a set of data for

selecting the structure and parameters of the synthesis methods (30 data points), and data for 30 simulated machining tests for comparison of the synthesis methods (30 data points each) were determined using the following relationship. Each data point consisted of the actual wear and three independent wear estimates.

$$x_i = y + \text{random}, \quad \text{for } i = 1, 2, 3 \tag{3-15}$$

where:

x_i = wear estimate (mm)

y = actual wear (mm) (starting at 0.01 mm and increasing in increments of 0.01 mm to 0.30 mm)

random = random number (normally distributed, mean=0, standard deviation=0.050 mm)

In the training data, selection data and in the data for the 30 simulated machining tests the random component in the wear estimates was from the same distribution; however, the actual values of the random component for corresponding points in these sets of data were different from each other.

The MSE was calculated for each of the 30 simulated machining tests. The sample mean and standard deviation of these MSEs were calculated for each sensor synthesis scheme in order to evaluate and compare the different schemes. For the 30 machining tests the sample means and standard deviations of the MSEs for the three simulated model wear estimates used directly, as well as for the synthesized estimates provided by the training and statistical methods are shown in Table 3.1. The sample mean and standard deviation of the MSEs provided by using the arithmetic mean of the three model estimates as the synthesized wear estimate is also shown in Table 3.1. Using the arithmetic mean as the synthesized wear estimate is a very simple method for sensor synthesis and could be

considered as a base-line for evaluation of the other sensor synthesis approaches.

For the GMDH method, several different criteria are available for evaluating each generation of quadratic polynomials during the training phase. In this study, the mean squared error (MSE), prediction sum of squares (PRESS) [4], root mean square (RMS) [97], unbiased [97], and combined root mean square and unbiased criteria [97] were implemented. The polynomial selected by the PRESS, RMS, Unbiased and Combined criteria provided the lowest MSE on the data used for selection of the structure and parameters for the synthesis methods. This polynomial was used for comparison with the other synthesis methods.

For the multi-layer perceptron two network structures were implemented: a simple network with one hidden layer containing four nodes and a more complex network with two hidden layers each containing eight nodes. The goal was to determine if a more complex network learns more effectively than a simple network. The inputs to these networks consisted of the three simulated wear estimates (3 input nodes). Training tolerances were implemented starting with a large tolerance (0.060 mm) where no significant training occurred and decreasing in increments of 0.001 mm until the network could not converge in 40,000 iterations through the training data set or within one hour of CPU time on a VAXstationII/RC. The objective was to see if changing the training tolerance would cause the network to overfit or underfit the data. The error between the network predictions and the actual wear in the training data set must be within the training tolerance without modifying the network connection weights or node thresholds in order for the training phase to be complete. The results for the network and training tolerance providing the lowest MSE on the data used for selection of the structure and parameters of the synthesis methods were used for comparison with the other methods. This network had two hidden layers each containing eight nodes and a 0.049 mm training tolerance.

		Wear Estimation Method	Mean of Mean Square Errors (mm^2) $MSE = \frac{1}{n}\sum_{i=1}^{n}(y_i - y_{ti})^2$	Standard Deviation of Mean Square Errors (mm^2)
Single Sensor Estimates		Simulated Force Model	2.29E-3	6.74E-4
		Simulated AE Model	2.55E-3	6.73E-4
		Simulated Temperature Model	2.59E-3	5.58E-4
Synthesized Estimates		Arithmetic Mean	8.39E-4	1.98E-4
	Methods Based on Training	Inverse Least Squares	9.41E-4	2.23E-4
		Multiple Regression	8.28E-4	2.16E-4
		GMDH	1.00E-3	2.72E-4
		Multi-Layer Perceptron 2 Hidden Layers, 8 Nodes/Hidden Layer, Training Tolerance = 0.049 mm	8.09E-4	2.03E-4
		Interpolation Network $\sigma = 0.028$	4.56E-3	1.41E-3
	Statistical Method	Approach Maximizing $\prod_{i=1}^{n} P_i(\theta/x_i)$ No Bias Compensation, Thresholds $r_{ij} = 1.0$	8.88E-4	2.02E-4

Table 3.1 Comparison of Wear Estimates for Simulation Case 1 (Ideal sensor operation and adequate process models)

The interpolation network implemented had 30 nodes in the input layer corresponding to the 30 data points in the training data. The input vectors for the interpolation net consisted of the three simulated wear estimates (vector dimension of three). Values of the Gaussian function width, σ, ranging from 0.010 to 0.100 in increments of 0.001 were implemented. The network with $\sigma = 0.028$ provided the lowest MSE on the data used for selection of the structure and parameters of the synthesis methods

and was used for comparison with the other synthesis methods.

For both of the statistical methods considered, several different thresholds, r_{ij}, which are used to determine the consensus group of sensors were implemented. The methods were implemented with and without compensation for the bias. In Table 3.1 the results are shown for the statistical method providing the lowest MSE on the data used for selection of the structure and parameters of the synthesis methods. This statistical method attempts to maximize expression (3-10) with no bias compensation and thresholds $r_{ij} = 1$.

Figure 3.8 compares the mean MSEs of the three simulated model estimates with the best performance provided by a synthesis method based on training and with the best performance provided by the statistical methods. The multi-layer perceptron neural network provided the lowest mean MSE among the methods based on training. Using the data shown in Figure 3.8, a two sample *t* test [86] was used to make inferences about the population mean MSEs for the sensor synthesis methods. The population mean MSE provided by the neural network could not be shown to be less than the population mean MSE provided by the statistical method nor less than the population mean MSE provided by using the arithmetic mean of the three wear estimates with a certainty of at least 95%. With at least 95% certainty the population mean MSEs provided by each of the synthesis approaches shown in Figure 3.8 were less than the lowest mean MSE provided by directly using one of the three wear estimates.

The results from this simulation indicate that under ideal circumstances when the deterministic component of the model estimates adequately reflect the actual state variable a statistical method and a synthesis method based on training will provide similar performance.

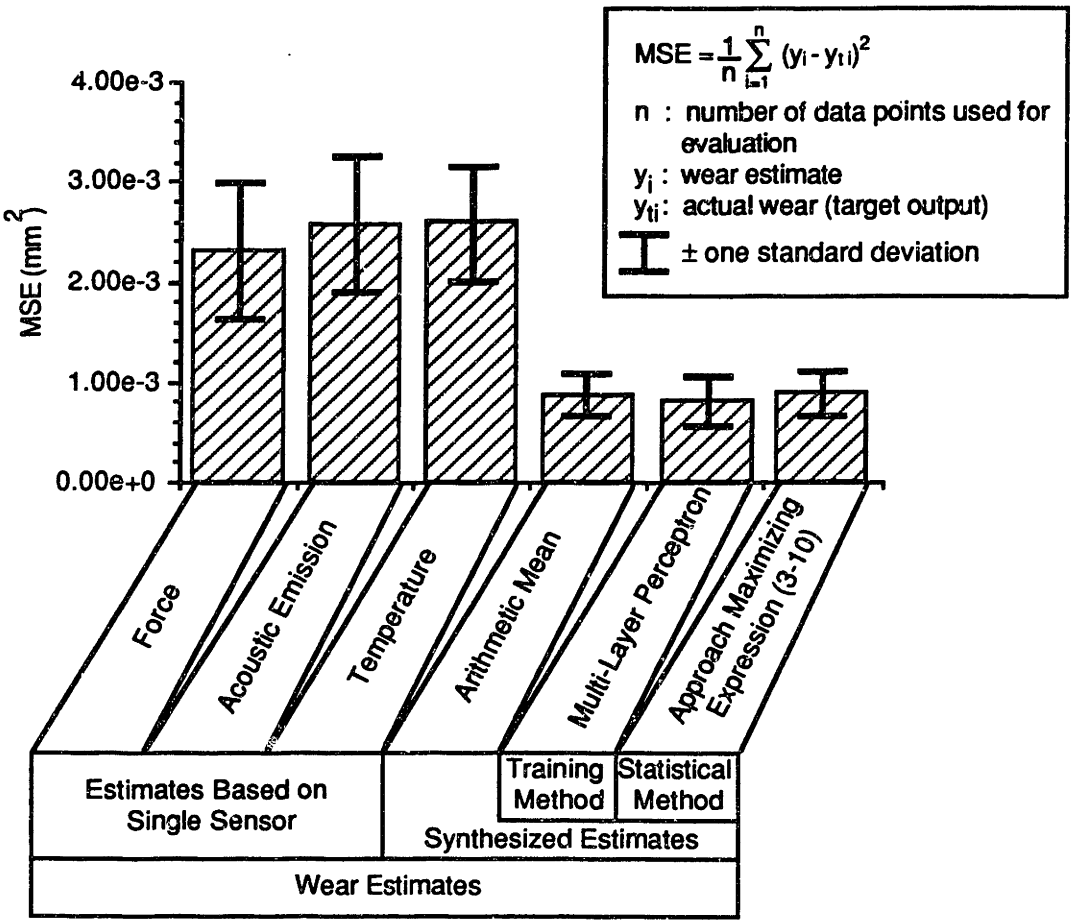

Figure 3.8 Evaluation of Best Wear Estimates for Simulation Case 1
(Ideal sensor operation and adequate process models)

Case 2: Ideal sensor operation and inadequate process models

In the second case considered, all of the sensors operate properly, but the process models do not adequately reflect the complexity of the process. In this case, there are deterministic errors between the wear estimates provided by the models and the actual wear. Models which adequately reflect the complexity of the machining process are difficult to build. The purpose of this simulation was to compare the methods for sensor synthesis under conditions which may more adequately reflect the circumstances in a real

machining operation than situation one. The simulation was also used to determine whether sensor synthesis provides a better estimate of the state variables than using the information from a single sensor in these non-ideal circumstances.

The values used to simulate the wear estimates provided by the process models were generated by including a deterministic component which is a nonlinear function of the actual wear. This nonlinear component was added to simulate a deterministic error between the estimates provided by the process models and the actual wear.

To simulate this case, a set of training data (30 data points), a set of data for selecting the structure and parameters of the synthesis methods (30 data points), and data for 30 simulated machining tests for comparison of the synthesis methods (30 data points each) were determined using the relationship:

$$x_i = y + 0.075\sin(y\pi/0.3) + \text{random}, \quad \text{for } i = 1, 2, 3 \tag{3-16}$$

The MSE sample means and standard deviations for each sensor synthesis method for the 30 simulated machining tests are shown in Table 3.2. For the GMDH method the polynomial selected by the RMS, unbiased and combined criteria provided the lowest MSE on the data for selecting the structure and parameters of the synthesis methods; this mean MSE is shown in Table 3.2. For the multi-layer perceptron training tolerances were implemented starting with a large tolerance (0.080 mm) where no significant training occurred and decreasing in increments of 0.001 mm until the network could not converge in 40,000 iterations through the training data set or within one hour of CPU time on a VAXstationII/RC. The multi-layer perceptron with two hidden layers each containing eight nodes with a 0.067 mm training tolerance provided the lowest MSE on the data for selecting the structure and parameters of the synthesis methods and was used for

		Wear Estimation Method	Mean of Mean Square Errors (mm^2) $MSE = \frac{1}{n}\sum_{i=1}^{n}(y_i - y_{ti})^2$	Standard Deviation of Mean Square Errors (mm^2)
Single Sensor Estimates		Simulated Force Model	4.87E-3	1.16E-3
		Simulated AE Model	5.66E-3	1.19E-3
		Simulated Temperature Model	5.25E-3	1.10E-3
Synthesized Estimates		Arithmetic Mean	3.62E-3	6.19E-4
	Methods Based on Training	Inverse Least Squares	1.48E-3	3.42E-4
		Multiple Regression	1.28E-3	2.98E-4
		GMDH	1.36E-3	3.97E-4
		Multi-Layer Perceptron 2 Hidden Layers, 8 Nodes/Hidden Layer, Training Tolerance = 0.067 mm	1.16E-3	2.71E-4
		Interpolation Network $\sigma = 0.029$	4.70E-3	1.38E-3
	Statistical Method	Approach Maximizing $\prod_{i=1}^{1} P_i(\theta/x_i)$ Bias Compensation, Thresholds $r_{ij} = 1.0$	1.46E-3	3.52E-4

Table 3.2 Comparison of Wear Estimates for Simulation Case 2
(Ideal sensor operation and inadequate process models)

comparison with the other synthesis methods. For the interpolation network values of the Gaussian function width, σ, ranging from 0.010 to 0.050 in increments of 0.001 were implemented. The network with $\sigma = 0.029$ provided the lowest MSE on the data used for selection of the structure and parameters of the synthesis methods. This network was used for comparison with the other synthesis methods. The results for the statistical method shown in Table 3.2 are for the specifications providing the lowest MSE on the data used

for selecting the structure and parameters of the synthesis methods. This statistical method attempts to maximize expression (3-10) with bias compensation and thresholds $r_{ij} = 1.0$.

In Figure 3.9 the mean MSEs of the three simulated model estimates are compared with the best performance provided by a synthesis method based on training and with the best performance provided by the statistical methods. Among the methods based on training the multi-layer perceptron provided the lowest mean MSE. Using a two sample *t* test, based on the the data shown in Figure 3.9 with at least 95% certainty the population mean MSEs provided by the multi-layer perceptron and by the statistical method were less than the lowest population mean MSE provided by using one of the simulated model wear estimates directly and less than the population mean MSE provided by using the arithmetic mean of the model wear estimates. With at least 95% certainty the population mean MSE provided by the multi-layer perceptron was less than the mean MSE provided by the statistical method.

The results from simulating this case indicate that when the deterministic component of the state variable estimates provided by the models do not accurately reflect the actual state variable a method based on training can more adequately account for these deterministic errors than a statistical method.

In simulation cases one and two for both multi-layer perceptron structures considered, an intermediate value of the training tolerance provided the lowest MSE on the data used for selection of the structure and parameters of the synthesis methods. This result indicates that the perceptron can overfit or underfit the data if the training tolerance is too small or too large, respectively. In simulation case one the sixteen hidden node network provided a somewhat lower MSE (MSE = 7.88E-4 mm^2) on the data used to select the network structure and parameters than the four hidden node network (MSE =

8.33E-4 mm^2); while the selected four hidden node network provided a somewhat lower mean MSE (MSE = 7.64E-4 mm^2) on the data used for comparison of the synthesis methods than the selected sixteen hidden node network (MSE = 8.09E-4 mm^2). In simulation case two the sixteen hidden node network provided a somewhat lower MSE on both the selection and comparison data (MSE = 1.38E-3 and MSE = 1.16E-3 mm^2, respectively) than the four hidden node network provided on the selection and comparison data (MSE = 1.40E-3 and MSE = 1.29E-3 mm^2, respectively). Because the MSEs provided by the two network structures were not significantly different it indicates that the network structures implemented were sufficiently complex for the data considered. However in simulation case two where the mapping between the wear estimates and actual wear was nonlinear, the sixteen hidden node network did provide a somewhat lower MSE than the four hidden node network on the data used for comparison of the synthesis methods. This result may indicate that the perceptron structure used must be sufficiently complex in order to obtain the lowest MSE.

In simulation cases one and two the multi-layer perceptron provided a lower sample mean MSE than the other synthesis methods based on training. The magnitude of this difference was greater in simulation case two where the relationship between the wear estimates provided by the models and the actual wear was nonlinear. The inverse least-squares and multiple regression techniques are based on a linear model of the relationship between the wear estimates provided by the models and the actual wear. The GMDH method is based on a high order polynomial model of the relationship between the inputs and outputs; however, a polynomial of an order high enough to closely approximate a nonlinear relationship will tend to be sensitive to random noise in the inputs to the polynomial. The multi-layer perceptron does not presuppose the form of the relationship between the network inputs and output, but rather learns this relationship based on the training data. In addition, the perceptron uses the sigmoid function as a processor at each

node in the network. This function is less sensitive to noise than a high-order polynomial.

The interpolation network in the form it was implemented in this work did not perform as well as the other sensor synthesis methods in simulation cases one and two. The performance of the interpolation network was also worse than the performance of the other methods in simulation cases three and four which are described in the following sections. The interpolation network as implemented in this work used the same value of the Gaussian function width, σ, at each of the input nodes. Implementing an algorithm

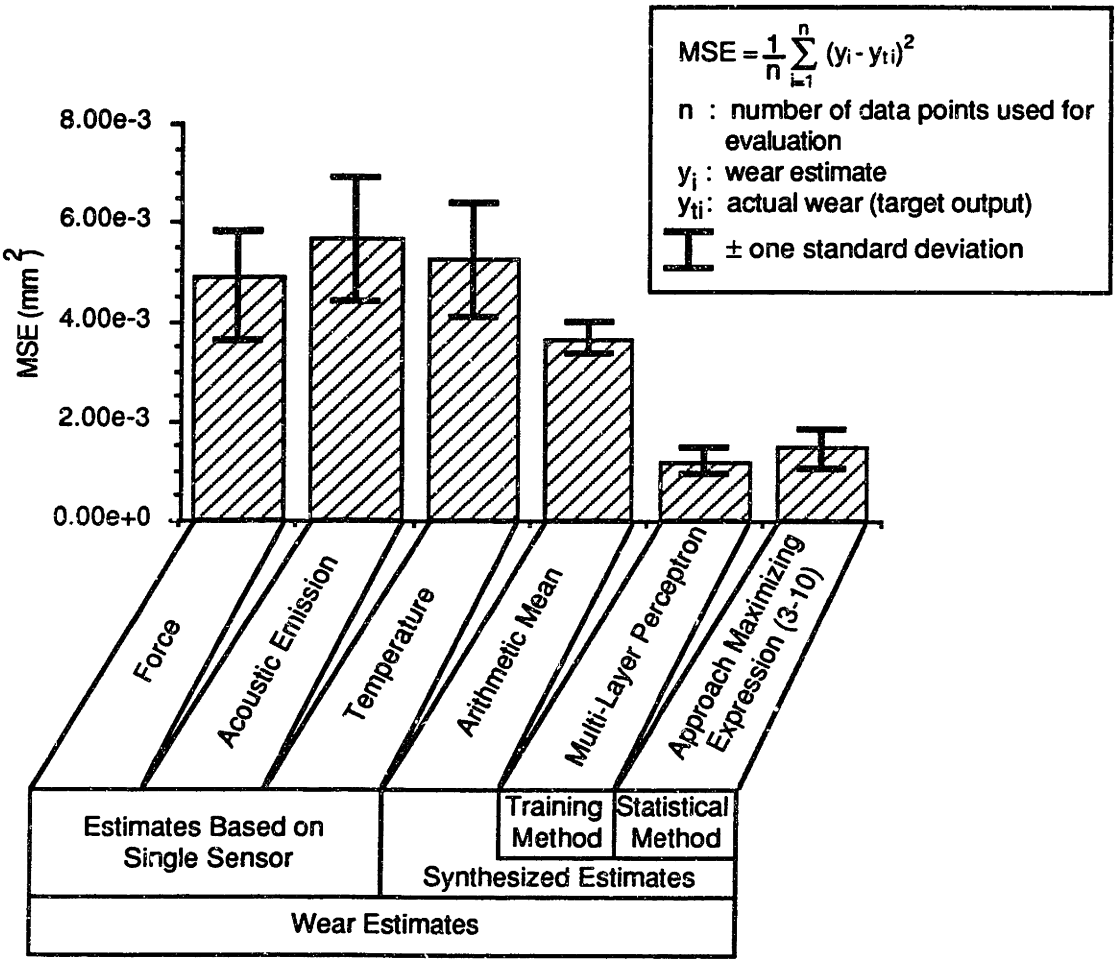

Figure 3.9 Evaluation of Best Wear Estimates for Simulation Case 2
(ideal sensor operation and inadequate process models)

where different values of σ can be learned for each of the input nodes during the training phase may improve the performance of this type of network.

Case 3: Inadequate sensor operation and ideal process models

In the third case considered, the process models adequately reflect the complexity of the process, but the tool or workpiece material properties change from one batch of material to the next or the behavior of the sensors drift from their characteristics at the time of calibration. In this case, the wear estimates provided by the models will show the same general trend as the development of the actual wear, but a deterministic error will develop between the estimates provided by the models and the actual wear. The purpose of simulating this situation was to study the robustness of the synthesis approaches with respect to variations in process conditions which can possibly occur in a machining operation.

Two simulations of this case were performed. In both of the simulations, the statistical method selected in simulation case one as indicated in Table 3.1 was used. The standard deviations determined from the training data in simulation case one were also used in the following simulations. For the methods based on training, the methods as trained in simulation case one (Table 3.1) were used. The sensor synthesis methods were used to predict the actual wear during 30 simulated machining tests based on wear estimates determined by the following relationship:

$$x_i = 1.5y + \text{random}, \quad \text{for } i = 1, 2, 3 \tag{3-17}$$

This relationship corresponds to an increase in the slope of the wear estimates with respect

to the actual wear described by the function used in the simulation of case 1. This change in slope was used to simulate the effect of changes in workpiece material properties or sensor drift on the wear estimates provided by the process models. For example, an increase in the workpiece material hardness might cause such an increase in the slope of the estimates. An increase in the workpiece hardness would tend to increase the magnitude of the sensor signals corresponding to a given level of tool wear. The errors in the tool wear estimates would tend to increase near the end of the tool life since the models described in Section 3.3.2 of this chapter attempt to adapt to the particular cutting conditions in the first call to the model when the tool is unworn. In the second simulation, the sensor synthesis methods were used to predict the actual wear during 30 simulated machining tests based on wear estimates determined from the following relationship:

$$x_i = 0.5y + \text{random}, \quad \text{for } i = 1, 2, 3 \tag{3-18}$$

This relationship corresponds to a decrease in the slope of the wear estimates with respect to the actual wear described by the function used in simulation one. If the increase in slope in expression (3-17) simulates the effect of an increase in the workpiece material hardness, a decrease in slope might be caused by a decrease in the workpiece material hardness.

For the first simulation, the sample means and standard deviations of the MSE for each sensor synthesis method are shown in Table 3.3a. In Table 3.3a and in all following simulations, only the structure and parameters selected in simulation case 1 as indicated in Table 3.1 were considered for the synthesis methods. For the second simulation, the MSE sample means and standard deviations for each synthesis method are shown in Table 3.3b.

For the first and second simulations Figures 3.10a and Figure 3.10b, respectively, compare the mean MSEs of the three simulated model estimates with the best performance

provided by a synthesis method based on training and with the best performance provided by he statistical methods. Among the methods based on training the multi-layer perceptron provided the lowest mean MSE in the first simulation while multiple regression provided the lowest mean MSE in the second simulation. Based on the data in Figures 3.10a and 3.10b, in both of the simulations with at least 95% certainty the population mean MSE provided by the best method based on training was less than the lowest population mean MSE provided by using one of the simulated model wear estimates directly and less than the population mean MSE provided by using the arithmetic mean of the model estimates. In both simulations with at least 95% certainty the population mean MSE provided by the statistical method was less than the lowest population mean MSE provided by using one of the simulated model wear estimates directly but was not less than the population mean MSE provided by using the arithmetic mean of the model estimates. In the first simulation, with at least 95% certainty the population mean MSE provided by the perceptron was less than the mean MSE provided by the statistical method. In the second simulation, with at least 95% certainty the population mean MSE provided by multiple regression was less than the mean MSE provided by the statistical method.

The results from the simulations of this case indicate that a method requiring a training phase is less sensitive than a statistical method to the types of errors in the model estimates which may be caused by variations in workpiece material properties or by sensor drift.

		Wear Estimation Method	Mean of Mean Square Errors (mm^2) $MSE = \frac{1}{n}\sum_{i=1}^{n}(y_i - y_{ti})^2$	Standard Deviation of Mean Square Errors (mm^2)
Single Sensor Estimates		Simulated Force Model	9.78E-3	1.48E-3
		Simulated AE Model	1.12E-2	1.79E-3
		Simulated Temperature Model	1.06E-2	1.17E-3
Synthesized Estimates		Arithmetic Mean	8.87E-3	6.89E-4
	Methods Based on Training	Inverse Least Squares	1.02E-2	7.01E-4
		Multiple Regression	8.33E-3	6.16E-4
		GMDH	9.10E-3	1.02E-3
		Multi-Layer Perceptron 2 Hidden Layers, 8 Nodes/Hidden Layer, Training Tolerance = 0.049 mm	2.69E-3	4.85E-4
		Interpolation Network $\sigma = 0.028$	1.95E-2	1.42E-3
	Statistical Method	Approach Maximizing $\prod_{i=1}^{1} P_i(\theta/x_i)$ No Bias Compensation, Thresholds $r_{ij} = 1.0$	8.95E-3	6.63E-4

Table 3.3a Comparison of Wear Estimates for Simulation Case 3
(Inadequate sensor operation and ideal process models, $x_i = 1.5y$ + random)

		Wear Estimation Method	Mean of Mean Square Errors (mm^2) $MSE = \frac{1}{n}\sum_{i=1}^{n}(y_i - y_{ti})^2$	Standard Deviation of Mean Square Errors (mm^2)
Single Sensor Estimates		Simulated Force Model	1.05E-2	1.42E-3
		Simulated AE Model	9.69E-3	1.49E-3
		Simulated Temperature Model	1.04E-2	1.30E-3
Synthesized Estimates		Arithmetic Mean	8.57E-3	6.31E-4
	Methods Based on Training	Inverse Least Squares	7.46E-3	5.43E-4
		Multiple Regression	6.93E-3	4.73E-4
		GMDH	7.50E-3	5.95E-4
		Multi-Layer Perceptron 2 Hidden Layers, 8 Nodes/Hidden Layer, Training Tolerance = 0.049 mm	7.02E-3	5.32E-4
		Interpolation Network $\sigma = 0.028$	1.39E-2	1.46E-3
	Statistical Method	Approach Maximizing $\prod_{i=1}^{1} P_i(\theta/x_i)$ No Bias Compensation, Thresholds $r_{ij} = 1.0$	8.59E-3	6.29E-4

Table 3.3b Comparison of Wear Estimates for Simulation Case 3
(Inadequate sensor operation and ideal process models, $x_i = 0.5y$ + random)

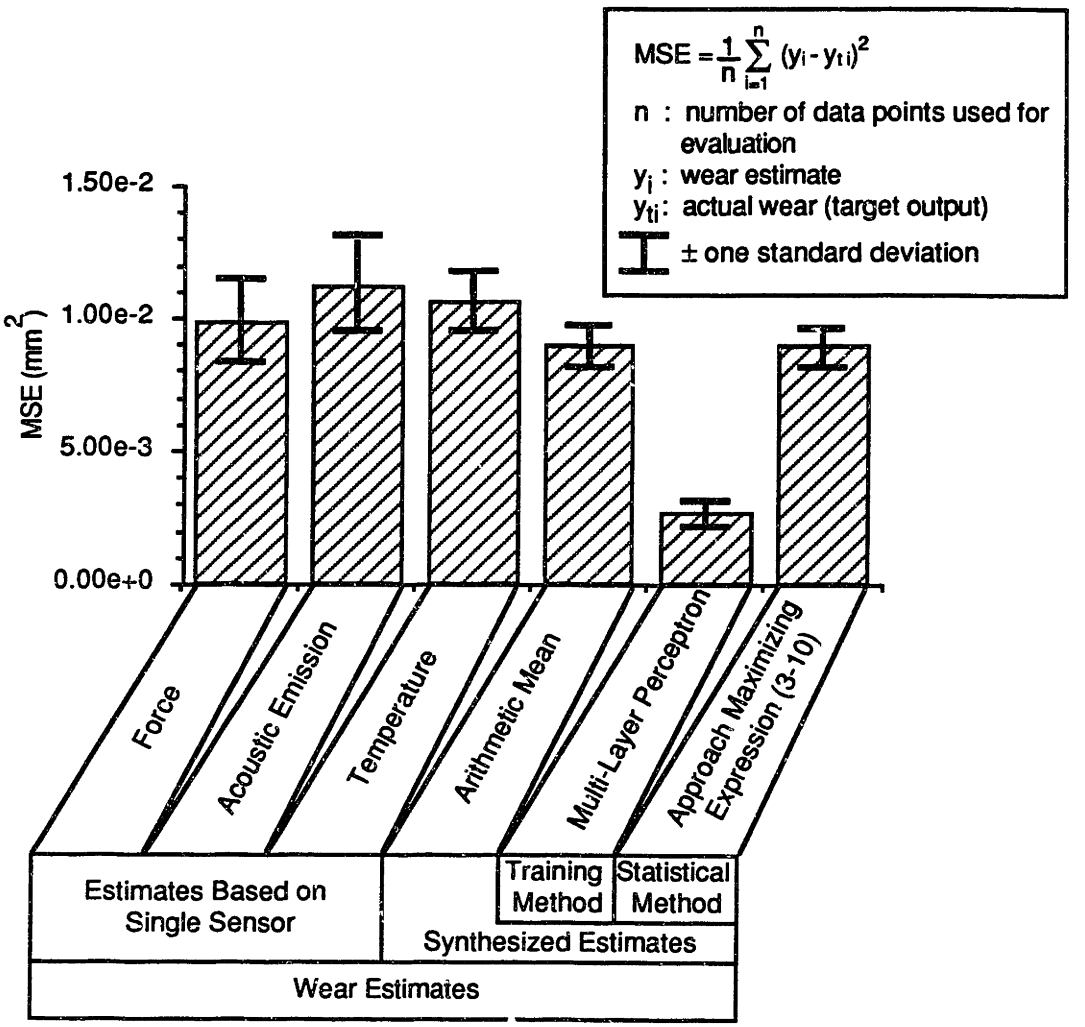

Figure 3.10a Evaluation of Best Wear Estimates for Simulation Case 3
(Inadequate sensor operation and ideal process models, $x_i = 1.5y + \text{random}$)

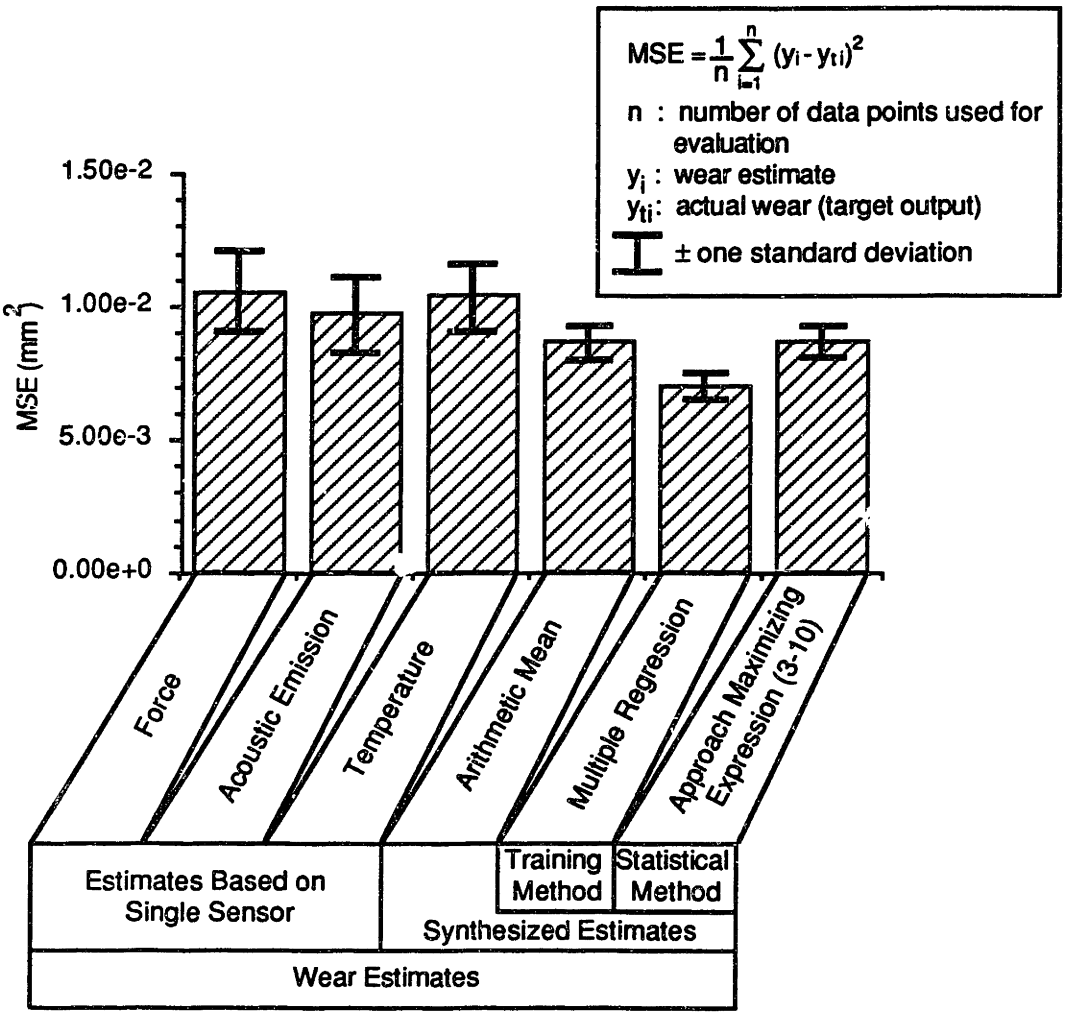

Figure 3.10b Evaluation of Best Wear Estimates for Simulation Case 3
(Inadequate sensor operation and ideal process models, $x_i = 0.5y + \text{random}$)

Case 4: Ideal process models and failure of one sensor

In the final case considered, the process models adequately reflect the complexity of the process, however one of the sensors fails. In this case, the wear estimates provided by one of the models will not contain any information which is useful for the prediction of the actual wear. The purpose of simulating this situation was to evaluate the robustness of the synthesis methods to the failure of one of the sensors.

Three simulations reflecting this case were performed. For all three simulations, the statistical method selected in simulation case one as indicated in Table 3.1 was used. The statistical method used the standard deviations determined from the training data in simulation case one. For the methods based on training, the methods as trained in simulation case one (Table 3.1) were used. In the simulations the sensor synthesis methods were used to estimate the actual wear during 30 simulated machining tests based on wear estimates determined using the following relationship:

$$x_j = \text{random, for } j = 1, 2 \text{ and } 3 \text{ in simulations 1, 2, and 3, respectively}$$
$$x_i = y + \text{random, for } i \neq j \text{ (i.e. } i = 2,3 \text{ in simulation 1)} \qquad (3\text{-}19)$$

The simulated model wear estimates x_i correspond to the same estimates used in case one. The wear estimate x_j, however, is a random number which contains no information about the actual wear, y. The estimates x_j are used to simulate the wear estimates provided by a model when the corresponding sensor fails. For each sensor synthesis method, the MSE sample mean and standard deviation for the 30 simulated machining tests where the first, second and third wear estimates "fail" are shown in Tables 3.4a, 3.4b and 3.4c, respectively.

		Wear Estimation Method	Mean of Mean Square Errors (mm^2) $MSE = \frac{1}{n}\sum_{i=1}^{n}(y_i - y_{ti})^2$	Standard Deviation of Mean Square Errors (mm^2)
Single Sensor Estimates		Simulated Force Model	3.46E-2	2.62E-3
		Simulated AE Model	2.55E-3	6.73E-4
		Simulated Temperature Model	2.59E-3	5.58E-4
Synthesized Estimates		Arithmetic Mean	4.24E-3	4.36E-4
	Methods Based on Training	Inverse Least Squares	2.89E-3	3.35E-4
		Multiple Regression	2.79E-3	3.00E-4
		GMDH	1.31E-3	3.07E-4
		Multi-Layer Perceptron 2 Hidden Layers, 8 Nodes/Hidden Layer, Training Tolerance = 0.049 mm	2.35E-3	2.68E-4
		Interpolation Network $\sigma = 0.028$	2.43E-2	1.13E-3
	Statistical Method	Approach Maximizing $\prod_{i=1}^{1} P_i(\theta/x_i)$ No Bias Compensation, Thresholds $r_{ij} = 1.0$	2.72E-3	4.07E-4
		Approach Maximizing $\prod_{i=1}^{1} P_i(\theta/x_i)$ No Bias Compensation, Thresholds $r_{ij} = 0.95$	2.41E-3	6.63E-4

Table 3.4a Comparison of Wear Estimates for Simulation Case 4
(Ideal process models and failure of force sensor)

		Wear Estimation Method	Mean of Mean Square Errors (mm^2) $MSE = \frac{1}{n}\sum_{i=1}^{n}(y_i - y_{ti})^2$	Standard Deviation of Mean Square Errors (mm^2)
Single Sensor Estimates		Simulated Force Model	2.29E-3	6.74E-4
		Simulated AE Model	3.26E-2	2.92E-3
		Simulated Temperature Model	2.59E-3	5.58E-4
Synthesized Estimates		Arithmetic Mean	4.24E-3	4.35E-4
	Methods Based on Training	Inverse Least Squares	2.60E-3	3.18E-4
		Multiple Regression	2.53E-3	2.86E-4
		GMDH	2.02E-3	5.84E-4
		Multi-Layer Perceptron 2 Hidden Layers, 8 Nodes/Hidden Layer, Training Tolerance = 0.049 mm	2.62E-3	2.88E-4
		Interpolation Network $\sigma = 0.028$	2.11E-2	1.30E-3
	Statistical Method	Approach Maximizing $\prod_{i=1}^{1} P_i(\theta/x_i)$ No Bias Compensation, Thresholds $r_{ij} = 1.0$	3.81E-3	4.55E-4
		Approach Maximizing $\prod_{i=1}^{1} P_i(\theta/x_i)$ No Bias Compensation, Thresholds $r_{ij} = 0.95$	2.29E-3	5.49E-4

Table 3.4b Comparison of Wear Estimates for Simulation Case 4
(Ideal process models and failure of acoustic emission sensor)

		Wear Estimation Method	Mean of Mean Square Errors (mm^2) $MSE = \frac{1}{n}\sum_{i=1}^{n}(y_i - y_{ti})^2$	Standard Deviation of Mean Square Errors (mm^2)
Single Sensor Estimates		Simulated Force Model	2.29E-3	6.74E-4
		Simulated AE Model	2.55E-3	6.73E-4
		Simulated Temperature Model	3.39E-2	2.35E-3
Synthesized Estimates		Arithmetic Mean	4.24E-3	4.35E-4
	Methods Based on Training	Inverse Least Squares	5.53E-3	4.65E-4
		Multiple Regression	5.19E-3	4.07E-4
		GMDH	6.38E-3	8.88E-4
		Multi-Layer Perceptron 2 Hidden Layers, 8 Nodes/Hidden Layer, Training Tolerance = 0.049 mm	5.86E-3	4.82E-4
		Interpolation Network $\sigma = 0.028$	2.69E-2	1.04E-3
	Statistical Method	Approach Maximizing $\prod_{i=1}^{1} P_i(\theta/x_i)$ No Bias Compensation, Thresholds $r_{ij} = 1.0$	6.08E-3	7.41E-4
		Approach Maximizing $\prod_{i=1}^{1} P_i(\theta/x_i)$ No Bias Compensation, Thresholds $r_{ij} = 0.95$	5.99E-3	2.50E-3

Table 3.4c Comparison of Wear Estimates for Simulation Case 4
(Ideal process models and failure of temperature sensor)

Among the methods based on training the GMDH method provided the lowest mean MSE in the first and second simulations and multiple regression provided the lowest mean MSE in the third. From the results in Tables 3.4a, 3.4b and 3.4c it cannot be conclusively determined that one of the methods based on training is less sensitive than the others to the "failure" of one of the sensors.

In Tables 3.4a, 3.4b and 3.4c the results are shown for the statistical method where the thresholds have been reduced from $r_{ij} = 1.0$ to $r_{ij} = 0.95$. This reduction of the value for the thresholds reduced the mean MSE provided by this method primarily because the lower value for the thresholds tends to eliminate the failed sensor from the consensus group of sensors used in the sensor synthesis.

For the first, second and third simulations Figures 3.11a, 3.11b and 3.11c, respectively, compare the mean MSEs of the three simulated model estimates with the best performance provided by a synthesis method based on training and with the best performance provided by the statistical methods (with thresholds $r_{ij} = 0.95$). Based on the data shown in these figures, with at least 95% certainty in all three simulations the population mean MSE for the best method based on training and for the statistical method was less than the mean MSE provided by using the failed wear estimates directly. In all three simulations with at least 95% certainty the best method based on training provided a lower population mean MSE than the statistical method.

The results from the simulations of this case indicate that a method based on training may be less sensitive to the failure of one of the sensors than a statistical method. The multi-layer perceptron has often been considered as a method which is robust with respect to noisy and incomplete information [11, 16, 46, 73, 96]; however, the results of the simulations indicate that approaches could be investigated for making the multi-layer

perceptron more "fault tolerant". One approach may be to include some data where each of the sensors had failed in the training data set.

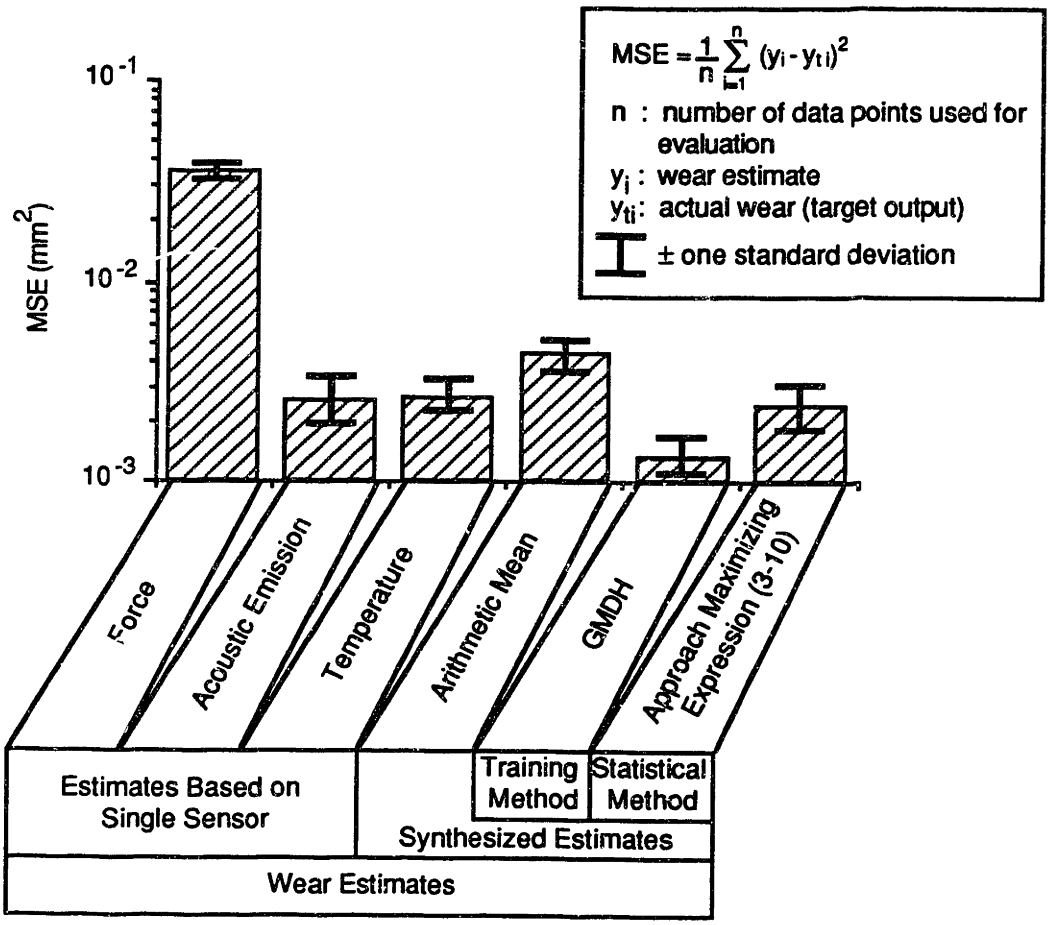

Figure 3.11a Evaluation of Best Wear Estimates for Simulation Case 4
(Ideal process models and failure of force sensor)

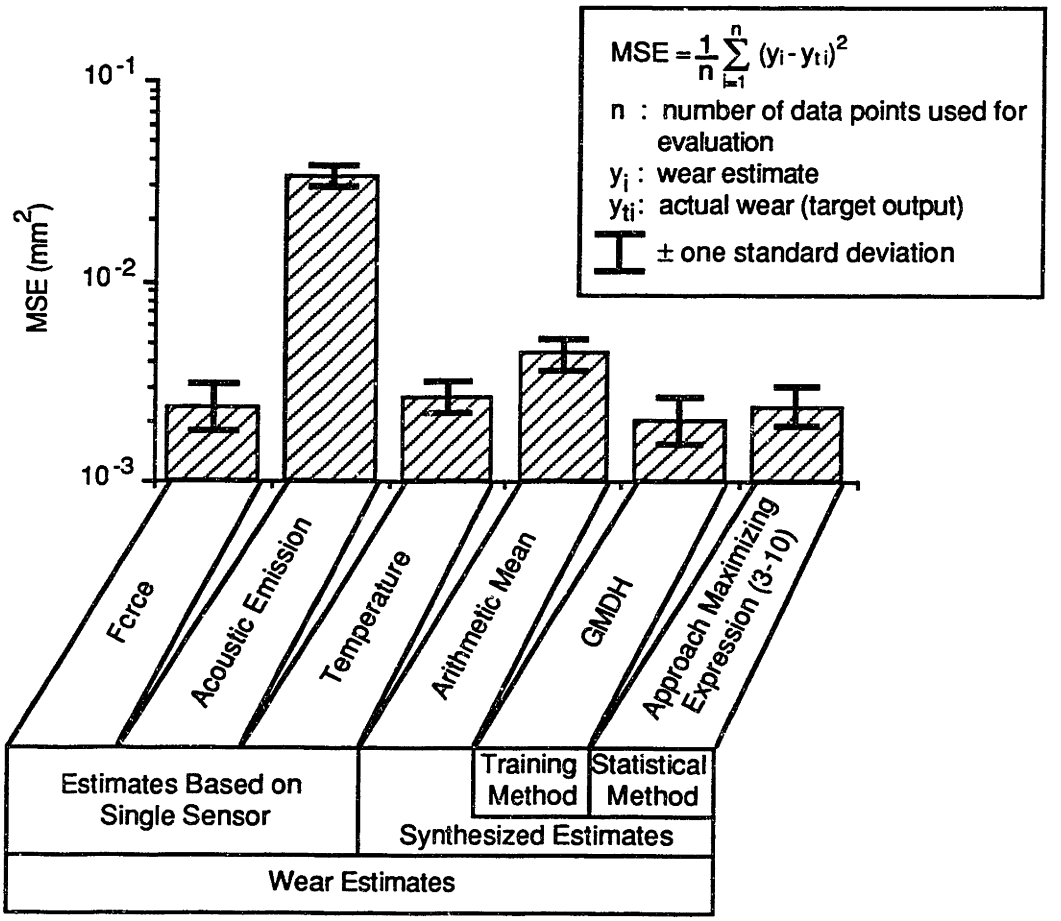

Figure 3.11b Evaluation of Best Wear Estimates for Simulation Case 4
(Ideal process models and failure of acoustic emission sensor)

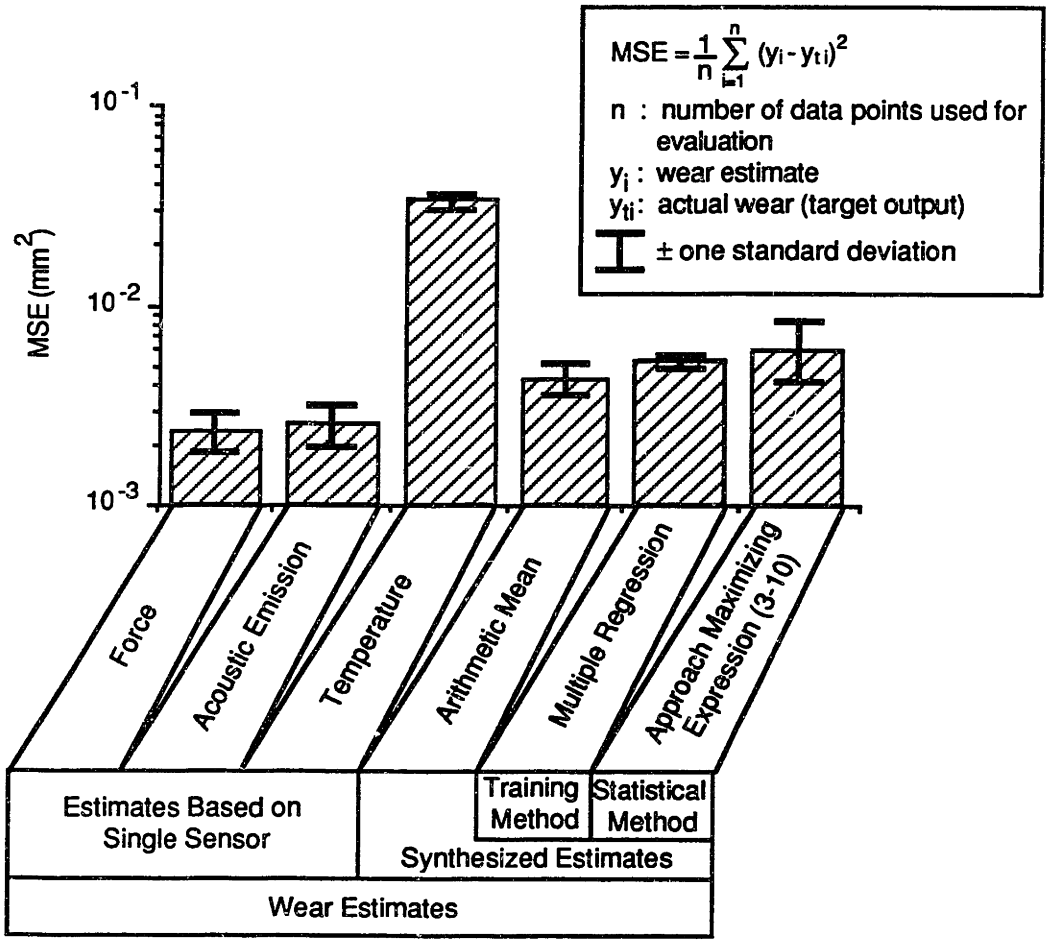

Figure 3.11c Evaluation of Best Wear Estimates for Simulation Case 4
(Ideal process models and failure of temperature sensor)

3.3.2 Experimentation

In order to experimentally evaluate and compare the sensor synthesis methods, a series of turning operations were performed during which force, temperature and acoustic emission (AE) sensor signals corresponding to measured values of tool wear were recorded. These variables are relatively easy to measure and a significant body of knowledge exists about them and their correlation with machining conditions. The sensor signals were fed into independent process models which estimated the tool wear during the turning operations based on each of the three types of sensor signals (Figure 3.12).

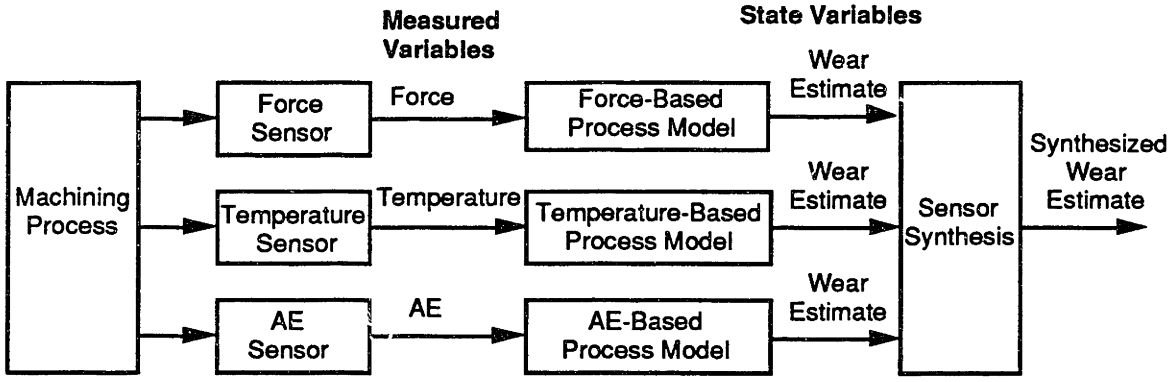

Figure 3.12 Wear Estimate Based on Multiple Sensor Synthesis

In the following section the force, temperature and acoustic emission based process models which were used in this work will be described. Methods will then be presented for establishing the probability density functions necessary for implementing the statistical approach to sensor synthesis. Next, the use of designed experiments in order to obtain the maximum amount of information for training the methods based on training from the fewest number of experiments will be discussed. Finally, the experimental procedure which was implemented will be described and the results of the experimental comparison of the sensor synthesis methods will be discussed.

Process modelling for sensor synthesis

During a turning process, the decision-making approach or an adaptive control approach operates the process by changing machine settings such as the speed and feed. Therefore it is essential that the process models are capable of estimating the tool wear during the process even as the machine settings are changed. In general, both tool wear and changes in the machine tool settings will affect process monitoring signals such as vibration, cutting forces, and tool temperature. The models presented in this section attempt to account for changes in the signal due to changes in the machine tool settings so that the models are adequate for wear monitoring in the context of an in-process operation scheme.

The geometry of the three-dimensional turning process is complex. In addition the behavior of the process is the product of a complex interaction between several physical phenomena. A model which attempted to reflect all of these phenomena in detail would require an unreasonably long time to evaluate, particularly in the context of in-process control. The objective of sensor synthesis is to use process models which may not adequately reflect the process behavior when considered individually, however, in combination they may provide sufficient information to provide a reasonable estimate of the tool wear. Consequently, the models presented below attempt to reflect only the general trends of the process behavior and do not include complex descriptions of the process geometry or the interactions between the physical phenomena occurring during the process.

Force-based turning process model

The force-based process model considers measurements of the cutting force along the cutting (horizontal) and feed (vertical) directions (Figure 3.13). The model utilizes fundamental physical relationships from the areas of tribology and applied mechanics, and can be used for a wide variety of cutting conditions [29].

As suggested by several researchers, the normal pressure distribution on the rake face (Figure 3.14) is assumed to be exponential [3,115,126]

$$P_r = P_1[1-(s/L_R)^k] \tag{3-20}$$

where

P_r = pressure distribution on the rake face

P_1 = maximum normal pressure on the rake face

s = distance from the cutting edge along the rake face

L_R = contact length between the chip and the tool on the rake face

k = exponent for the normal pressure distribution on the rake face

From the theory of plasticity, it is assumed that the maximum normal pressure on the rake face can be determined as [17]

$$P_1 = 2\,\tau_s\,(1.3 - \alpha) \tag{3-21}$$

where

τ_s = shear strength of the workpiece material

α = rake angle

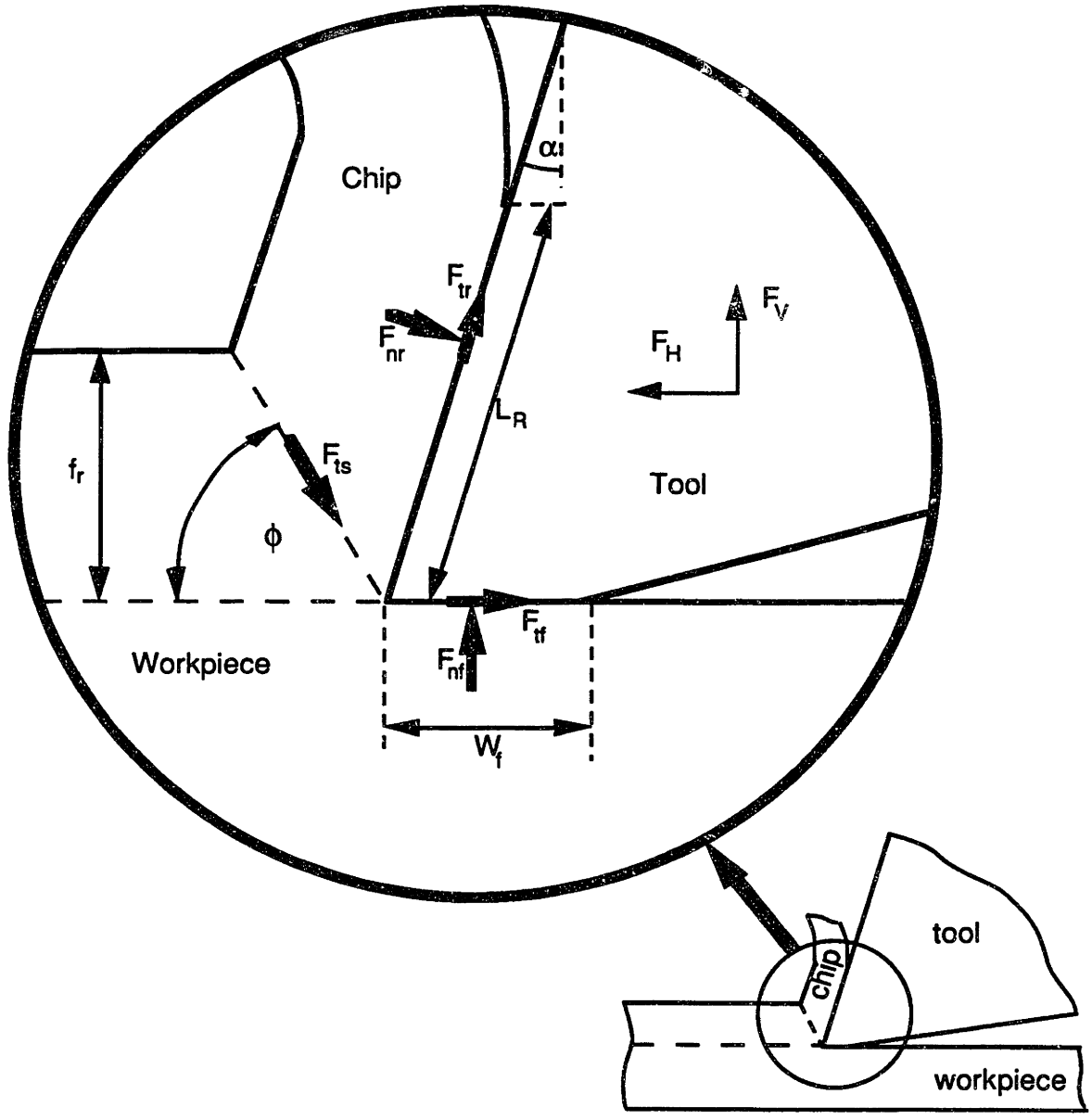

Figure 3.13 Forces in Cutting

(F_H = measured force component along horizontal axis, F_V = measured force component along vertical axis, F_{nf} = normal force on the flank face, F_{nr} = normal force on the rake face, F_{tf} = tangential force on the flank face, F_{tr} = tangential force on the rake face, F_{ts} = tangential force along shear plane, f_r = feed, L_R = contact length between the chip and the tool on the rake face, W_f = length of flank wear land, α = rake angle, ϕ = shear angle)

Based on published experimental data [126] the contact length between the chip and tool on the rake face is assumed to be a function of the feed as expressed in the following relationship.

$$L_R = C_4 f_r^{3/4} \tag{3-22}$$

where

f_r = feed

C_4 is a constant of proportionality.

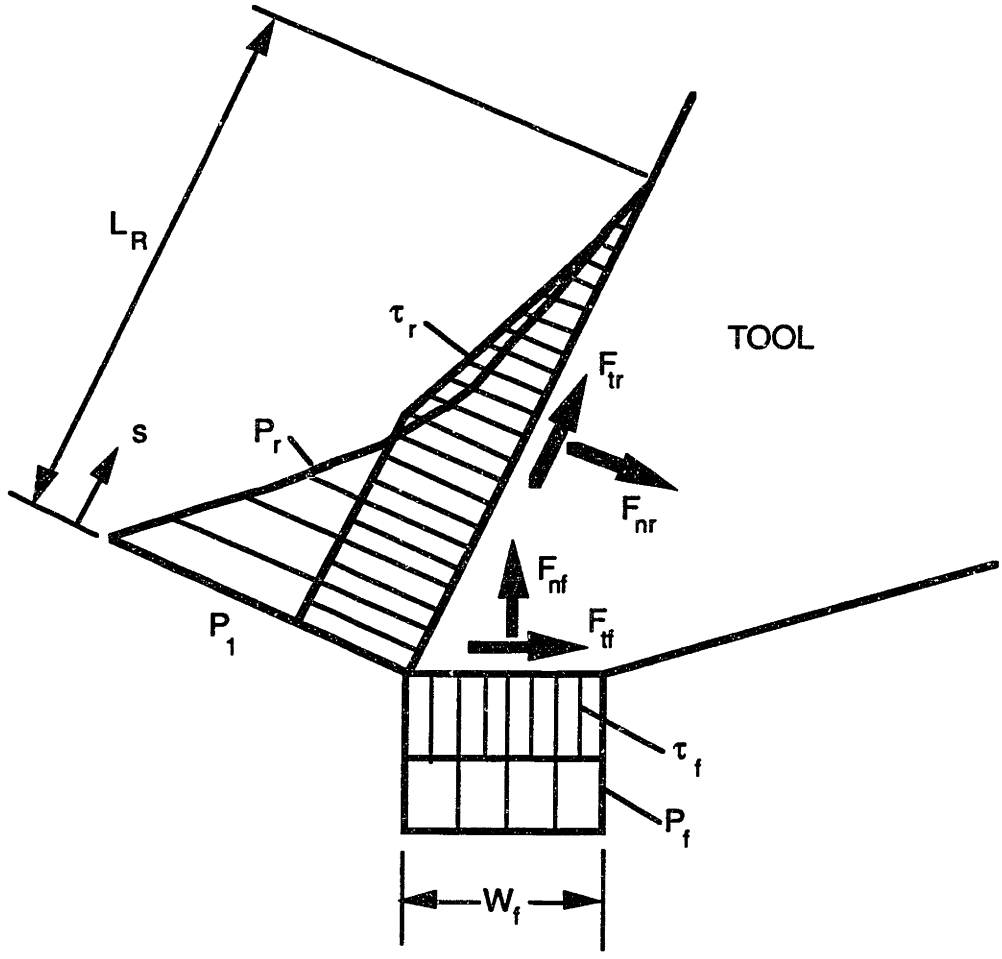

Figure 3.14 Pressure and Shear Stress Distributions

Integrating the normal pressure distribution over the contact area between the chip and the rake face provides the following expression for the normal force on the rake face.

$$F_{nr} = d\, P_1\, L_R \left[\frac{k}{k+1}\right] \tag{3-23}$$

where

F_{nr} = normal force component on the rake face

d = depth of cut

The shear stress distribution on both the rake and flank faces of the tool is assumed to be related with the corresponding normal pressure distributions according to the following expressions [13,48,100,107,114].

$$\tau = \mu\, P \qquad \text{for} \qquad P < \tau_s/\mu \tag{3-24}$$

$$\tau = \tau_s \qquad \text{for} \qquad P \geq \tau_s/\mu$$

where

τ = shear stress on the tool face

μ = friction coefficient between the workpiece material and the tool

P = pressure on the tool face

Integrating the resulting shear stress distribution over the rake face yields

$$F_{tr} = d\, L_R \left[\tau_s\, L_{st} + \mu\, P_1 \left[\frac{k}{k+1} - L_{st} + \frac{L_{st}^{k+1}}{k+1}\right]\right] \tag{3-25}$$

where

$$L_{st} = \left[1 - \frac{\tau_s}{\mu P_1} \right]^{1/k} \qquad \text{for } P_1 \geq \tau_s/\mu$$

$$L_{st} = 0 \qquad \text{for } P_1 < \tau_s/\mu$$

F_{tr} = tangential force component on the rake face

L_{st} = length of the sticking region on the rake face

It is assumed that over the entire flank face of the tool the normal pressure between the tool and workpiece exceeds the critical pressure at which the workpiece material sticks to the flank face. The shear stress on the flank face is therefore assumed to be equal to the shear strength of the workpiece material. Integrating this shear stress over the flank face yields

$$F_{tf} = \tau_s \, d \, W_f \qquad (3\text{-}26)$$

where

F_{tf} = tangential force component on the flank face

W_f = length of flank wear land

The chip is assumed to be sheared along a shear plane. Based on this assumption the tangential force along the shear plane can be determined as

$$F_{ts} = \tau_s \, A_s \qquad (3\text{-}27)$$

where

F_{ts} = tangential force component along the shear plane

A_s = shear plane area

The area of the shear plane is calculated as

$$A_s = df_r/\sin(\phi) \tag{3-28}$$

where

ϕ = shear angle

The chip above the shear plane is assumed to behave as a rigid body and thus the forces exerted on the chip the by the tool and through the shear plane can be equated along a direction parallel to the shear plane.

$$F_{ts} = F_{nr} \cos(\alpha - \phi) - F_{tr} \sin(\alpha - \phi) \tag{3-29}$$

It is assumed that the force components on the rake and flank faces of the tool do not directly influence each other and thus can be equated with the measured force components along the horizontal and vertical axes according to the following expressions (Figure 3.13).

$$F_H = \cos(\alpha) F_{nr} + \sin(\alpha) F_{tr} + F_{tf} \tag{3-30a}$$

$$F_V = \sin(\alpha) F_{nr} - \cos(\alpha) F_{tr} - F_{nf} \tag{3-30b}$$

where

F_H = measured force component along the horizontal axis

F_V = measured force component along the horizontal axis

F_{nf} = normal force component on the flank face

The force-based model operates in two stages: first a procedure is followed for identifying the shear angle, ϕ, coefficient of friction, μ, and a constant C_4 based on the initial measured cutting forces (Figure 3.15a). This initial procedure is executed in order to adapt the model to the particular process conditions. Following this initial stage, the model

is used to estimate the tool wear during the remainder of the process (Figure 3.15b).

In step ① (Figure 3.15a) of the initial identification procedure, the tangential and normal components on the tool rake face, F_{nr} and F_{tr}, are determined based on the measured cutting force components in the horizontal and vertical directions F_H, F_V (Figure 3.13). In this step the tool is considered to be unworn with the flank wear $W_f = 0$, and the force components on the flank face of the tool, F_{tf} and F_{nf}, equal to zero. Based on the values of F_{nr} and F_{tr}, the shear angle, ϕ, is estimated in step ② (Figure 3.15a) of the procedure. In step ③ the maximum pressure between the chip and tool rake face is estimated. Using this maximum pressure, the contact length between the chip and tool on the rake face is estimated in step ④. From the estimated contact length, the coefficient C_4, which relates the contact length with the feed, is identified in step ⑤. In step ⑥ two equations are solved iteratively in order to determine the coefficient of friction, μ, between the tool and workpiece materials. It is assumed that the values for the parameters identified in the first pass through the model remain constant for the remainder of the tool life. In the initial identification procedure it is assumed that the parameter k, which is the exponent for the exponential pressure distribution used to model the normal pressure on the rake face of the tool, has a nominal value of 0.333. This initial value for k is based on equating normal forces on the rake face determined using the assumed exponential pressure distribution with normal forces found experimentally [17,115,125] and with normal forces predicted by an analysis of the pressure distribution found between a beam supported on an elastic surface (the chip supported by the rake face of the tool). These forces were equated on the basis of an equivalent maximum normal pressure and an equivalent contact length between the chip and rake face.

In the second stage of the model operation (Figure 3.15b) the maximum pressure between the chip and tool on the rake face is estimated in step ①. In step ②, the total

length of contact between the chip and the tool on the rake face is estimated. In step ③, four equations are solved iteratively in order to estimate the tangential and normal components of the force on the rake face of the tool, F_{nr} and F_{tr}. During the solution of these equations in step three the value of the parameter k is reidentified. In step ④, the estimated force components on the rake face of the tool as well as the measured force component in the horizontal direction (Figure 3.13) are used to identify the tangential component of the force on the flank face of the tool, F_{tf}. This force component is used in step ⑤ to estimate the flank wear, W_f.

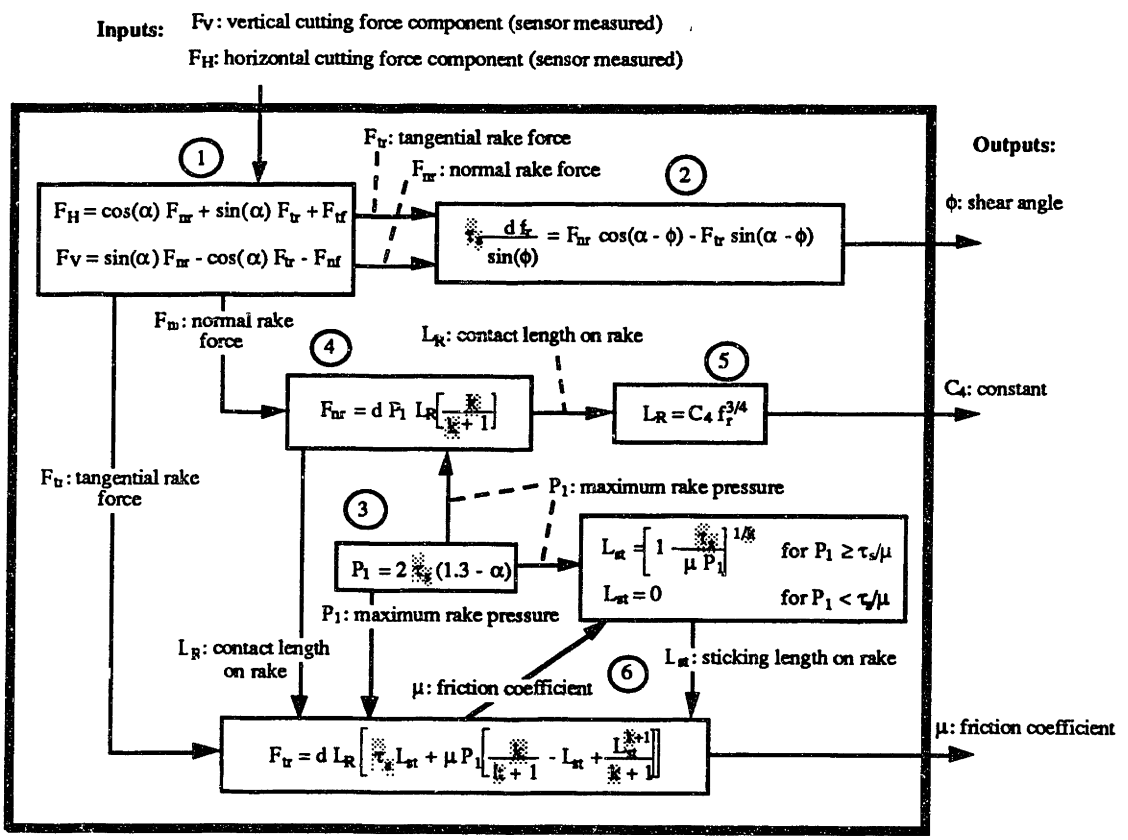

Figure 3.15a Procedure for Force-Based Model Operation: Identification of Shear Angle, ϕ, Friction Coefficient, μ, and Constant C_4. (Numbers in circles indicate the sequence of the procedure steps; Uncertain model parameters (shaded) are workpiece shear strength, τ_s, and initial value of the exponent k)

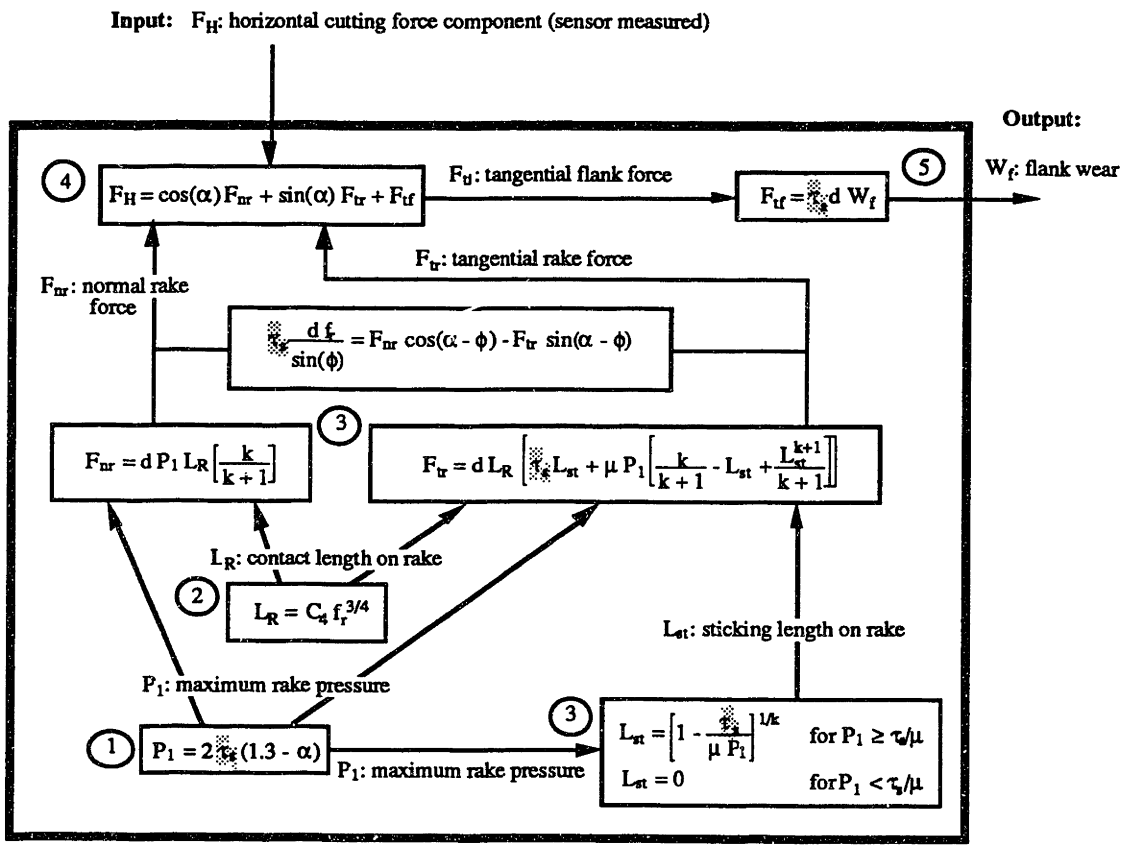

Figure 3.15b Procedure for Force-Based Model Operation: Estimation of Tool Wear. (Numbers in circles indicate the sequence of the procedure steps; Uncertain model parameter (shaded) is workpiece shear strength, τ_S)

Acoustic emission-based turning process model

The form of the acoustic emission model utilized was developed in Chapter 2.

$$RMS = C_1 v^m \left[F_{ts} \frac{\cos[\alpha]}{\cos[\phi-\alpha]} + F_{tr} \frac{\sin[\phi]}{\cos[\phi-\alpha]} + F_{tf} \right]^n \qquad (3\text{-}31)$$

where

RMS = root mean square of the AE signal

C_1 = proportionality constant which takes into account factors such as amplifier gains and attenuation coefficients

v = cutting speed

n, m = constant exponents

The AE model operates in two stages: first a procedure is followed for identifying an attenuation coefficient, C_1, in order to adapt the AE model to the particular process conditions (Figure 3.16a). The model is then used to estimate the tool wear during the remainder of the process (Figure 3.16b).

Steps ①, ② and ③ in the first stage of the AE-based model operation (Figure 3.16a) are similar to steps ①, ② and ③ in the second stage of the force-based model operation (Figure 3.15b). In the first stage of the AE model operation the tool is considered to be unworn with the flank wear $W_f = 0$, and the tangential force component on the flank face of the tool F_{tf} equal to zero. The tangential shear force and tangential rake face force components determined in the first three steps are used to determine the attenuation coefficient, C_1, in step ④.

In the second stage of the AE-based model operation (Figure 3.16b), steps ①, ② and ③ are similar to steps ①, ② and ③ in the second stage of the force-based model operation (Figure 3.15b). The tangential shear force and tangential rake face force components determined in these three steps are used to determine the tangential flank force component, F_{tf}, in step ④. Based on this force component, the flank wear is calculated in step ⑤.

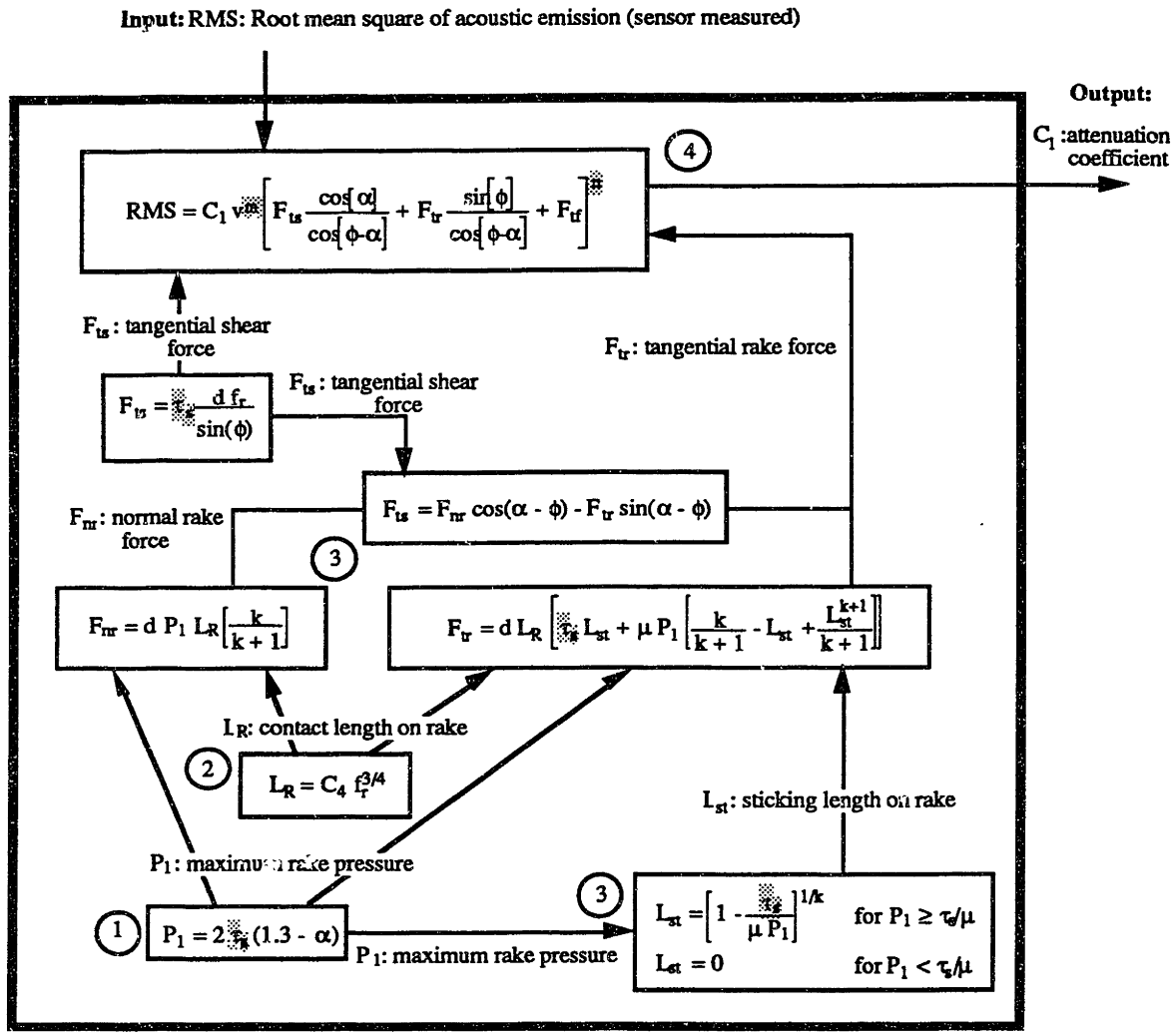

Figure 3.16a Procedure for Acoustic-Emission Based Model Operation: Identification of Attenuation Coefficient C_1. (Numbers in circles indicate the sequence of the procedure steps; Uncertain model parameters (shaded) are workpiece shear strength, τ_S, and exponents m and n)

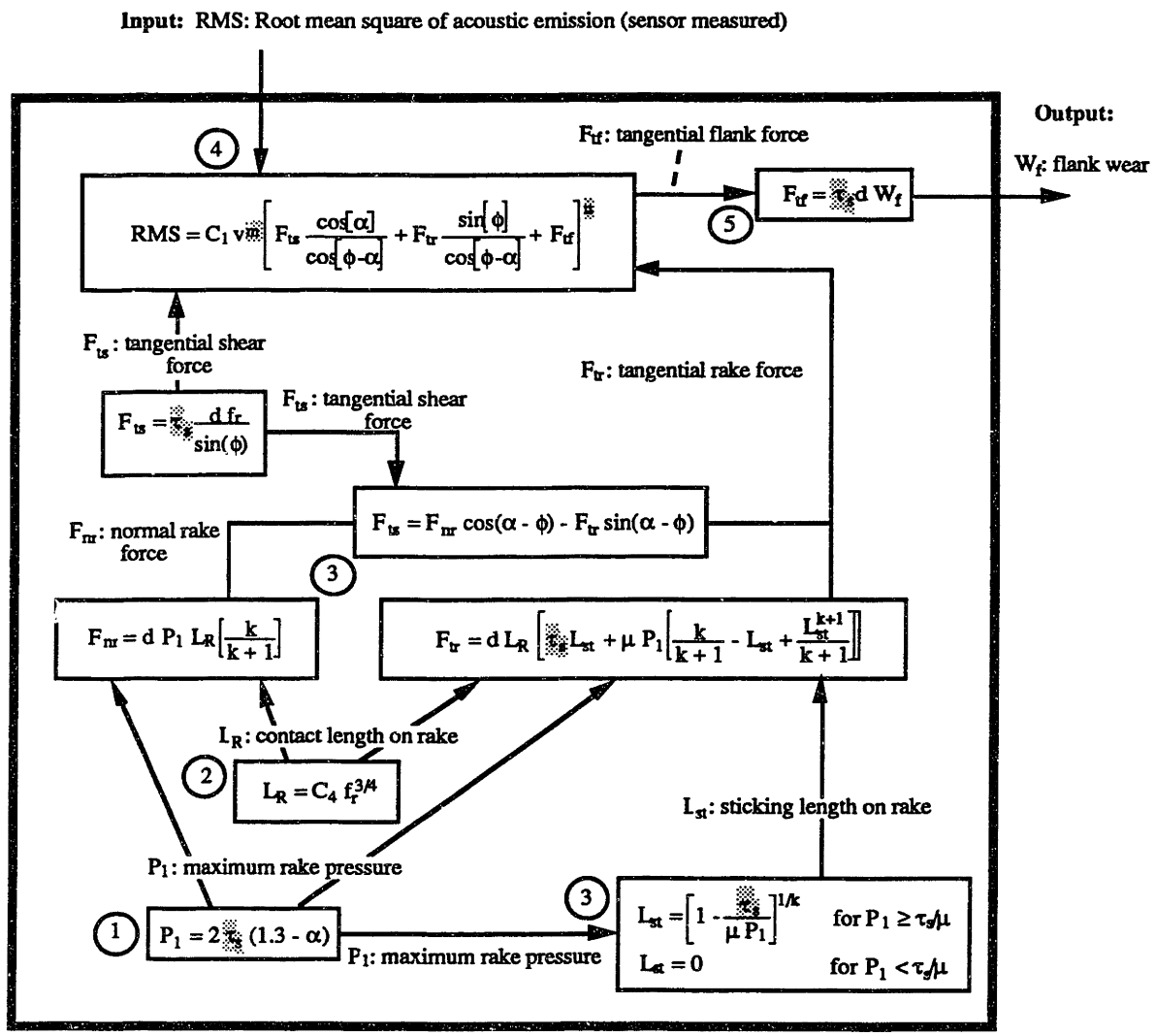

Figure 3.16b Procedure for Acoustic-Emission Based Model Operation: Estimation of Tool Wear. (Numbers in circles indicate the sequence of the procedure steps; Uncertain model parameters (shaded) are workpiece shear strength, τ_S, and exponents m and n)

Temperature-based turning process model

The temperature-based model utilizes relationships which correlate the tool wear rate with the measured tool temperature. At least three mechanisms are known to contribute to the development of flank wear; abrasion, adhesion and diffusion. In general it is believed that adhesion and abrasion, which are mechanically activated mechanisms, are the

major contributors to flank wear during the early stages of cutting while diffusion, which is a thermally activated mechanism, dominates later in the process when the temperature on the flank face of the tool is higher. One of the simplest wear rate models developed was presented by Koren and Lenz [62]. This model assumes that abrasion and diffusion are the dominant wear mechanisms. The flank wear rate is separated into a component cause by abrasion, $\dot{W}_{f1}$, and a component caused by diffusion, $\dot{W}_{f2}$.

$$\dot{W}_{f1} = \left[\frac{v}{l_o}\right]\left[K_1 \cos(\alpha) \frac{F_H}{f_r d} - W_{f1}\right] \tag{3-32}$$

$$\dot{W}_{f2} = K_2 \sqrt{v} \exp\left[\frac{-K_3}{273 + \theta_f}\right] \tag{3-33}$$

where

l_o = constant

K_1, K_2, K_3 = constants

θ_f is the measured flank temperature which may be approximated by the temperature measured by the tool/workpiece thermocouple method.

The total wear rate is then

$$\dot{W}_f = \dot{W}_{f1} + \dot{W}_{f2} \tag{3-34}$$

In step ① of the temperature-based model operation (Figure 3.17), the diffusive wear rate is determined based on the measured temperature. In step ② the tangential force component on the flank face of the tool, F_{tf}, is calculated based on the previous estimate of the flank wear. Steps ③, ④ and ⑤ in the operation of the temperature model (Figure 3.17) are similar to steps ①, ② and ③ in the second stage of the force-based model operation (Figure 3.15b) and are used to estimate the normal and tangential force

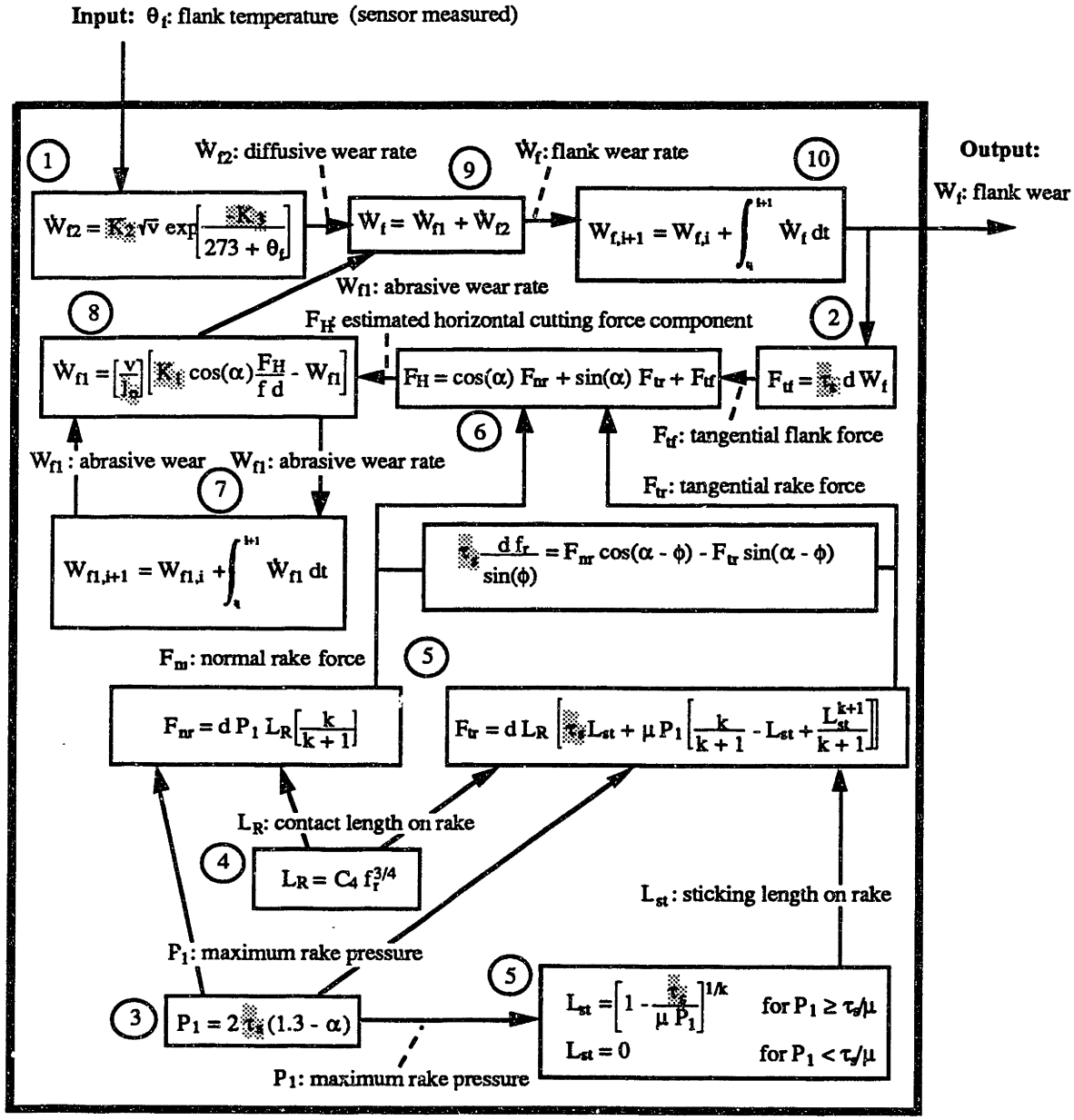

Figure 3.17 Procedure for Temperature-Based Model Operation: Estimation of Tool Wear. (Numbers in circles indicate the sequence of the procedure steps; Uncertain model parameters (shaded) are workpiece shear strength, τ_s, and the constants K_1, K_2, K_3 and l_o)

components on the rake face of the tool. In step ⑥ these force components and the tangential force component determined in step ② are used to estimate the horizontal cutting force component, F_H. The abrasive wear rate estimated during the previous iteration through the model is integrated with respect to time in step ⑦ in order to estimate the current level of abrasive wear. Based on this value of the abrasive wear and the estimated value of F_H the abrasive wear rate is calculated in step ⑧. The total wear rate is determined in step ⑨ by adding the abrasive and diffusive wear rate components. In step ⑩ the wear rate is integrated with respect to time to determine the flank wear.

Establishment of probability density functions for statistical synthesis

In order to implement the statistical approach to sensor synthesis discussed in Section 3.2.2 probability density functions, $P_i(x_i)$, must be established. Given an estimate of a state variable, x_i, this density function describes the probability that the actual value of the state variable, x, is in a certain range (Figure 3.6). These distributions could be established by performing special experiments similar to those required for the synthesis methods based on training. In this case, sensor signals recorded during training experiments can be fed into the models. The state variable estimates provided by the models are subtracted from the actual measured values for the state variable in order to establish histograms for the uncertainty in the estimates provided by each model (Figure 3.18a). The histograms are then normalized in order to determine probability density functions for the uncertainty. During the operation of the process (Figure 3.18b) the probability density functions for the uncertainty in the state variable can be added to the corresponding nominal estimates for the state variable provided by each model in order to determine probability density functions for the state variable. Statistical sensor synthesis can then be performed using the probability density functions for the state variable.

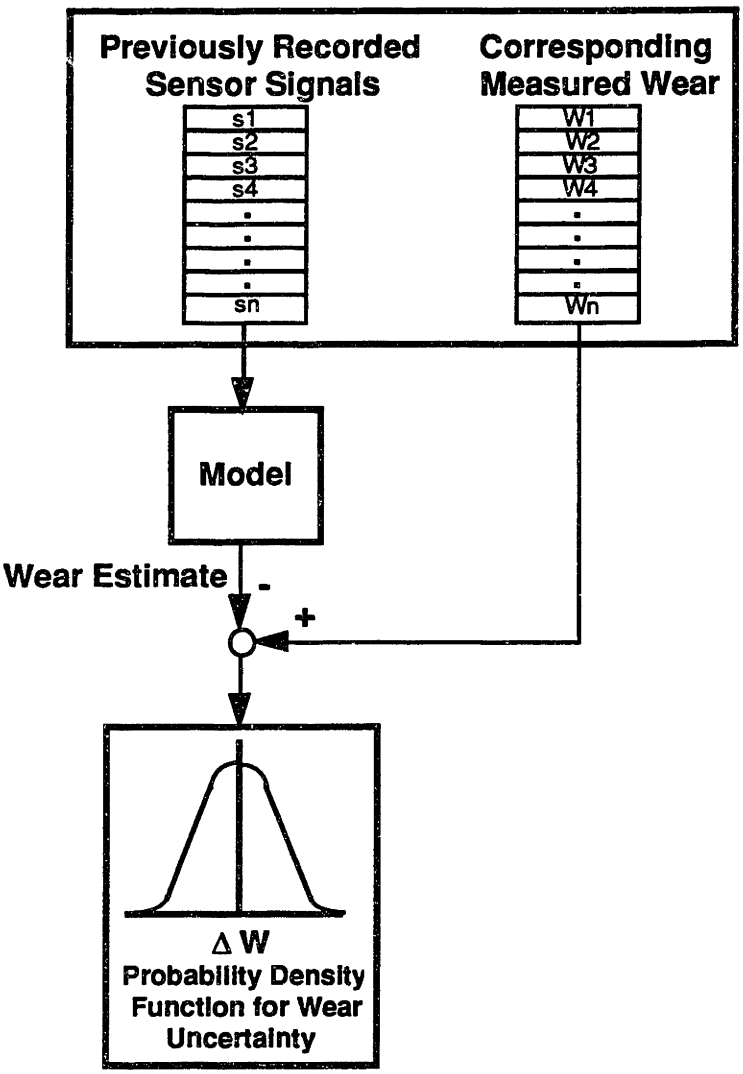

Figure 3.18a Determination of Probability Density Function for Wear Uncertainty Using Previously Recorded Data

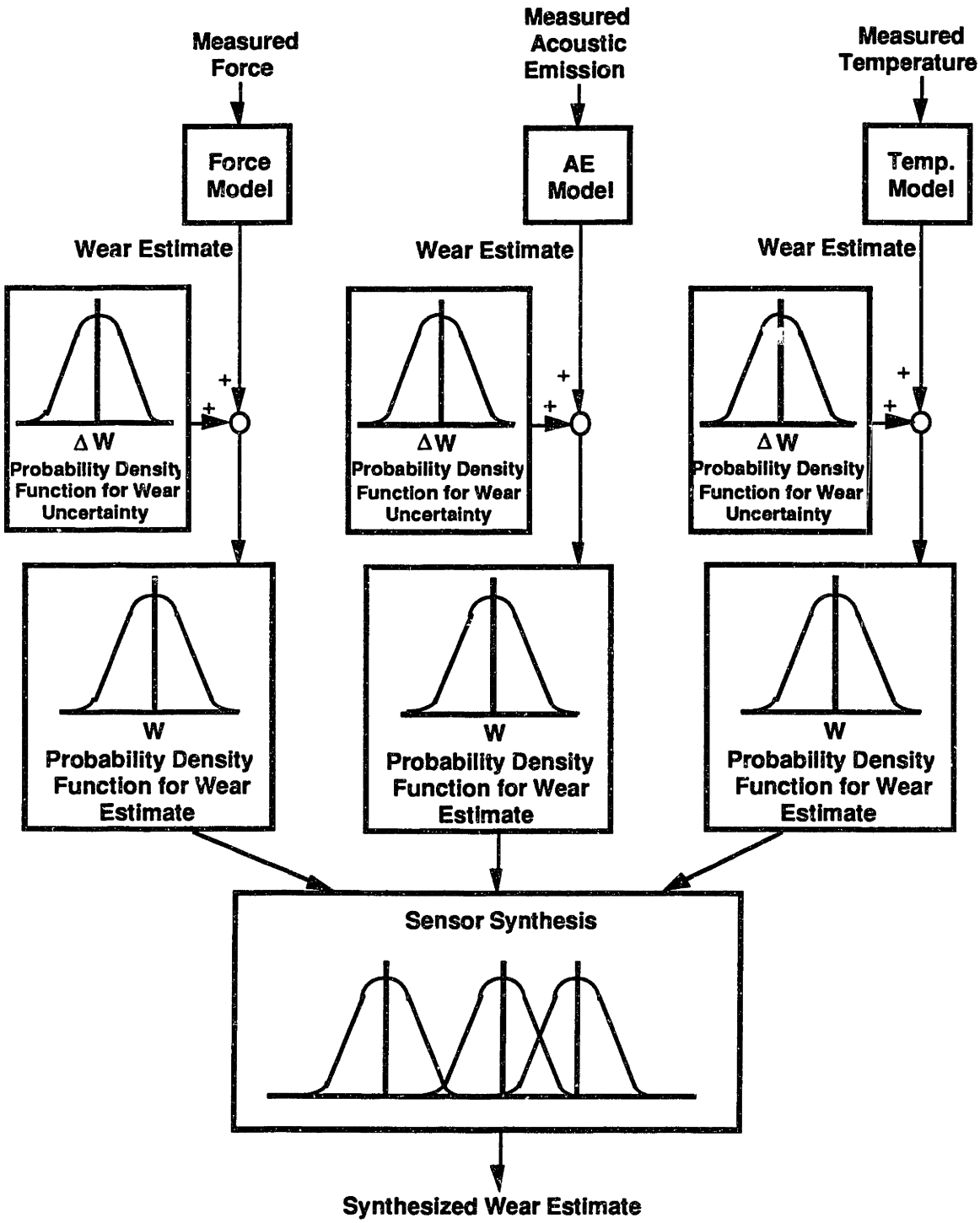

Figure 3.18b Statistical Sensor Synthesis Using Probability Density Functions Determined from Previously Recorded Data

It may be impractical to run experiments to obtain training data whenever process conditions, such as the workpiece material, are changed. Additionally, in some processes it may not be possible to measure the state variable which is to be estimated even during special experiments; in this case a set of training data cannot be established. As an alternative to an approach based on training data, a method is presented below for obtaining the distributions, $P_i(x_i)$, in-process through evaluation of process models which are based on a physical understanding of the process. Because this method can be implemented without extensive pre-process experimentation, it may have a significant advantage over synthesis methods requiring training.

Given accurate values for the sensor signals a process model may not provide correct estimates of a state variable because of *parametric* uncertainty. *Parametric* uncertainties occur when the correct values of *constants*, such as material properties, utilized in a process model are somewhat uncertain. To illustrate this type of uncertainty, the models of the machining process presented in Figures 3.15 through 3.17 can be considered. The values used for the shear strength τ_s, exponents k, m and n and the constants K_1, K_2, K_3 and l_o may not reflect the actual values for these parameters. In particular, such inaccuracies may occur if the tool or workpiece material properties change or if a wide range of cutting conditions are utilized. In the method presented below for determining the probability density functions $P_i(x_i)$, the assumption is made that the uncertainty in the state estimates is due to the physical constants used in the models.

When determining the probability density functions in-process, each time a synthesized estimate for the wear must be determined the probability density function, $P_i(x_i)$, is re-evaluated for each model (Figure 3.19). The models are provided with values for the uncertain model parameters which in this thesis were randomly selected according to a Gaussian distributions which are centered on the nominal value for each parameter. A set

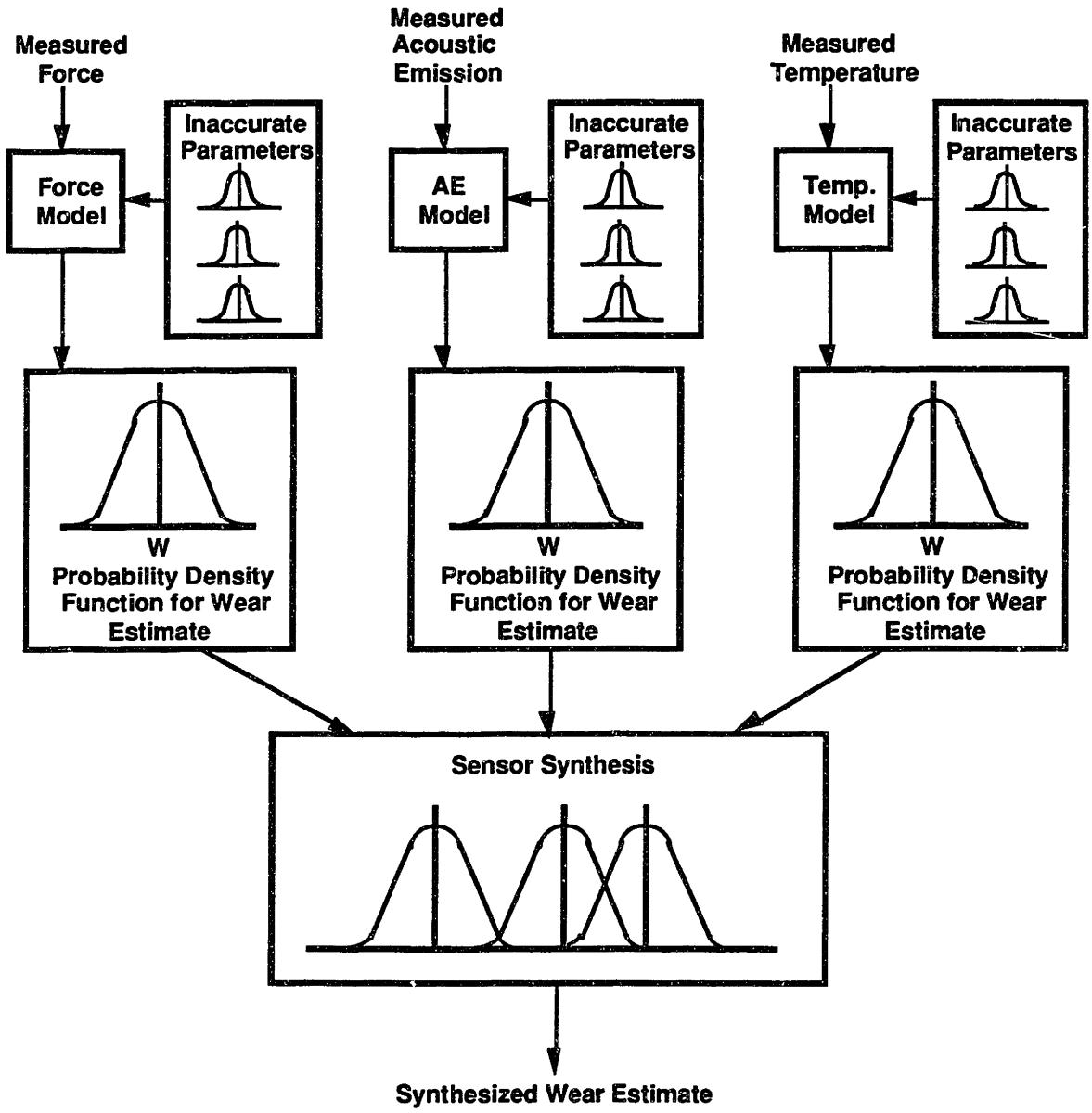

Figure 3.19 Statistical Sensor Synthesis Using Probability Density Functions Determined In-Process

of estimates for the state variable corresponding to different randomly selected values of the uncertain model parameters are determined based on the current values of the sensor measurements. For each model, these estimates are accumulated in the form of a histogram

which is then normalized in order to obtain the corresponding probability density function, $P_i(x_i)$.

The synthesized state variable estimate can be determined relatively easily using expressions (3-11 to 3-13) presented in Section 3.2.2 if the density functions, $P_i(x_i)$, can be assumed to have a Gaussian form. The biases and standard deviations of the state variable estimates provided by the process models must be determined in order to implement these solutions for the synthesized estimate; the probability density functions themselves need not be determined. When determining the biases and standard deviations based on training data, the mean of the differences between the estimates given by the models and the actual measured state variable is considered as the bias, and the standard deviation of these differences is considered as the standard deviation for the probability density function, $P_i(x_i)$, in expressions (3-11 to 3-13). When determining the biases and standard deviations in-process, every time a synthesized estimate must be determined a set of estimates for each model corresponding to different randomly selected values of the uncertain model parameters are determined based on the current values of the sensor measurements. The standard deviation for each of these sets of wear estimates is considered as the standard deviation for the corresponding probability density function, $P_i(x_i)$. The means for each of the sets of wear estimates rather than the nominal estimates (where all the uncertain parameters are set at their nominal values) are synthesized. Therefore to implement the solutions given in expressions (3-11 to 3-13) the biases are determined by subtracting the mean wear estimates from the nominal estimates. If the density functions cannot be assumed to be Gaussian then the solutions for the synthesized state estimate presented in Section 3.2.2 are not applicable and more elaborate solutions must be developed.

Statistical design of experiments for sensor synthesis methods requiring training

A manufacturing process may be operated using a wide range of workpiece materials, geometries of the tooling and values of process input settings such as speed and feed. In an effort to optimize the process, a controller may specify in-process variations of the controlled input variables over a wide range of values. Therefore a synthesis method which uses a mechanism based on training must be trained to adequately synthesize the variable estimates for a wide range of process conditions. If a method is trained for a wide variety of process conditions the method will likely perform adequately for conditions within the range and for conditions somewhat outside of the range of conditions for which the method has been trained.

For most manufacturing processes the experiments necessary to obtain data for training are time consuming and expensive. Therefore it is desirable to obtain the most information for training from the fewest number of experiments. In experimental design, the input settings for the experiment are usually referred to as factors. These factors are considered at several discrete levels over the range for which the factor is to be varied. In a full factorial design an experiment is run for every possible combination of the levels for each of the factors. This type of design ensures that the process characteristics throughout the entire range of experimental conditions are reflected in the recorded data; however, this approach requires an unreasonable number of experiments to be performed even when considering only a few factors and a small number of levels for each factor.

An alternative to a full factorial design is to specify the conditions for each experiment according to an orthogonal array [95,104]. In general, an orthogonal array requires a much smaller number of experiments to be performed than a full factorial design.

In the array each column corresponds to a factor to be varied and the rows of values in the array specify the levels of the factors for each experiment. An orthogonal array can be determined by eliminating experiments from a full factorial design while maintaining that for any pair of columns all combinations of the factor levels must occur and they must occur an equal number of times. This property ensures that the effect of one factor on the variables measured during the experiments is not coupled with a particular value for any of the other factors. Orthogonal arrays can be used to design experiments to obtain training data for any variety of variables specifying the process conditions, including workpiece and tooling material as well as input variables such as speeds and feeds. In addition, the arrays can accommodate any number of materials or levels for the input variables.

A turning process can be considered as an example of the application of an orthogonal array for experimental design. A large variety of tool and workpiece materials can be utilized in a turning process. In addition, many different values can be selected for variables such as the feed, cutting speed, width of cut, tool rake angle and tool relief angle. Ideally, a synthesis method should be comprehensively trained over the full range of conditions which may occur in a turning operation so that the method will provide adequate synthesized estimates of the tool wear and wear rate for any typical turning process. If five classifications are considered for the workpiece material, tool material, speed, feed, rake angle, clearance angle, machining time and width of cut, a full factorial experimental design would require 390625 experiments. In contrast, the number of tool and workpiece materials and levels for the other factors listed above can be accommodated in an orthogonal array of 8 factors with 5 levels for each of the factors which specifies 125 experiments.

As shown by the above example, statistical design of experiments can greatly reduce the number of experiments needed to obtain training data for any manufacturing

process. In the example, the number of experiments was reduced by a factor of 3125 from the number required by a full factorial experimental design. Utilizing an orthogonal array rather than a full factorial design for obtaining training data may reduce the accuracy of the training for some of the operating conditions of a manufacturing process. However, by maintaining that for any pair of columns all combinations of the factor levels must occur and they must occur an equal number of times, an orthogonal array ensures that the specified experiments are well distributed throughout the operating conditions for the process.

Experimental procedure and apparatus

In order to complete the experiments used to evaluate the synthesis methods in a reasonable amount of time the wide range of tool and workpiece materials which can be considered for any turning operation were limited to HSS M2 for the tool and SAE 4340 steel for the workpiece. Appropriate ranges for the feed, cutting speed and depth of cut were selected according to recommended conditions for these tool and workpiece materials [80]. In the experimental design used for obtaining data for the methods requiring training, nine levels were considered for the factors of feed and speed, and three levels were considered for the factors of rake angle, relief angle and depth of cut. The orthogonal array which describes the experiments performed for obtaining the training data is shown in Table 3.5. Each experiment consisted of machining for an incremental tool travel distance of 1.0 inch as measured axially along the workpiece. After each experiment, the flank wear was measured under a microscope before proceeding with the next experiment. The tool travel distance was kept constant for each experiment in order that the increase in tool wear during each experiment would be similar regardless of the speed and feed utilized. As indicated in Table 3.5, a machining test was defined as 9 consecutive experiments; a new tool was used at the beginning of each test.

Test	Experiment	Rake Angle (degrees)	Relief Angle (degrees)	Tool Travel Distance (m)	Feed Rate (mm/rev)	Cutting Speed (m/min)	Depth of Cut (mm)
1	1	0	2	0.025	0.102	9.14	0.508
	2	0	2	0.051	0.279	17.68	0.508
	3	0	2	0.076	0.152	11.58	0.508
	4	0	2	0.102	0.305	18.90	0.762
	5	0	2	0.127	0.127	10.36	0.762
	6	0	2	0.152	0.229	15.24	0.762
	7	0	2	0.178	0.178	12.80	1.016
	8	0	2	0.203	0.254	16.46	1.016
	9	0	2	0.229	0.203	14.02	1.016
2	1	0	7	0.025	0.203	16.46	1.016
	2	0	7	0.051	0.102	14.02	1.016
	3	0	7	0.076	0.279	9.14	1.016
	4	0	7	0.102	0.152	17.68	0.508
	5	0	7	0.127	0.305	11.58	0.508
	6	0	7	0.152	0.127	18.90	0.508
	7	0	7	0.178	0.229	10.36	0.762
	8	0	7	0.203	0.178	15.24	0.762
	9	0	7	0.229	0.254	12.80	0.762
3	1	0	12	0.025	0.254	15.24	0.762
	2	0	12	0.051	0.203	12.80	0.762
	3	0	12	0.076	0.102	16.46	0.762
	4	0	12	0.102	0.279	14.02	1.016
	5	0	12	0.127	0.152	9.14	1.016
	6	0	12	0.152	0.305	17.68	1.016
	7	0	12	0.178	0.127	11.58	0.508
	8	0	12	0.203	0.229	18.90	0.508
	9	0	12	0.229	0.178	10.36	0.508
4	1	7.5	2	0.025	0.178	18.90	0.508
	2	7.5	2	0.051	0.254	10.36	0.508
	3	7.5	2	0.076	0.203	15.24	0.508
	4	7.5	2	0.102	0.102	12.80	0.762
	5	7.5	2	0.127	0.279	16.46	0.762
	6	7.5	2	0.152	0.152	14.02	0.762
	7	7.5	2	0.178	0.305	9.14	1.016
	8	7.5	2	0.203	0.127	17.68	1.016
	9	7.5	2	0.229	0.229	11.58	1.016
5	1	7.5	7	0.025	0.229	17.68	1.016
	2	7.5	7	0.051	0.178	11.58	1.016
	3	7.5	7	0.076	0.254	18.90	1.016
	4	7.5	7	0.102	0.203	10.36	0.508
	5	7.5	7	0.127	0.102	15.24	0.508
	6	7.5	7	0.152	0.279	12.80	0.508
	7	7.5	7	0.178	0.152	16.46	0.762
	8	7.5	7	0.203	0.305	14.02	0.762
	9	7.5	7	0.229	0.127	9.14	0.762

Table 3.5 Orthogonal Array Specifying Experiments for Obtaining Training Data

(continued on next page)

Test	Experiment	Rake Angle (degrees)	Relief Angle (degrees)	Tool Travel Distance (m)	Feed Rate (mm/rev)	Cutting Speed (m/min)	Depth of Cut (mm)
6	1	7.5	12	0.025	0.127	14.02	0.762
	2	7.5	12	0.051	0.229	9.14	0.762
	3	7.5	12	0.076	0.178	17.68	0.762
	4	7.5	12	0.102	0.254	11.58	1.016
	5	7.5	12	0.127	0.203	18.90	1.016
	6	7.5	12	0.152	0.102	10.36	1.016
	7	7.5	12	0.178	0.279	15.24	0.508
	8	7.5	12	0.203	0.152	12.80	0.508
	9	7.5	12	0.229	0.305	16.46	0.508
7	1	15	2	0.025	0.305	12.80	0.508
	2	15	2	0.051	0.127	16.46	0.508
	3	15	2	0.076	0.229	14.02	0.508
	4	15	2	0.102	0.178	9.14	0.762
	5	15	2	0.127	0.254	17.68	0.762
	6	15	2	0.152	0.203	11.58	0.762
	7	15	2	0.178	0.102	18.90	1.016
	8	15	2	0.203	0.279	10.36	1.016
	9	15	2	0.229	0.152	15.24	1.016
8	1	15	7	0.025	0.152	10.36	1.016
	2	15	7	0.051	0.305	15.24	1.016
	3	15	7	0.076	0.127	12.80	1.016
	4	15	7	0.102	0.229	16.46	0.508
	5	15	7	0.127	0.178	14.02	0.508
	6	15	7	0.152	0.254	9.14	0.508
	7	15	7	0.178	0.203	17.68	0.762
	8	15	7	0.203	0.102	11.58	0.762
	9	15	7	0.229	0.279	18.90	0.762
9	1	15	12	0.025	0.279	11.58	0.762
	2	15	12	0.051	0.152	18.90	0.762
	3	15	12	0.076	0.305	10.36	0.762
	4	15	12	0.102	0.127	15.24	1.016
	5	15	12	0.127	0.229	12.80	1.016
	6	15	12	0.152	0.178	16.46	1.016
	7	15	12	0.178	0.254	14.02	0.508
	8	15	12	0.203	0.203	9.14	0.508
	9	15	12	0.229	0.102	17.68	0.508

Table 3.5 Orthogonal Array Specifying Experiments for Obtaining Training Data
(continued from previous page)

Turning was performed on a Daewoo Puma10 CNC lathe with 20 HP maximum spindle power. The tool holder was equipped for measuring the cutting forces along three orthogonal axes (Figure 3.20). The tool-workpiece thermocouple method was used for measuring the temperature at the tool-workpiece interface. An insulating guard attached to the tool holder was used to prevent the chip from making contact with the workpiece after leaving the tool face. A physical acoustics WD wideband transducer mounted on the tool holder was used to detect the AE signal. The signal from the AE transducer was preamplified using a Physical Acoustics 1220A preamplifier and then amplified by a Physical Acoustics AE1A postamplifier for a total gain of 40 db. The AE signal was highpass filtered with a 50 KHz cutoff frequency in order to remove components due to machine vibration and other low-frequency noise from the signal. An Analog Devices AD636 true RMS to dc converter chip was used to determine the RMS of the AE signal. The RMS signal was then lowpass filtered with a cutoff frequency of 1.59 Hz in order to remove high-frequency components from the RMS AE signal associated with chip breaking. All sensor signals were recorded using a Compaq Deskpro 286 computer with a Data Translation DT2801 data acquisition board. For all the tool wear tests, M2 HSS tools by Enco Mfg. were used and SAE 4340 steel cylinders were used as the workpiece material.

The sensor-based models were used to estimate the wear during each experiment specified by the orthogonal array in Table 3.5 based on the corresponding sensor signals which were recorded. For these computations the parameter shear strength, τ_s, in the models was assigned a typical value (Table 3.6) found in materials handbooks, parameter k was assigned the value 0.333 for the reasons given in the description of the force-based model, the parameters m and n in the acoustic-emission model were assigned values reflecting those given in Chapter 2 for steel machined with a HSS tool, and the parameters K_1, K_2, K_3 and l_o in the temperature-based model were assigned values reflecting those

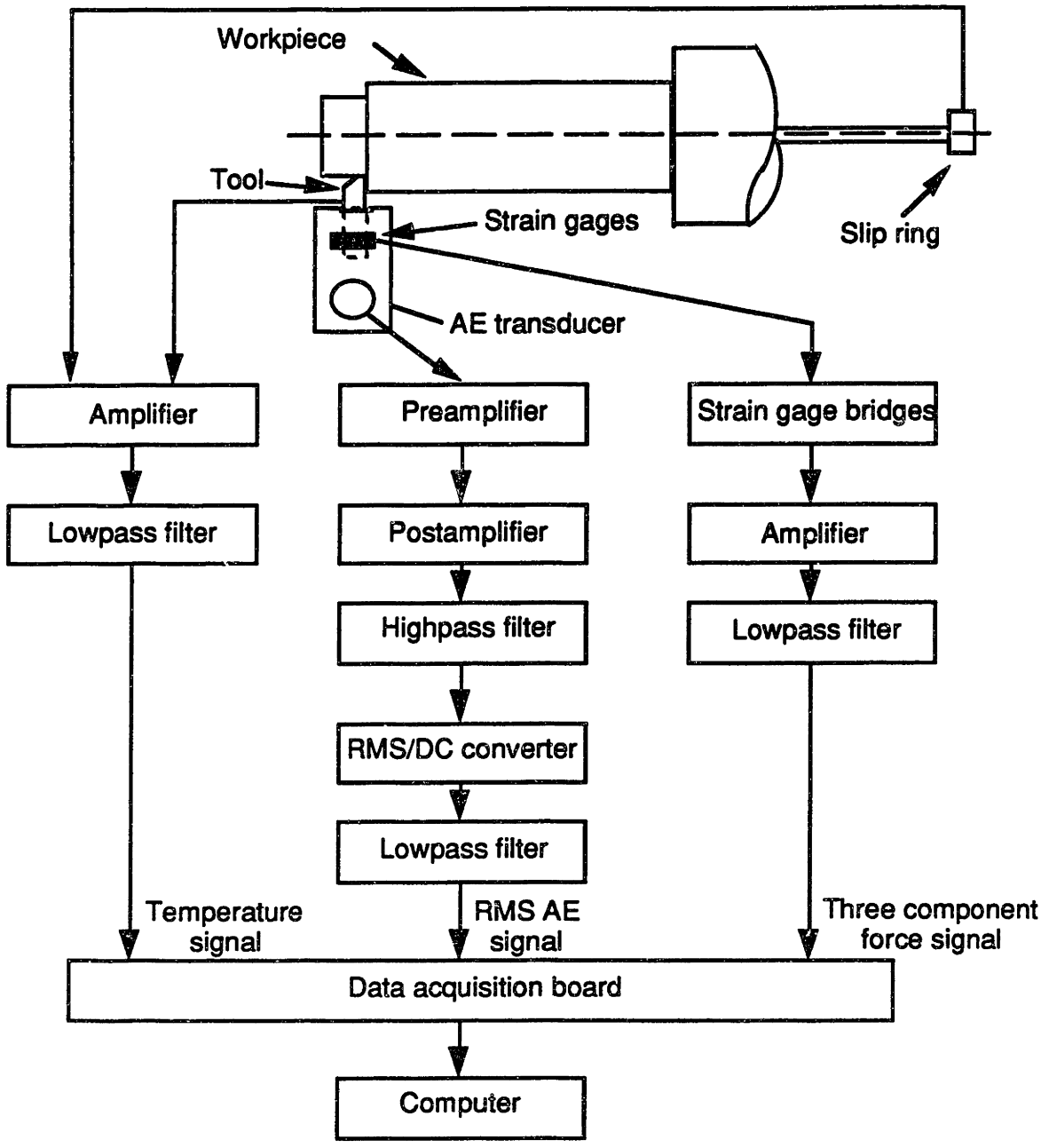

Figure 3.20 Experimental Apparatus

Parameter	Value Used
τ_s	1068 N/mm^2
k	0.333
m	0.654
n	0.137
K_1	5.2E-5
K_2	15.0
K_3	10,000 ^oK
l_o	500 m

Table 3.6 Values for Parameters in Sensor-Based Models

reported in [30]. The synthesis methods requiring training were trained to estimate the actual wear based on the wear estimates provided by the process models.

After the sensor synthesis methods requiring training had been trained, all of the synthesis methods, including the statistical approach, were compared using data from a tool wear test which was not included in the training data. In order to quantitatively evaluate the synthesis approaches, the mean squared error between the synthesized wear estimates and the actual wear was determined for the evaluation test. This criterion is expressed in equation (3-14) which is repeated below.

$$MSE = \frac{1}{n}\sum_{i=1}^{n}(y_i - y_{t,i})^2 \qquad (3\text{-}14)$$

where:

MSE = mean squared error

y_i = synthesized wear estimate

$y_{t,i}$ = actual wear (target output)

n = number of data points in evaluation test

Different network structures and training tolerances in the case of the multi-layer perceptron, different values of sigma, σ, in the case of the interpolation network, different training criteria in the case of the GMDH method, and different threshold values used to determine the consensus group of sensor in the case of the statistical approach, will all result in different values of the MSE for the data used to evaluate the sensor synthesis methods. To ensure that the particular structure or parameters used in the synthesis methods were not unfairly tailored to the particular data used for evaluation of the methods, the same approach to comparison of the synthesis methods used in the simulations was also used in the experimental comparison. Three sets of data were used: one for training, a second data set for selecting the best structure or parameters for the synthesis methods and a third data set for comparing the performance of the synthesis methods. This approach to the comparison of the methods is particularly appropriate when the amount of data available for comparison of the methods is limited [46]. Obtaining a large amount of experimental data is time consuming and expensive.

The experiments used to obtain the training data are specified in Table 3.5. The tool wear test used for selecting the best structure or parameters for the synthesis methods is specified in Table 3.7. The test performed based on the conditions in Table 3.7 used levels of the experimental factors, such as speed and feed, which were identical to those in the training data; however in this test the combinations for these levels of the factors for each experiment were different than in the experiments used to obtain the training data. Table 3.8 specifies the conditions for the tool wear experiment used to compare the performance of the synthesis methods. In most cases it would be unreasonable to train a network for all possible conditions which may be anticipated during a turning operation. Consequently, the experiment specified in Table 3.8 used levels of the factors which were not utilized in

the training data. All of the tool wear experiments were performed with a 4340 steel workpiece and M2 HSS tools.

Test	Experiment	Rake Angle (degrees)	Relief Angle (degrees)	Tool Travel Distance (m)	Feed Rate (mm/rev)	Cutting Speed (m/min)	Depth of Cut (mm)
1	1	7.5	7	0.025	0.178	12.80	0.762
	2	7.5	7	0.051	0.305	11.58	0.762
	3	7.5	7	0.076	0.102	15.24	0.762
	4	7.5	7	0.102	0.127	17.68	0.508
	5	7.5	7	0.127	0.229	14.02	0.508
	6	7.5	7	0.152	0.152	9.14	0.508
	7	7.5	7	0.178	0.254	18.90	1.016
	8	7.5	7	0.203	0.203	10.36	1.016
	9	7.5	7	0.229	0.279	16.46	1.016

Table 3.7 Array Specifying Experiments for Selection of Best Structure and Parameters for Sensor Synthesis Approaches

Test	Experiment	Rake Angle (degrees)	Relief Angle (degrees)	Tool Travel Distance (m)	Feed Rate (mm/rev)	Cutting Speed (m/min)	Depth of Cut (mm)
1	1	11	4.5	0.032	0.216	12.19	0.635
	2	11	4.5	0.064	0.267	17.07	0.635
	3	11	4.5	0.095	0.140	14.63	0.635
	4	11	4.5	0.114	0.191	10.97	0.889
	5	11	4.5	0.133	0.292	19.51	0.889
	6	11	4.5	0.165	0.318	15.85	0.889
	7	11	4.5	0.197	0.165	9.75	0.381
	8	11	4.5	0.216	0.241	18.29	0.381
	9	11	4.5	0.235	0.114	13.41	0.381

Table 3.8 Array Specifying Experiments for Evaluation of Sensor Synthesis Approaches

Results

The results for the evaluation test (Table 3.8) are shown in Figure 3.21. In this figure the quality of the synthesized wear rate estimates are compared with the wear estimates provided directly by the force, temperature and acoustic emission based process models. The MSE provided by using the arithmetic mean of the three model estimates as the synthesized wear estimate is shown in Figure 3.21 as a base-line for evaluation of the other sensor synthesis approaches. The MSEs for the wear estimates provided by the AE-based model were significantly greater than those for the other two models. This result probably occurred because the wear estimates provided by the AE model were particularly sensitive to even low levels of vibration and chatter during the machining tests.

For all of the synthesis methods requiring training, including the multi-layer perceptron network, interpolation network, multiple regression and GMDH methods, the inputs to the synthesis methods included the wear estimates provided by each of the three process models, the cutting velocity, feed rate, depth of cut, tool rake angle and tool relief angle.

For the multi-layer perceptron neural network, the same network structures used in the simulations in Section 3.3.1 were implemented: a simple network with one hidden layer containing four nodes and a more complex network with two hidden layers each containing eight nodes. In order to accommodate all of the inputs, each of these networks had eight input nodes. The error between the network predictions and the actual wear in the training data set must be within a specified training tolerance without modifying the network connection weights or node thresholds in order for the training phase to be complete. Different training tolerances were implemented, starting with a large tolerance (0.300 mm) where no significant training occurred and decreasing in increments of 0.001 mm until the

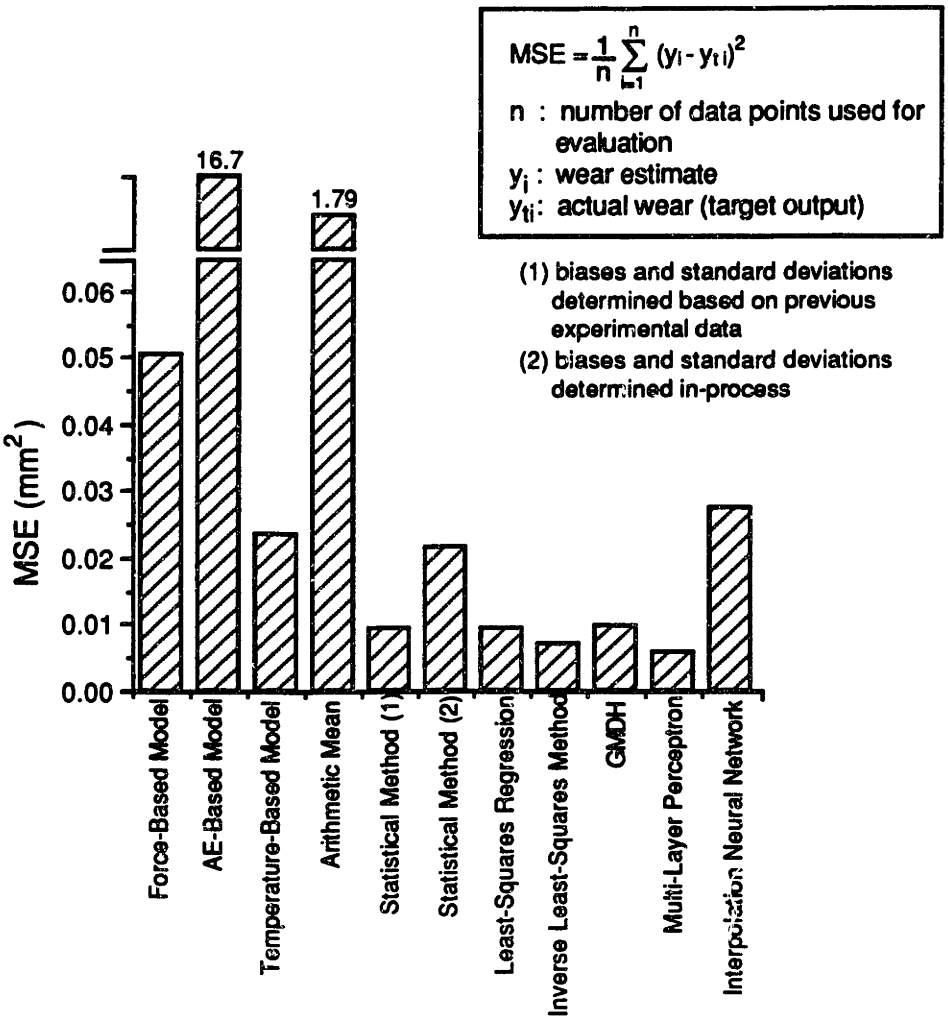

Figure 3.21 Experimental Comparison of Wear Estimates

network could not converge within 40,000 iterations through the training data set or one hour of CPU time on a VAXstationII/RC. The neural network providing the lowest MSE on the data from the tool wear experiment specified by Table 3.7 was selected for comparison with the other synthesis methods. The one hidden layer network with 0.032 mm training tolerance provided the lowest MSE on this data. The one-hidden layer network provided a lower MSE than the two hidden-layer network on the data used for

selection of the structure and parameters for the synthesis methods; this result indicates that the network structures that were implemented were sufficiently complex for the experimental data which was considered.

The interpolation network implemented had 81 nodes in the input layer corresponding to the 81 data points in the training data (Table 3.5). In order to accommodate all of the inputs, the input vectors had a dimension of eight. Values of the Gaussian function width, σ, ranging from 0.010 to 0.140 in increments of 0.001 were considered. The network with $\sigma = 0.115$ was found to provide the lowest MSE for the experiments specified by Table 3.7. This value of σ was used in comparing the interpolation net with the other synthesis methods.

For the GMDH method, several different criteria are available for evaluating each generation of quadratic polynomials during the training phase. The criteria were the same as those considered in the simulations: the mean squared error (MSE), prediction sum of squares (PRESS) [4], root mean square (RMS) [97], unbiased [97], and combined root mean square and unbiased [97] criteria. The polynomial selected by the combined criterion provided the lowest MSE on the data from the experiments described by Table 3.7. This polynomial was used for comparison with the other synthesis methods.

The statistical synthesis methods were implemented where the bias and standard deviations of the wear estimates provided by the models were determined in two different ways: (1) based on the mean error and the standard deviation of the error between the wear estimates provided by the process models and the actual wear measured during the experiments specified in Table 3.5, (2) using in-process evaluation of the uncertainty in the wear estimates due to uncertainties in the model parameters as outlined earlier in this section. For method (2) above, the values used in the models for the shear strength τ_s,

exponents k, m and n and the constants K_1, K_2, K_3 and l_o were considered to be uncertain (Figures 3.15 through 3.17). These uncertain parameters were assumed to be distributed according to Gaussian distributions with the means and standard deviations shown in Table 3.9. A standard deviation of 20% of the mean value was used for each of the uncertain parameters. For method (2), at each point the wear estimates were synthesized the biases and standard deviations for the wear estimates were determined in-process based on 100 estimates of the wear determined using randomly selected values for the model parameters; using more than 100 wear estimates for determining the biases and standard deviations did not significantly change the results on the data from the experiments used to select the structure or parameters for the synthesis methods (Table 3.7).

Uncertain Parameter	Mean	Standard Deviation
τ_s	1068 N/mm^2	214 N/mm^2
k	0.333	0.067
m	0.654	0.131
n	0.137	0.027
K_1	5.2E-5	1.04E-5
K_2	15.0	3.0
K_3	10,000 ^{o}K	2000 ^{o}K
l_o	500 m	100 m

Table 3.9 Means and Standard Deviations for Uncertain Model Parameters

The performance of the statistical synthesis approach where the bias and standard deviations for the wear uncertainty were determined using each of the two methods discussed above are shown in Figure 3.21 for the experiments specified by Table 3.8. The synthesis approaches which attempt to maximize expressions (3-9) and (3-10) were implemented and all possible combinations of eleven potential values (0.0 to 1.0 in

increments of 0.1) for each of the thresholds $r_{force\text{-}AE}$, $r_{force\text{-}temperature}$ and $r_{AE\text{-}temperature}$, which are used to determine the consensus group of sensors, were considered. The results shown in Figure 3.21 are for the statistical approach and thresholds providing the lowest MSE on the data used for selection of the structure and parameters of the synthesis methods (Table 3.7). The statistical approach which attempts to maximize expression (3-10) with thresholds $r_{force\text{-}AE} = 0.0$, $r_{force\text{-}temperature} = 0.2$ and $r_{AE\text{-}temperature} = 1.0$ provided the lowest MSE on the selection data when the biases and standard deviations were determined based on the data recorded during the experiments specified by Table 3.5. The statistical approach which attempts to maximize expression (3-10) with thresholds $r_{force\text{-}AE} = 0.8$, $r_{force\text{-}temperature} = 0.4$ and $r_{AE\text{-}temperature} = 0.8$ provided the lowest MSE on the selection data when the biases and standard deviations were determined in-process.

Based on Figure 3.21, statistical synthesis provided a lower MSE when the biases and standard deviations for the wear estimates are determined directly from measurements of the wear made during special tool wear experiments. However, this approach requires many experiments to be performed similar to those required by the methods based on training. In-process determination of the biases and standard deviations does not require as much experimentation prior to implementing the method.

As shown in Figure 3.21, all of the sensor synthesis methods implemented provided significantly lower MSEs than the MSE for the arithmetic mean of the wear estimates from the three models. All of the synthesis methods implemented except for the interpolation neural network also provided a lower MSE than the lowest MSE provided by using the wear estimates directly from a single model. The interpolation network was implemented in a simple form in this work. Implementing a more sophisticated form of this network, allowing features such as different values of σ corresponding to each of the input nodes, may improve the performance of this type of network. Aside from the

interpolation network, the results in Figure 3.21 do not conclusively show that any one of the sensor synthesis methods implemented is significantly better than the others.

3.4 CONCLUSIONS

This chapter evaluated the performance of several synthesis methods which require a training phase as well as an approach which synthesizes the sensor information based on a statistical criterion. The methods based on training included neural networks, multiple least-squares regression, inverse least-squares regression and the GMDH approach. In this chapter, sensor synthesis was considered for providing estimates of the tool wear during a turning operation. The synthesis methods were first evaluated and compared in a simulated environment using test data composed of linear, sinusoidal and random signals. Simulations conducted using the test data indicated that synthesis of multiple sensor information will generally provide better estimates of tool wear than information from only one sensor. As compared to the GMDH, multiple least-squares regression, interpolation neural network and inverse least-squares techniques, a multi-layer perceptron neural network appeared to be more effective at learning a relationship for providing synthesized estimates, particularly when the relationship between the sensor-based information and the actual process variable is nonlinear. The simulations indicate that when the sensors operate properly and the corresponding process models adequately reflect the complexity of the process a synthesis method based on training and a method based on a statistical criterion will not provide significantly different performance. However, when the process models do not adequately reflect the process complexity, and when sensor drift or variations in material properties occur, the simulations indicate that a method requiring training will provide better estimates of the wear than a statistical synthesis method. In addition, the simulations indicate that a method based on training may also be somewhat less sensitive to

failure of one of the sensors than a method based on a statistical criterion.

After performing the simulations, the synthesis approaches were evaluated using data from tool wear experiments during which force, temperature and acoustic emission signals were recorded. The results of the experiments indicate that synthesis of multiple sensor information will provide better estimates of the tool wear than using information from only a single sensor. Except for the interpolation network, all of the synthesis approaches considered provided better estimates of the wear than using the wear estimates directly from each individual sensor and its corresponding process model. These methods also provided better estimates of the wear than taking the arithmetic mean of the estimates provided by the independent models.

Implementation of a sensor synthesis approach based on statistical information about the state variables estimated through different sensors and their corresponding process models requires probability density functions for these state variables to be derived. This chapter presented a method of determining these density functions based on the evaluation of process models relating sensor signals with state variables necessary for the monitoring and operation of a manufacturing process. This method determines the probability density functions in-process and it has the advantage that it does not require extensive pre-process experimentation.

A general indication from the evaluation of the sensor synthesis approaches under the conditions which were simulated as well as based on experimental data is that sensor synthesis will provide better estimates of the tool wear in a turning operation than using information from a single sensor. The synthesized estimates may be better in terms of being more accurate, more reliable, and less sensitive to random sensor noise than estimates based on information from a single sensor. Although not explored in this

chapter, one implication of the work presented here is that the monitoring and operation of other manufacturing processes may potentially benefit from the synthesis of multiple sensor information.

4 DECISION-MAKING APPROACH TO PROCESS OPERATION

4.1 INTRODUCTION

As discussed in Chapter 1, several approaches can be taken for the operation of manufacturing equipment and processes. The simplest approach is to use an open-loop control system with fixed input variables determined off-line during planning [1,47,99]. Recent efforts to control manufacturing processes have primarily focussed on the development of adaptive control (AC) schemes. In this chapter the term "adaptive control" is used in the sense that it is used in the manufacturing literature. In the manufacturing literature "adaptive control" refers to any process operation scheme which automatically adjusts the process input settings on-line in response to the actual process conditions. A variety of adaptive control approaches have been presented over the past 25 years [8, 35, 41, 43, 44, 49, 55, 60, 68, 69, 72, 74, 76, 81, 82, 94, 102, 109, 110, 113, 116, 121, 122, 124]. While in Adaptive Control Constraint (ACC) the objective is primarily to control the input variables in order to maintain a measured parameter at a specified value, in Adaptive Control Optimization (ACO) the objective is to optimize the process with respect to specified criteria.

As an alternative to the AC approaches which have been presented in the literature, this chapter considers the approach to manufacturing process operation outlined in Chapter 1. The objective of this approach is to select the process input parameters in a manner which will operate the process in accordance with a set of performance objectives. The approach accomplishes this objective with the help of functions which explicitly relate

performance objectives, such as cost or rate, with the input parameters and with the sensor signals used to monitor the process. The synthesis of information from multiple sensor-based models which was explored in Chapter 3 is also incorporated into the process operation scheme considered in this chapter. Synthesis of multiple sensor information is used to overcome process monitoring difficulties caused by the lack of reliable sensors for manufacturing processes and the difficulty in developing one model which adequately reflects the complexity of the process.

The approach proposed in this thesis proceeds by periodically searching the feasible space of process input parameters with the help of functions which explicitly relate the performance objectives with the input parameters and with sensor signals in order to find the optimal set of inputs. In contrast, most adaptive control approaches presented in the literature attempt to apply control theory to a process by considering the process as the "plant" to be controlled. These AC approaches use a typical PID controller at some point in the operation scheme. Such a controller specifies changes of the process inputs in proportion to the error between a measured variable and a reference value. Because of this characteristic of a PID controller, it is susceptible to problems of unacceptably poor performance and instability, particularly under the circumstances of noisy and inaccurate sensor information and inadequate process models which are typical in a manufacturing environment. Unlike AC schemes, the approach considered in this thesis does not select the process input parameters based on the magnitude of an error between a reference value and a measured signal, but instead selects optimal, or at least "good", input parameters based on a set of performance objectives. Provided the input parameters are selected from a set of feasible inputs that will not lead to undesirable process behavior, the approach considered in this thesis is not susceptible to instability in the same sense of a typical closed-loop control scheme.

The concept of sensor synthesis which was investigated in Chapter 3 can be used in tandem with any process operation approach. However, because the approach considered in this thesis does not select the process input parameters based on the magnitude of an error between a measured signal an a reference value it is not susceptible to the instability which can be caused by time lags when using PID controller [24,27]. Sufficiently large time lags will cause a PID controller to become unstable. Therefore the operation approach considered in this thesis may allow a more sophisticated sensor synthesis scheme to be used than an approach which utilizes PID control.

In a manufacturing process, the relationships which are used to reflect the physical aspects of the process as well as the relationships which are used to determine values for the performance objectives based on the physical state of the process are typically complex and contain nonlinear terms. Often the mathematical models for a manufacturing process cannot be solved in closed form, a numerical approach is required for their solution. In addition, if a sophisticated synthesis approach such as a neural network is included in the process operation scheme it would not be reasonable to write out a closed form expression for the performance objectives as a function of the process input parameters. For the above reasons, in most circumstances a numerical technique would be required to search for the most appropriate input parameters in the feasible input space.

A numerical technique such as a gradient descent method could be used to search for the best process input parameters. However, when selecting an appropriate search method one must consider that the selection of the input parameters in the process operation approach considered in this thesis occurs in-process. Consequently, the method which is used to select the input parameters must be very reliable. An optimization technique which may occasionally fail to converge or which may get stuck in a local maximum (or minimum) would not be acceptable.

Based on the above considerations, a decision-making procedure is implemented in this thesis for the selection of the input parameters. This approach can be illustrated by considering a typical manufacturing process which requires several operating parameters; for example, in a machining/turning process, the operating parameters could include the feed and cutting speed. For generality, assume that there are k such operating parameters, i.e., (OP_1, OP_2,....., OP_k). An operating point of the process is described by the specific values of each of these operating parameters. If these parameters are continuous in nature, they can be discretized so that the interval of separation determines the number of operating points. Each of these operating points is an alternative for the process. If the discretization is fine, the number of alternatives is large and if the discretization is coarse, the number of alternatives is small. Due to process constraints, some of the operating parameters may not be feasible and would have to be removed from the set of alternatives. The remaining elements of the set form a feasible solution space of operating points.

These operating points form the options of a "decision maker;" criteria are used to evaluate and select an alternative. A consequence or outcome can be calculated for each alternative criterion pair. A typical decision matrix for a machining/turning process (Figure 4.1) can be conceived as having combinations of feed, f_r, and cutting speed, v, as alternatives and production rate and workpiece quality as criteria.

A matrix entry, a_{ij}, for an alternative i and a criterion j is calculated based on the definition of the criterion j and the particular value(s) of the alternative i. In order to make the comparison among the different alternatives independent of the different units, a normalization procedure can be applied to normalize the matrix entries so that their values do not have units and are bounded between 0 and 1 [75]. Once the matrix has been normalized, a number of different methods can be applied [56,75,106] in order to select the

best alternative.

The operation of the decision-making approach can be briefly described as follows: Measurement of process variables are performed by several sensing devices which in turn feed their signals into independent process models (Figure 4.2). Each of these models contains mathematical expressions based on the physics of the process which relate the measured variables to process state variables, namely process parameters which cannot be directly measured. The state variables are calculated for each alternative, namely for each possible input variable(s); if the value of the state variable exceeds the process constraints the corresponding alternative is not considered any further. For machining, the input variables may include the feed and speed and the state variables may include the tool wear

Alternatives	**Criteria**		
	Production rate	**Workpiece quality**	...
$(f_{r\,1}, v_1)$	a_{12}	a_{13}	...
$(f_{r\,2}, v_2)$	a_{22}	a_{23}	...
$(f_{r\,3}, v_3)$	a_{32}	a_{33}	...
⋮	⋮	⋮	⋮
⋮	⋮	⋮	⋮
$(f_{r\,n}, v_n)$	a_{n2}	a_{n3}	...

Figure 4.1 A Decision Matrix for Operating a Turning Process
$(f_{r\,i}, v_i)$: alternative pair operating point,
a_{ij} : value of alternative i with respect to criterion j

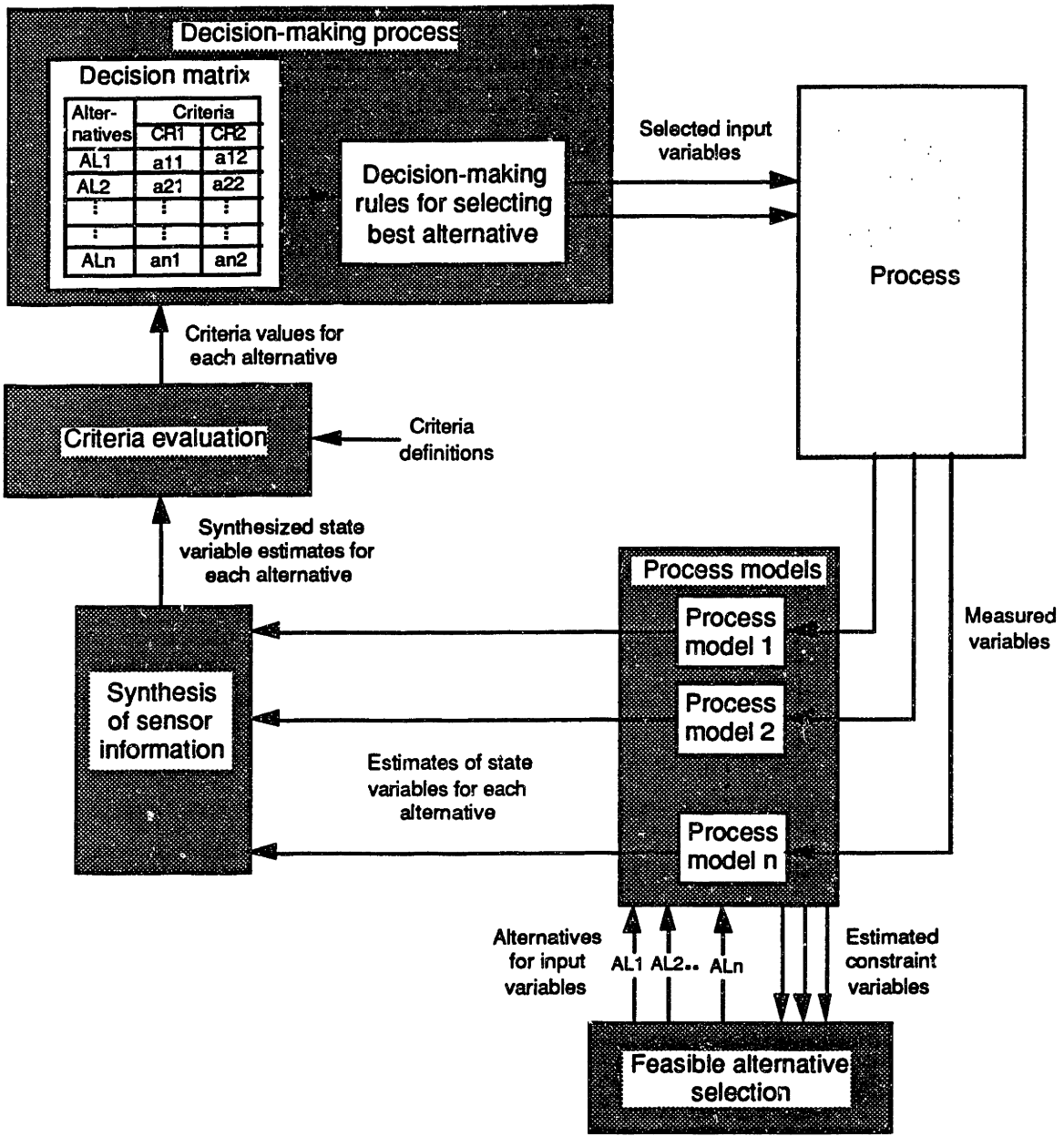

Figure 4.2 Block Diagram of Decision-Making Approach

and tool wear rate. For another manufacturing process such as injection molding, an input variable could be the screw speed and the state variable may be the part density. The proposed decision-making approach includes an integration or synthesis of state variable

estimates provided by several process models since a single process model which is accurate and reliable over a wide range of conditions is difficult to build for many processes [29]. The criteria values corresponding to each alternative are determined based on the criteria definitions, and decision-making rules are then applied to this information in order to select the best alternative.

The decision-making approach outlined above provides a straight-forward method for the selection of the process input parameters. Such an approach provides a number of unique features:

- The decision-making approach is one of several methods which can be used for selection of the most appropriate values for the input parameters. One would not necessarily have to consider the alternatives as being discrete in order to select values for the input parameters. However, by considering the input parameters as discrete alternatives, the decision-making approach provides a very robust method which is not susceptible to convergence problems and which will not get stuck in a local minimum. Considering the decision alternatives as discrete may cause the optimal point provided by the method to be somewhat off from the absolute best point since it considers a limited number of discrete points in the operating space; however this may not be a major drawback since using the optimal inputs at each point during a process does not necessarily lead to optimal operation for the overall process. This phenomenon occurs because it is difficult for any optimization method to reliably predict the behavior of a process significantly into the future.

- For many manufacturing processes it is desirable to operate the process in accordance with several different performance objectives. The decision-making approach provides a framework in which additional performance objectives can be

taken into account by adding more criteria to the decision matrix (Figure 4.1). The addition of these criteria does not significantly increase the complexity of the approach. The decision-making approach also provides the flexibility to respond to changes in the performance objectives for the overall manufacturing system by allowing the relative weighting on the decision-criteria to be changed even in-process. Other methods of searching for the best values for the input parameters may not provide this degree of responsiveness to changes in the performance objectives.

- Because the decision-making approach is modular, it can be easily adapted to a wide variety of process conditions and processes. For example, it may be possible to change one or more of the process models used in the approach without changing the other components of the decision-making approach.

- When considering multiple performance objectives it is frequently desirable to normalize the values for the criteria in some manner since the dimensional units for different criteria may not be the same. In order to implement a normalization procedure the maximum and minimum values for the criteria must be known for the range of input settings which is being considered. A normalization procedure can easily be implemented in the decision-making approach because maximum and minimum values for each criterion are found in the process of evaluating the decision alternatives.

- The operation of manufacturing processes and their control is associated with a degree of uncertainty, primarily due to changes in material properties and process modelling inaccuracies. The adaptive control approaches presented in the literature usually utilize a typical PID controller. The decision-making approach provides the

option of using concepts developed in decision theory for making decisions based on uncertain information which are different from the concepts utilized in control theory. Concepts from decision theory are not explored in detail in this chapter, but the decision-making approach provides a framework in which such concepts could be considered.

The objective of this chapter is to discuss the feasibility and the limitations of the decision-making approach to machining (in particular turning) and to compare the decision-making approach with typical ACC and ACO schemes. The work presented in this chapter is particularly concentrated on machining for the reasons discussed in Chapter 1.

4.2 ADAPTIVE CONTROL OPTIMIZATION VS. DECISION-MAKING APPROACH FOR MACHINING PROCESSES

In one recent scheme, which is representative of the ACO approaches, a locus of optimal points are established in the input variable space based on a cost function with each point corresponding to a value of a measurable process variable [60]. The optimal locus is determined prior to the process using a model relating the input variables with the measurable process variable and with the state variables influencing the cost function. The approach is based on the assumption that either (1) the process can be operated using fixed optimal input variables determined independent of constraints or (2) a constraint on the measured process variable prevents the use of the inputs determined in case (1) and therefore the input variables would lie on the constraint. When such a scheme is applied to machining, the optimization algorithm determines a value for the speed which corresponds to a given feed; this pair of variables is input to the process (Figure 4.3). Based on the values of the input variables the system determines the constraint, P_b, to be imposed on the measured variable, which in the case of machining may be the calculated power of the

machine. The constraint is used as a reference value to a control loop in which the feed is adjusted in order to reduce the difference, e, between the constraint, P_b, and the measured variable, P_c. The controller is based on some combination of proportional, integral and derivative control action (PID).

As an alternative to such a concept, a decision-making approach to machining presumes that measured variables such as the cutting force and tool temperature are fed into process models for estimating the tool wear (Figure 4.4). Based on these estimates of the tool wear, the wear rates corresponding to a set of feasible alternatives are calculated. Alternatives are feasible if the process constraints are not violated. The independent wear rate estimates provided by each model are synthesized in order to determine the best estimate. A decision matrix is determined according to the criteria definitions, and decision-making rules are applied to the decision matrix in order to determine the optimal alternative, namely the best input variables.

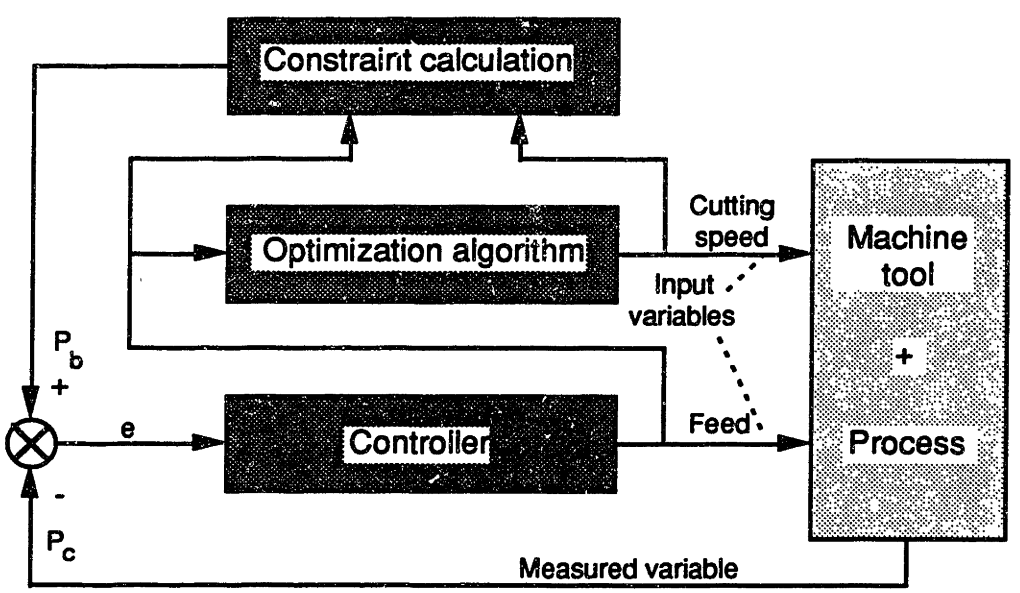

Figure 4.3 Block Diagram of an ACO Approach, [60]

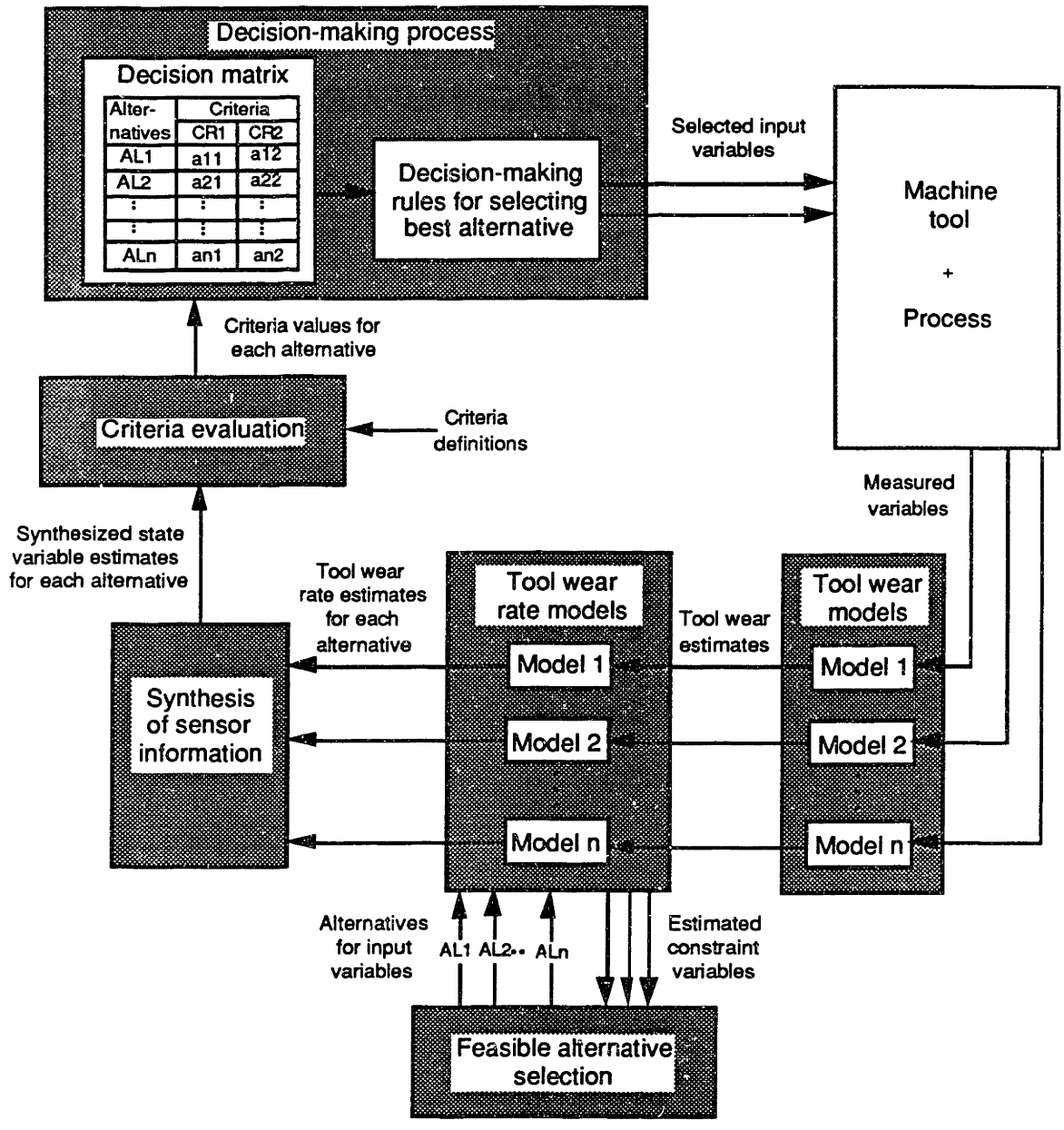

Figure 4.4 Block Diagram of Decision-Making Approach as Applied to Machining

The major differences between such a decision-making approach and a typical ACO approach can be summarized as follows:

- The decision-making approach can easily adapt to changes in the optimization criteria by changing the decision-making rules, whereas an ACO approach is more rigid regarding the optimization aspects of the process.

- The ACO approach is limited to account for only the changes that the state variable causes to the constraints (e.g. state variable: tool wear, constraint: machine power). In contrast the decision-making concept, with adequately structured process models, accounts for the effects of the state variables on the overall process behavior.

- In the ACO approach the input variables must be on the constraint when the constraint restricts the process from operating at the optimal point. In contrast, the input variables selected according to the decision-making approach need only to satisfy the constraints but not necessarily to lie on them.

- Decision-making requires more in-process computation than most ACO approaches. However, computing power is becoming less expensive and computational speed will increase as computer technology advances.

4.2.1 IMPLEMENTATION

In order to evaluate the feasibility and limitations of the proposed decision-making strategy to process operation, this approach was implemented in a simulated environment and compared with the ACO approach. During the simulations the tool wear was estimated

using available experimental data consisting of curves for flank wear versus time for steel machined on a lathe with a carbide tool with a feed of 0.25 mm/rev at cutting velocities of 80, 100, 125, 160, 200 and 260 m/min [67]. A tool life criterion of 0.3 mm was used; the tool was replaced when the flank wear reached 0.3 mm. For the purpose of simplicity the ACO and decision-making approaches were executed with speed as the only input variable. The feed was held constant at 0.25 mm/rev.

For comparison reasons a performance measure related to the process cost per part, C, was defined. This performance measure is the ratio of the total cost, including machining cost ($M\,t_m$), part changing cost ($N_p\,M\,t_L$), and tool replacement cost ($N_t\,C_c + N_t\,M\,t_d$), to the number of parts machined (N_p):

$$C = \frac{M\,t_m + N_t\,C_c + N_t\,M\,t_d + N_p\,M\,t_L}{N_p} \qquad (4\text{-}1)$$

where

t_m = total time the tool is in contact with the workpiece

M = machine operating rate including machinist's wages, machine depreciation and expendables

N_t = number of tools used

C_c = cost of a new tool

t_d = time required for tool change

N_p = total number of parts completed

t_L = time required for a part change

The number of parts completed, N_p, was determined by dividing the total distance traveled by the tool when in contact with the workpiece divided by the length of one part. The values in Table 4.1 were used in computing the value of the cost-per-part performance

measure. The turning process was assumed to be "active" for eight hours and the performance measure was calculated when the process was controlled by the ACO scheme and by the decision-making approach.

C_c = \$10.00	t_d = 1 minute	t_L = 1 minute

Table 4.1 Assumed Values for Computing the Value of the Performance Measure

Implementation of adaptive control optimization

For implementing the ACO approach the cost function was assumed to be identical with the performance measure in equation (4-1); furthermore a tool life equation is required which has been assumed to be the Taylor's relationship:

$$T = C_1/v^n \tag{4-2}$$

where

n = constant exponent

v = cutting speed

T = tool life

C_1 = constant

The total time the tool is in contact with the workpiece, t_m, can be determined as:

$$t_m = N_t T \tag{4-3}$$

When the process is operated at a constant speed the number of parts produced can be determined as:

$$N_p = \frac{v\, N_t\, T}{L_c} \tag{4-4}$$

where

L_c = length on the surface of the workpiece with which the tool is in contact needed for the completion of one part

L_c can be approximated as:

$$L_c = \frac{L}{f_r}\,\pi\, D \tag{4-5}$$

where

L = part length

f_r = feed

D = part diameter

It was assumed that the diameter of the parts was 0.04 meters and the length of the parts was 0.3 meters. Substituting expressions (4-3) and (4-4) into the performance measure, C, defined in equation (4-1):

$$C = \frac{M\, N_t\, T + N_t\, C_c + N_t\, M\, t_d + \left[\frac{v\, N_t\, T}{L_c}\right] M\, t_L}{\left[\frac{v\, N_t\, T}{L_c}\right]} \tag{4-6}$$

After substituting equation (4-2) for the tool life, T, into equation (4-6) and rearranging terms:

$$C = \frac{M\, L_c + (C_c + M\, t_d)\, L_c\, v^n / C_1}{v} + M\, t_L \tag{4-7}$$

Differentiating equation (4-7) with respect to the speed, v, and setting the resulting expression equal to zero yields the following expression for the unconstrained optimal speed:

$$v_{opt} = \left[\frac{M\,C_1}{(C_c + M\,t_d)(n-1)}\right]^{1/n} \tag{4-8}$$

The constants C_1 and n in Taylor's tool life equation were determined from least-squares regression based on the tool wear experimental data used for the simulation of the process; C_1 was determined as 9.92E4 and the value of the exponent, n, was found to be 1.7, where the tool life is in units of minutes and the speed is in units of m/min. The speed settings were constrained to be between 80 and 260 m/min; if the optimization algorithm prescribed $v_{opt} > 260$ m/min the process operated at v = 260 m/min.

The following constraint was imposed on the process:

$$P_b(v,d,f_r) - P_c(v,d,f_r,W_f) \geq 0 \tag{4-9}$$

where

P_b = calculated cutting power

P_c = measured cutting power

v = cutting speed (m/min)

d = depth of cut (mm)

f_r = feed (mm/rev)

W_f = width of flank wear (mm)

Based on the literature [60] P_b was determined as:

$$P_b = K_{11} d\, v\, f_r^{n4} \qquad (4\text{-}10)$$

P_c was determined from the literature [30] as:

$$P_c = \left[K_6 f_r^{n4}(1 - K_7\alpha) - K_8 - K_9 v\right] v\, d + K_{10} v\, d\, W_f \qquad (4\text{-}11)$$

where

K_6, K_7, K_8, K_9, K_{10}, K_{11} and n_4 are constants and α is the tool rake angle in radians

For the simulations, the constants and cutting conditions used in the expressions for the constraint above (Table 4.2) were assumed to have values which reflected those reported in [30] and also to reflect the experimental data reported in [67].

Because the ACO approach was implemented with only one input variable, when the varying constraint restricted the process from operating at v_{opt} the speed setting was determined by solving the relationship (4-9) as an equality.

$K_6 =$ 1960	$K_9 =$ 0.1	$n_4 =$ 0.76
$K_7 =$ 0.57	$K_{10} =$ 500	$\alpha =$ 5 degrees
$K_8 =$ 86	$K_{11} =$ 1616	d = 2.0 mm

Table 4.2 Constants and Cutting Conditions Assumed for Constraint on the Turning Process

Implementation of in-process decision making

Although the decision-making approach can simultaneously optimize the process with respect to several criteria, for the purpose of this discussion the process cost per part was considered as the only criterion. The use of this criterion will tend to minimize the process-cost-per-part performance measure. The definition of this criterion includes in its denominator the fraction of a part(s) (ΔN_p) completed during the decision interval Δt, which is the time between two subsequent decisions. The numerator includes the machine operating cost ($M\Delta t$) the cost of a new tool C_c and the cost of a tool change (Mt_d) prorated by the fraction of the tool life used during the decision interval, and the cost of a part change (Mt_L) prorated by the fraction of a part(s) completed during the decision interval. Thus the process-cost-per-part criterion, c, can be expressed as:

$$c = \frac{M\,\Delta t + \frac{\dot{W}_f}{W_{max}}\,\Delta t\,(C_c + M\,t_d) + \Delta N_p\,M\,t_L}{\Delta N_p} \qquad (4\text{-}12)$$

where the fraction of a part(s) completed during the interval Δt is determined as:

$$\Delta N_p = \frac{v\,\Delta t}{L_c} \qquad (4\text{-}13)$$

where

M = machine operating rate including machinist's wages, machine depreciation and expendables

$\dot{W}_f$ = flank wear rate

W_{max} = tool life criterion

C_c = cost of a new tool

t_d = time required for tool change (Table 4.1)

t_L = time required for a part change (Table 4.1)

v = cutting speed

L_c = length on the surface of the workpiece with which the tool is in contact needed for the completion of one part as defined in expression (4-5)

A five second decision interval was used in the simulations of the decision-making approach. Ten alternatives were evaluated at each decision point, which consisted of cutting speeds from 80 to 260 m/min in increments of 20 m/min. The constraint expressed in equation (4-9) was also imposed in the implementation of the decision-making approach; alternative speeds were only considered to be feasible if the constraint was not violated.

The wear rate estimates, $\dot{W}_f$, can be determined by synthesizing information from a variety of sensors. However, for the discussion in this section the wear rate estimates were obtained directly from the tool wear experimental data.

4.2.2 RESULTS AND DISCUSSION

Figure 4.5 shows the relative performance of the decision-making and ACO approaches with respect to the process-cost-per-part performance measure, C, as a function of the ratio of machine operating rate to tool cost, M/C_c. The relative performance of these two approaches is dependent on the ratio of the machine operating rate to the tool cost. For ratios of M/C_c from 0 to 0.25, the decision-making approach provides a 5.38 percent average reduction in cost per part as compared with the ACO approach. When the ratio of machine operating rate to tool cost is greater than 0.25 the ACO and decision-making approaches provide approximately the same cost per part. This is because when the machine operating rate is very high relative to the tool cost both approaches tend to select the highest allowable speed. The difference in cost per part for the two approaches can be

primarily attributed to the fact that by selecting the optimal input settings based on the overall tool life equation, the ACO approach does not take into consideration that the tool wear rate can vary significantly during the process, whereas the decision-making approach accounts explicitly for this dynamic change.

An adjustment in the length of the decision interval affects the performance of the decision-making approach (Figure 4.6). Intuitively it would be expected that by using the smallest decision interval the best performance could be achieved. However, this may not always be true since optimizing in the small intervals does not necessarily lead to the overall optimum. Through selection of the length of the decision interval execution of decisions can be tailored in accordance with available computation power and desired performance.

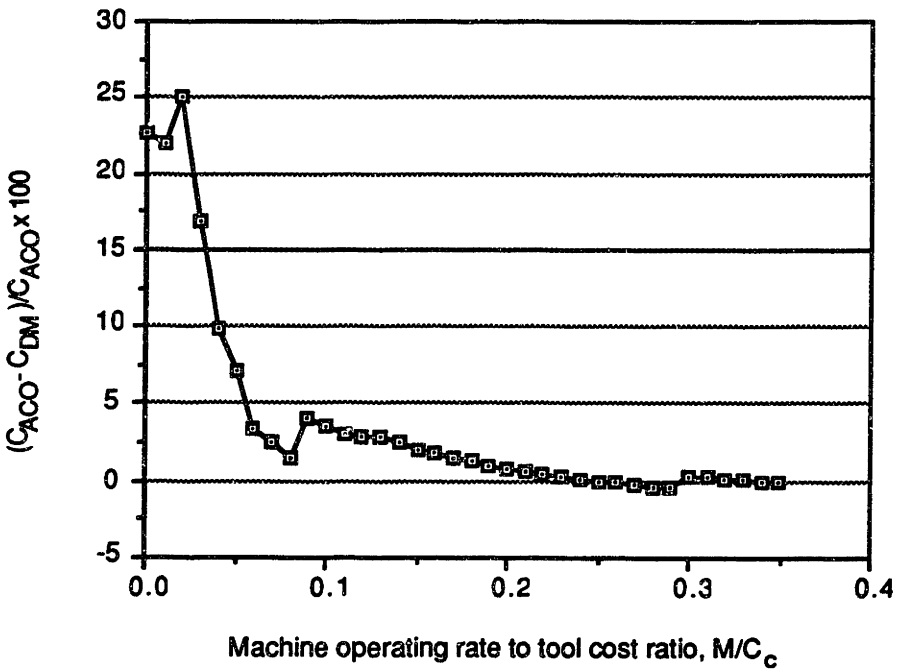

Figure 4.5 Percent Reduction in Performance Measure, C, Provided by Decision-Making Approach as a Function of Machine Operating Rate to Tool Cost Ratio, M/C_c
(C_{DM} = Performance measure, C, provided by decision-making,
C_{ACO} = Performance measure, C, provided by ACO)

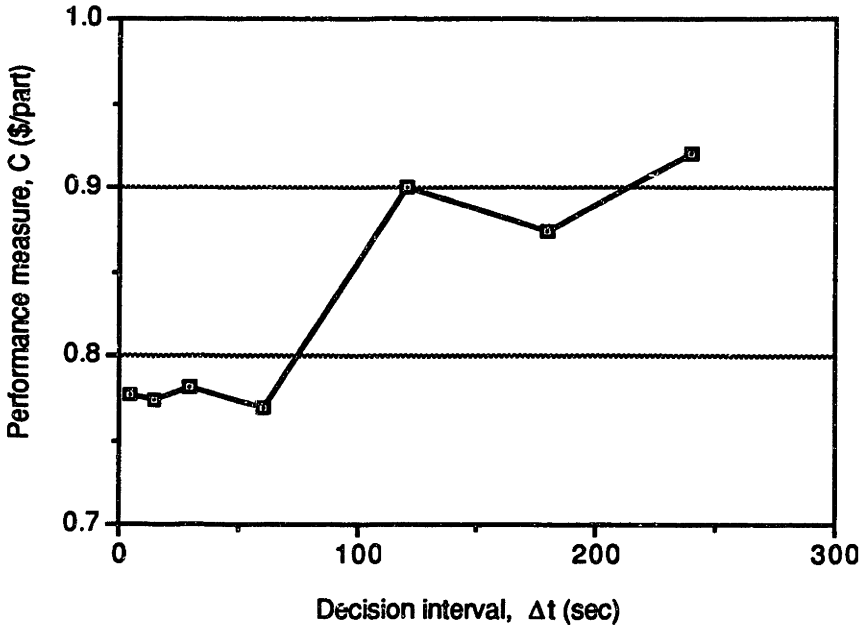

Figure 4.6 Effect of Changing the Decision Interval on the Performance of Decision-Making Approach, $M/C_c = 0.02$

During an actual machining operation the actual wear rates will not correspond exactly to the estimated wear rates used in the decision-making process. Simulations were run in order to examine the sensitivity of the decision-making approach to these estimation errors. For these simulations the wear rate estimates were determined as

$$(dW/dt)_e = (1 + e)\,(dW/dt)_s \qquad (4\text{-}14)$$

where

$(dW/dt)_e$ = wear rate estimate provided to decision-making approach including random error

e = random error factor

$(dW/dt)_s$ = wear rate determined from wear versus time data

In general, the wear rate estimates during an actual process would tend to have mean values near the actual values but would show a significant amount of scatter about the mean. The random error factors used for the simulations were uniformly distributed with a mean of zero.

Figure 4.7 shows the effect of increasing the maximum magnitude of the random error on the relative performance of the decision-making and ACO approaches with respect to the performance measure, C. Even with a significant level of error in the wear rate estimates, the decision-making approach provides a lower cost per part than the ACO approach for ratios of the machine operating rate to tool cost from 0 to 0.12.

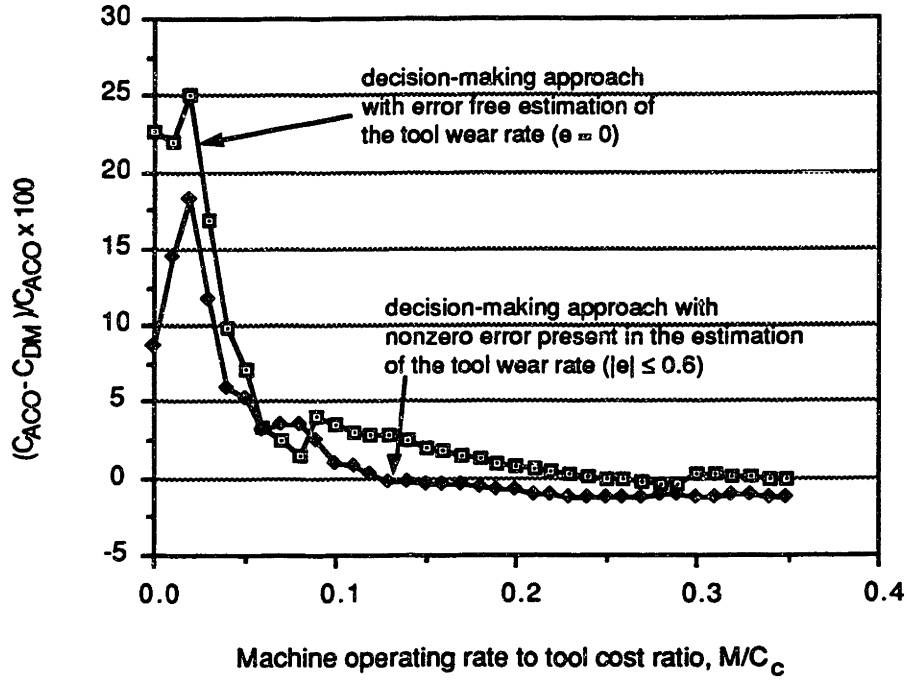

Figure 4.7 Effect of Error in Wear Rate Estimates on Percent Reduction in Performance Measure, C, Provided by Decision-Making Approach
(C_{DM} = Performance measure, C, provided by decision-making,
C_{ACO} = Performance measure, C, provided by ACO)

4.3 ADAPTIVE CONTROL CONSTRAINT VS. DECISION-MAKING APPROACH FOR MACHINING PROCESSES

Adaptive Control Constraint (ACC) schemes attempt to select the input variables in order to maintain a measured parameter at a specified value. Automatic control techniques have frequently been used in the implementation of ACC schemes for machining processes. The application of such techniques requires a mathematical description of the process which may be very complex because a number of physical phenomena interact during the actual process [40,116]. In addition, some of the parameters in the model may be uncertain, often due to uncertainties in material properties. This problem has been addressed by means of adaptation (Figure 4.8) whereby efforts are made to adapt the model parameters in such a manner that the model behavior closely reflects the behavior of the actual process.

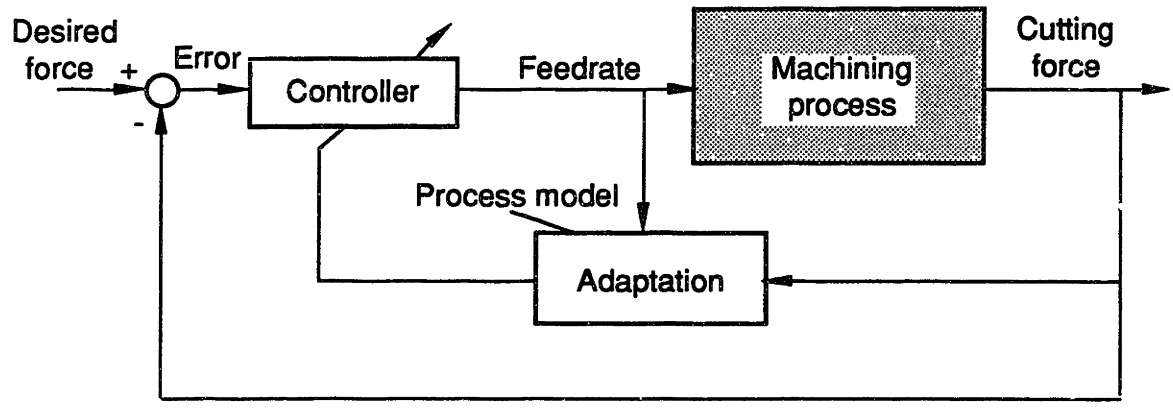

Figure 4.8 Adaptive Control Scheme for Controlling Force in Machining

The design and implementation of a model reference adaptive control (MRAC) schemes have been considered for force control in milling and turning [40,68,109]. In these control schemes the speed is held constant while the feedrate is adjusted in an attempt

to maintain a constant cutting force. The MRAC approach consists of two control loops. The first loop is the ordinary feedback loop consisting of a controller and the process. The parameters of the controller are adjusted in the second loop so that the error between the outputs of the process and a reference model is minimized [5]. The small gain theorem has been used to design an adaptive controller for a turning operation in which the feedrate was used as the control input [18]. A self tuning regulator (STR) has also been used to control a turning process [37]. The STR consists of two control loops, where the first is the ordinary feedback loop consisting of the process and a controller. In the second control loop, a recursive estimation of the parameters in the process model is performed based on the input and output of the process. The estimated model parameters are then used to adjust the parameters of the controller [18].

Because ACC schemes attempt to maintain a measured variable at a reference value, the implementation of these approaches first requires the choice of an appropriate, measurable variable, such as force or temperature, to be controlled, and the selection of a reference value for this variable. With a few exceptions [93], ACC approaches for machining reported in the literature rely on a single sensing variable, which in many cases is force. These schemes typically attempt to maintain the cutting force at a preselected value because it is believed that such a strategy leads to a "better" machining process (Figure 4.9). However, it is not evident that maintaining the cutting force at a constant value will necessarily optimize a machining process with respect to any criteria such as cost or production rate. In the attempt to maintain the measured variable at a reference value, the process operation may become unstable. Furthermore, the issue of selecting an appropriate reference cutting force which will lead to adequate process operation has not been sufficiently considered.

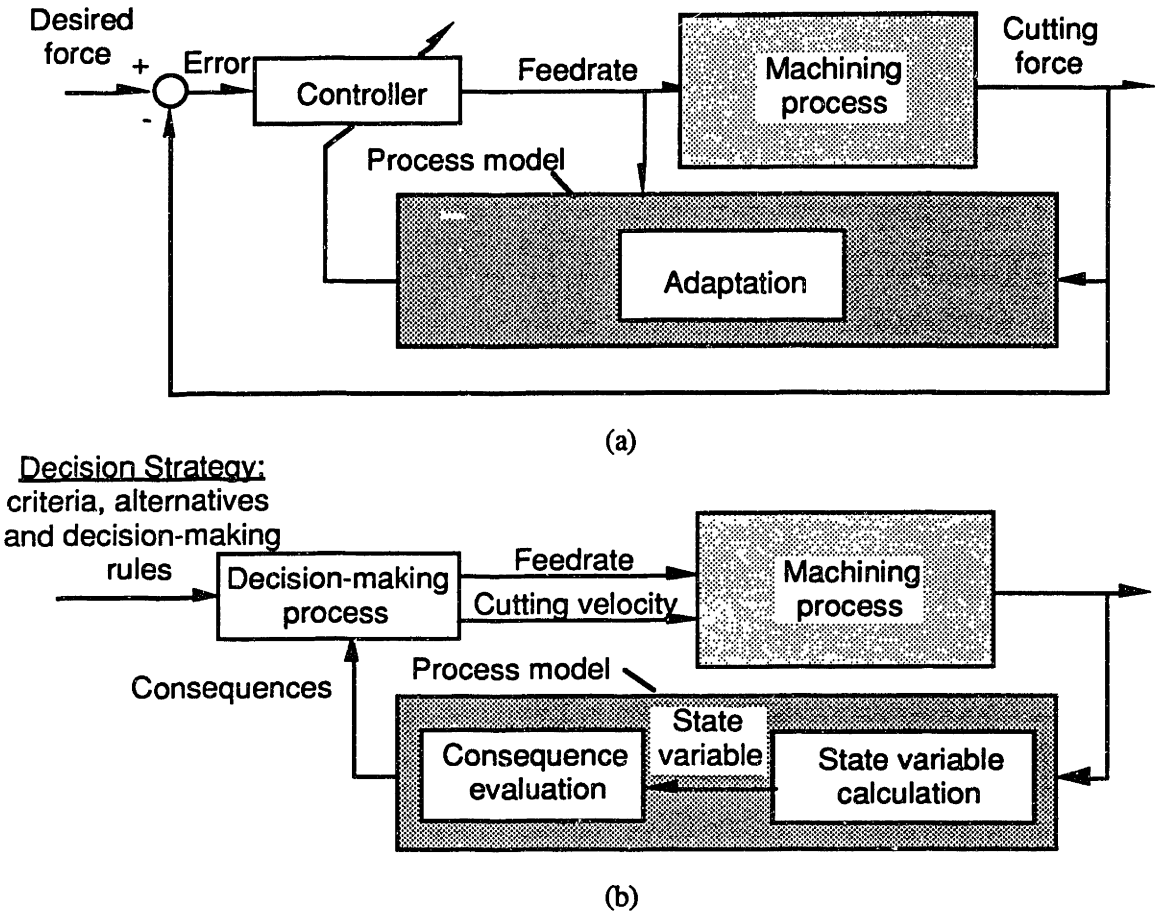

Figure 4.9 Adaptive Control (a) vs. Decision-Making (b) Approach for Machining

4.3.1 IMPLEMENTATION

In order to demonstrate the differences between an ACC and a decision-making approach, the turning process was used as a "test bed" for comparison purposes. The ACC approach considered in this section attempts to maintain a constant cutting force [109] by controlling the feed, f_r, whereas the decision-making approach chooses the cutting speed, v, and feed, f_r, based on the evaluation of several decision-making criteria.

The turning process

The comparison of the two approaches was made with the help of the turning process, which was simulated based on a model with the feedrate command U_c as input (Figure 4.10) and the cutting force F_m as output [109]. This model, in its original form accounted for:

a) Carriage motion dynamics

$$\frac{U_a}{U_c} = \frac{0.552z + 0.4529}{z^2 + 0.215z + 0.2466} \tag{4-15}$$

where

U_c = command feedrate (volts)

U_a = actual feedrate (cm/sec)

b) Feedrate/chip thickness dynamics

$$\frac{f_r}{U_a} = \frac{B\,(z^4 + z^3 + z^2 + z + 1)}{z^5} \tag{4-16}$$

where B = 0.01 for the uncut chip thickness/feed, f_r, and actual feedrate, U_a, in cm and cm/sec, respectively. This transfer function [109] depends on the sampling time and the spindle speed.

c) Cutting process

$$F = K\,d\,f_r^P \tag{4-17}$$

where

Turning Process (simulated)

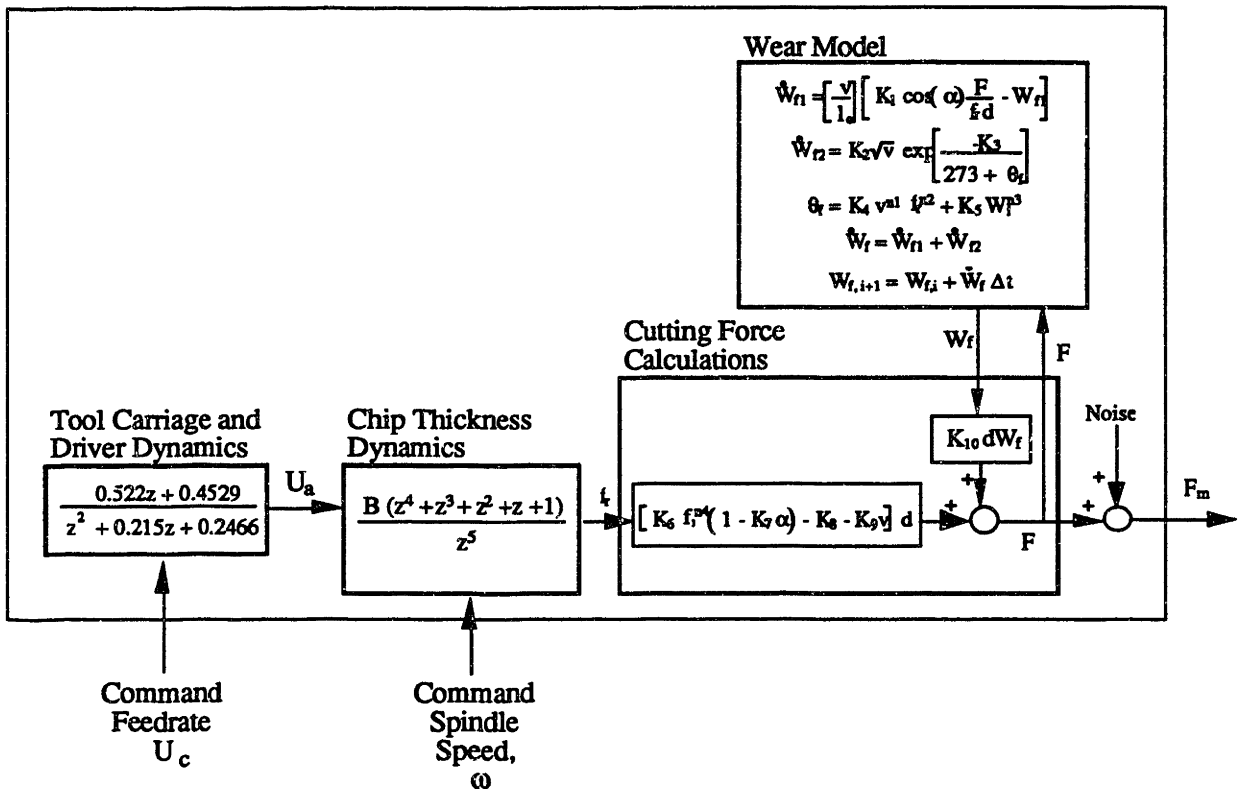

Figure 4.10 Model of a Turning Process

F = cutting force

K = constant

d = depth of cut

p = constant exponent

f_r = feed

This initial model was augmented by considering the effect of tool wear on the cutting force [90] so that instead of Equation (4-17) the following relationship was used.

$$F = \left[K_6 f_r^{n4}(1 - K_7\alpha) - K_8 - K_9 v\right] d + K_{10} d\, W_f \qquad (4\text{-}18)$$

where

$K_6, K_7, K_8, K_9, K_{10}$ = constants

n_4 = constant exponent

α = rake angle

v = cutting speed

W_f = flank wear

The data reported in [67] reflects the development of tool wear with respect to machining time for different cutting speeds. However, for the simulations discussed in this section the ACC scheme used the feed as the control input and the decision-making approach used both the feed and cutting speed as inputs to the process. Therefore expressions reported in [90] for modelling the development of tool wear which take into account both the speed and feed were used in the simulations for comparing the ACC scheme with a decision-making approach. In these expressions presented below, the cutting conditions and constants K_i, n_i and l_o (Table 4.3) were assumed to have values partially reported in [90], and partially to reflect experimental data reported in [67] (Figure 4.11). The expressions assume that abrasion and diffusion are the dominant mechanisms in the development of flank wear, W_f, for the carbide tools considered in the model. The flank wear rate, $\dot{W}_f$, is separated into a component caused by abrasion, $\dot{W}_{f1}$, and a component caused by diffusion, $\dot{W}_{f2}$.

$$\dot{W}_{f1} = \left[\frac{v}{l_o}\right]\left[K_1 \cos(\alpha)\frac{F}{f_r\, d} - W_{f1}\right] \qquad (4\text{-}19)$$

$$\dot{W}_{f2} = K_2 \sqrt{v} \exp\left[\frac{-K_3}{273 + \theta_f}\right] \qquad (4\text{-}20)$$

$K_1 = 5.2 \times 10^{-5}$	$K_7 = 0.57$	$n_3 = 1.45$
$K_2 = 15$	$K_8 = 86$	$n_4 = 0.76$
$K_3 = 8000$	$K_9 = 0.1$	$l_o = 300$
$K_4 = 72$	$K_{10} = 500$	$\alpha = 5$ degrees
$K_5 = 2500$	$n_1 = 0.4$	$d = 2.0$ mm
$K_6 = 2160$	$n_2 = 0.48$	

Table 4.3 Constants and Cutting Conditions Assumed for the Turning Process

where

l_o = constant

K_1, K_2, K_3 = constants

and the flank temperature, θ_f, in Equation (4-20) is estimated using the following relationship:

$$\theta_f = K_4 \, v^{n1} \, f_r^{n2} + K_5 \, W_f^{n3} \tag{4-21}$$

where

K_4, K_5 = constants

n_1, n_2, n_3 = constant exponents

The total wear rate, $\dot{W}_f$, is then

$$\dot{W}_f = \dot{W}_{f1} + \dot{W}_{f2} \tag{4-22}$$

This wear rate is integrated with respect to time in order to model the development of tool wear.

In an actual turning operation, the cutting force signal provided by a force sensor may contain a noise component, the magnitude of which may vary as a function of conditions such as the tool and workpiece materials or the machine on which the turning is performed. In order to account for this noise, the turning process model used in this investigation included a noise component for the cutting force. For a force, F, calculated by the deterministic expressions of the process model (Figure 4.10), a "measured" force F_m was estimated using the following expression

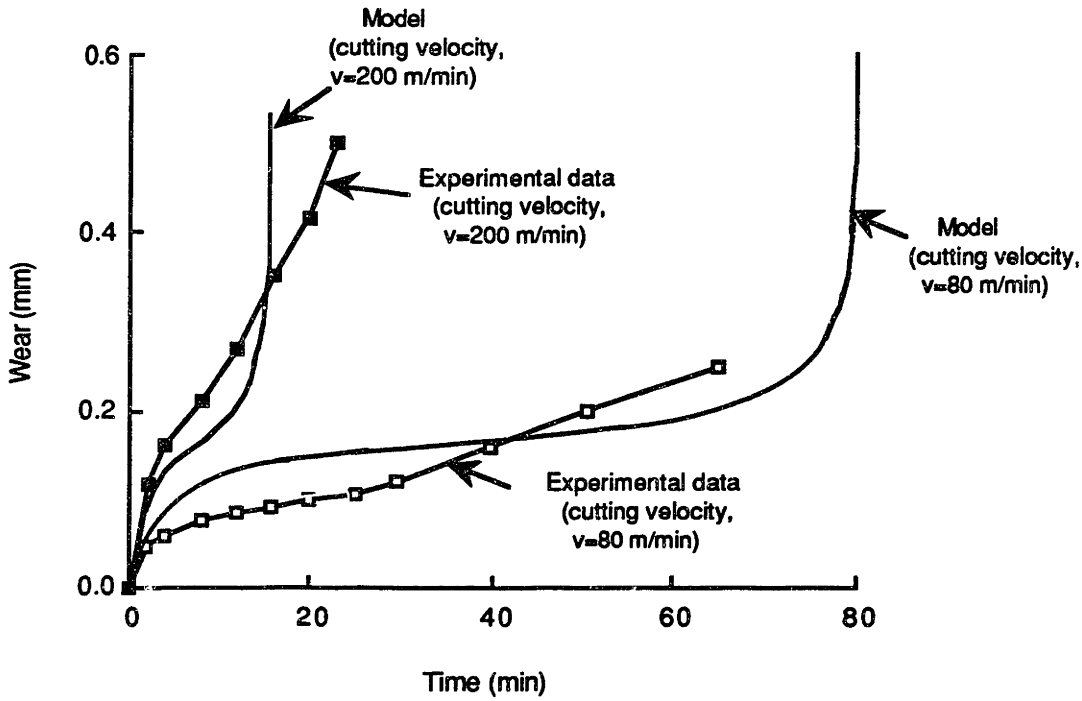

Figure 4.11 Experimental and Calculated Tool Wear
(feed = 0.25 mm/rev, depth of cut = 2.0 mm)

$$F_m = F[1 + N_F \times N_R] \tag{4-23}$$

where

F_m = "measured" force value assumed to be provided by a force sensor

F = force value calculated using the model of Figure 4.10

N_F = noise factor (assumed to be 0.1 for this investigation)

N_R = a normally distributed random number with mean zero and variance of one

In the simulations for both the decision-making and ACC approaches, the measured force, F_m, was filtered using the lowpass filter used in [109].

$$\frac{F_f}{F_m} = \frac{0.454}{z - 0.5464} \tag{4-24}$$

where

F_f = filtered force signal

Performance measures

Production rate, process cost and part quality are typical measures used to evaluate the performance of a manufacturing process. For machining processes, the surface roughness of the parts can be used as a measure of the part quality. Therefore the comparison of the decision-making approach with the ACC scheme is based on the following performance measures.

a) **Process cost per part, C**

This performance measure is the ratio of the total cost, including machining cost ($M\ t_m$), part changing cost ($N_p\ M\ t_L$), and tool replacement cost ($N_t\ C_c + N_t\ M\ t_d$), to the number of parts machined (N_p) and is defined in expression (4-1) which is

repeated below:

$$C = \frac{M\, t_m + N_t\, C_c + N_t\, M\, t_d + N_p\, M\, t_L}{N_p} \qquad (4\text{-}1)$$

where

t_m = total time the tool is in contact with the workpiece

M = machine operating rate including machinist's wages, machine depreciation and expendables

N_t = number of tools used

C_c = cost of a new tool

t_d = time required for tool change

N_p = total number of parts completed

t_L = time required for a part change

The number of parts completed, N_p, was determined by dividing the total distance traveled by the tool when in contact with the workpiece divided by the length of one part.

b) **Production rate, P**

This performance measure is the ratio of the number of parts completed (N_p), to the length of time during which the parts were machined ($t_m + N_t\, t_d + N_p\, t_L$):

$$P = \frac{N_p}{t_m + N_t\, t_d + N_p\, t_L} \qquad (4\text{-}25)$$

c) **Surface roughness, R**

This performance measure was assumed to be related to the feed, f_r, with which the tool was advancing on the workpiece surface. A lower value for the time average

of the feed indicates that the surface roughness of the completed parts is reduced.

$$R = \frac{\Sigma (f_r \times \Delta t)}{t_m} \qquad (4\text{-}26)$$

where Δt is the sampling time for the ACC approach and the decision interval for the decision-making approach.

Using the performance measures defined above, an assumed value for the machine operating rate of M=$50.00/hour and the values in Table 4.1, one can compare the effectiveness of a turning process controlled by an ACC scheme with one operated by the decision-making approach. For this purpose, the turning process described above was "active" for eight hours and its performance measures were calculated when the process was controlled by an ACC and by the decision-making approach.

Implementation of in-process decision making

In the decision-making approach, a decision matrix is periodically formulated during the process; the evaluation of the matrix leads to the selection of an operating point during a decision interval. In the application of the decision-making approach to a turning process, the operating point may correspond to a pair of settings for the cutting speed, v, and feed, f_r. The performance of the decision-making approach is influenced by the number of alternatives considered in the decision matrix and by the frequency of the matrix evaluation; both of these factors are limited by the available computation power. The criteria in the decision matrix can be defined to reflect relevant performance measures. However, there are different definitions for criteria and performance measures. The relationship for a particular criterion is used to evaluate, on-line, the consequence of each

individual alternative with respect to this criterion in order for the decision making process to select the best alternative. Performance measures, on the other hand, are "globally" estimated, over a relatively long period of time. Thus the major differences between criteria and performance measures are that the former must be estimated on line and for the decision interval Δt, while the latter are estimated over a longer period of time, e.g. a shift, and off-line at the end of the selected time period. The point here is that if the performance metrics according to which the overall process is to be measured are known, then one can establish properly defined criteria which can be used for on-line decision making. The criteria implemented in the decision-making approach for the purpose of this discussion were production rate, p, and surface roughness, r, and are defined below.

a) **Production rate criterion, p.** The use of this criterion will tend to maximize the production rate and minimize the cost per part. The definition of this criterion includes in its numerator the fraction of the part(s) completed during the decision interval, Δt, which is the time between two subsequent decisions. The denominator must include not only the decision interval, Δt, but also a portion of the tool change time, t_d, prorated by the fraction of the tool life used during the decision interval, and a portion of the part change time, t_L, prorated by the fraction of a part(s) completed during the decision interval. Thus the production rate decision criterion p can be expressed as:

$$p = \frac{\Delta N_p}{\Delta t + \frac{\dot{W}_f}{W_{max}} \Delta t\, t_d + \Delta N_p\, t_L} \qquad (4\text{-}27)$$

where the fraction of a part completed during the interval can be determined from expression (4-13) which is repeated below:

$$\Delta N_p = \frac{v\,\Delta t}{L_c} \tag{4-13}$$

where

$\dot{W}_f$ = flank wear rate

W_{max} = tool life criterion

t_d = time required for tool change (Table 4.1)

t_L = time required for a part change (Table 4.1)

v = cutting speed

L_c = length on the surface of the workpiece with which the tool is in contact needed for the completion of one part as defined in expression (4-5). It was assumed that the diameter of the parts was 0.04 meters and the length of the parts was 0.3 meters.

b) **Surface roughness criterion, r.** The surface roughness produced by the turning process has a direct correlation with the feed. As the feed is decreased, the surface roughness of the machined part tends to also decrease. The surface roughness criterion is defined as the feed used during the decision interval, Δt. Use of this criterion will tend to reduce the surface roughness of the completed parts.

$$r = f_r \tag{4-28}$$

where

f_r = feed

After the criteria values have been calculated, the decision matrix can be evaluated using several different methods [56,75,106]. In the implementation of the decision-making approach considered in this section the decision matrix was evaluated by first normalizing

the criteria in unitless values between 0 and 1 according to the following expressions.

For a "benefit" criterion where it is desirable to select an alternative which maximizes the criterion:

$$a_{i,j}^{norm} = \frac{a_{i,j} - a_{min\ i,j}}{a_{max\ i,j} - a_{min\ i,j}} \tag{4-29}$$

For a "cost" criterion where it is desirable to select an alternative which minimizes the criterion:

$$a_{i,j}^{norm} = 1 - \frac{a_{i,j} - a_{min\ i,j}}{a_{max\ i,j} - a_{min\ i,j}} \tag{4-30}$$

where

$a_{i,j}^{norm}$ = normalized criterion value

$a_{i,j}$ = original criterion value

$a_{min\ i,j}$ = minimum over all i alternatives for criterion j

$a_{max\ i,j}$ = maximum over all i alternatives for criterion j

The relative importance of each criterion depends on the overall objectives for the manufacturing system. For example, in a finishing operation it is generally most important to reduce the surface roughness of the parts, whereas the production rate is more significant in a roughing operation. Thus in the utility function used in the decision-making approach each decision criterion is assigned a weight which reflects its importance.

$$u_i = w_1 a_{i,1}^{norm} + w_1 a_{i,2}^{norm} + \ldots + w_n a_{i,n}^{norm} \tag{4-31}$$

where

u_i = utility for alternative i

w_j = weight for criterion j

The alternative with the highest utility, u_i, is selected.

The production rate criterion in equation (4-27) contains a wear rate term, $\dot{W}_f$, and therefore the tool wear rate must be estimated for each alternative in order for this criterion to be evaluated. A decision-making approach can use a variety of sensor inputs to estimate the process state variables [26]. However, for the work presented in this section, the decision-making approach was provided with only a measurement of the cutting force, F_f, for the purpose of estimating the tool wear rate. Equations (4-18) through (4-22) were used to estimate the cutting force, F, and the wear rate, $\dot{W}_f$, corresponding to each alternative. A detailed illustration of the decision-making approach as applied to the turning process is shown in Figure 4.12.

The minimum decision interval that can be utilized by a decision-making approach is limited by the speed of the computing hardware. Longer decision intervals may lead to suboptimal performance of the decision-making approach with respect to the performance measures; however, for the reasons discussed in Section 4.3, longer decision intervals will not cause the decision-making approach to become unstable. For the results presented in this section, a decision interval of five seconds was used in the simulations of the decision-making approach. Sixty-five alternatives were evaluated at each decision point, which consisted of all possible combinations of five different cutting speeds, v, (150, 175, 200, 225 and 250 m/min) and 13 different feeds, f_r, (ranging from 0.100 to 0.400 in increments of 0.025 mm/rev). The tool life criterion used was 0.3 mm; the tool was replaced when the flank wear reached 0.3 mm.

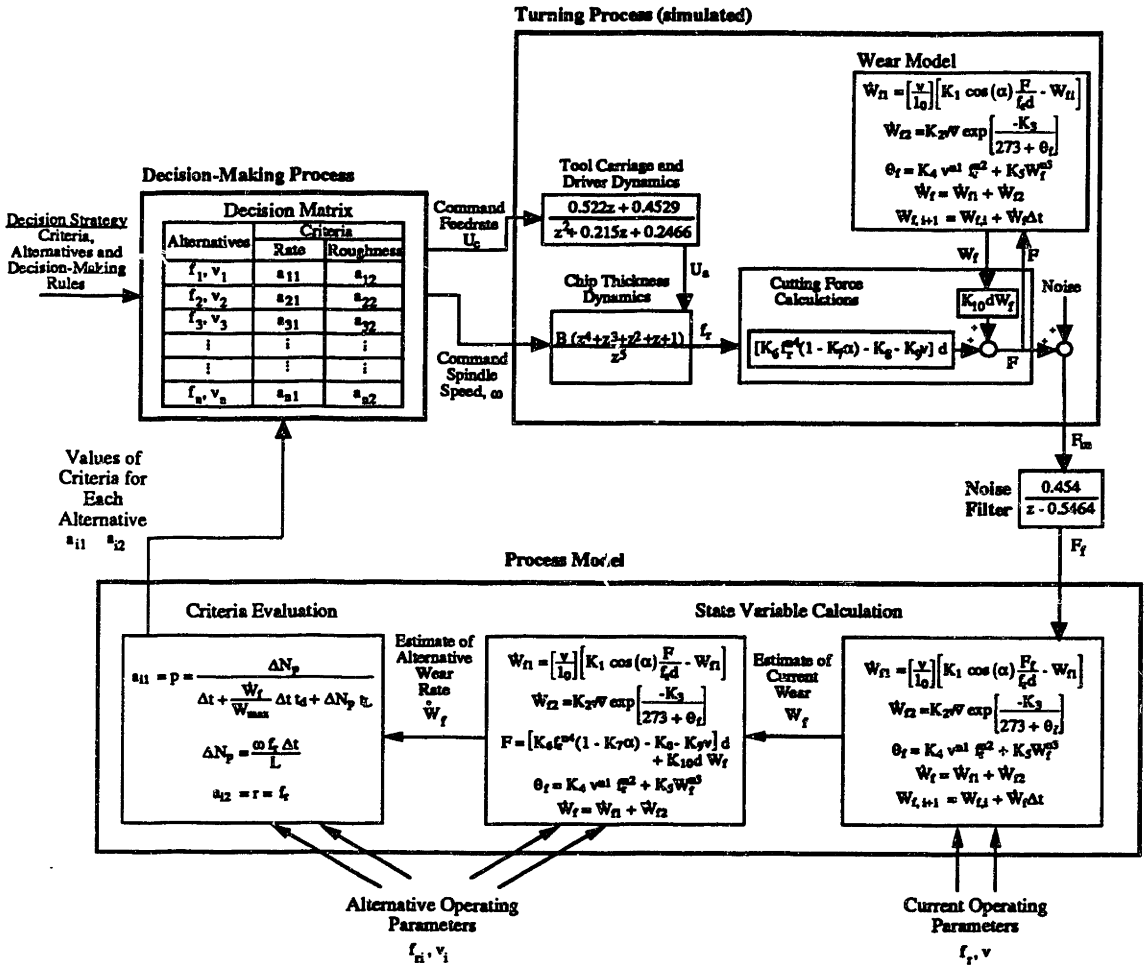

Figure 4.12 Decision-Making Approach Applied to a Turning Process

Implementation of adaptive control constraint

The adaptive control constraint approach implemented is a model reference adaptive control (MRAC) scheme in which a proportional-integral (PI) controller with an adjustable gain is employed [109]. The objective of this control approach is to maintain the cutting force, F_f, at a desired value, F_d, by making appropriate adjustments to the command feedrate, U_c while the cutting speed remains constant. The controller consists of two

control loops (Figure 4.13). The first loop is a standard feedback loop utilizing a PI controller; the second loop tunes the gain, $\hat{K}_p$, so that the difference between the cutting force estimated by the model, $\hat{F}_f$, and the measured cutting force, F_f, is minimized. The adaptation model contains the equations for the tool carriage driver dynamics (equation 4-15), the chip thickness dynamics (equation 4-16), and the lowpass filter for the measured force (equation 4-24).

In the simulations of the adaptive control approach, the cutting speed remained constant at v=200 m/min. Tools were replaced when the flank wear land, W_f, reached 0.3 mm. K_{po} was set to $0.454K_6Bd$, where K_6 is a proportionality constant relating the cutting conditions with the cutting force (equation 4-18), B depends on the spindle speed

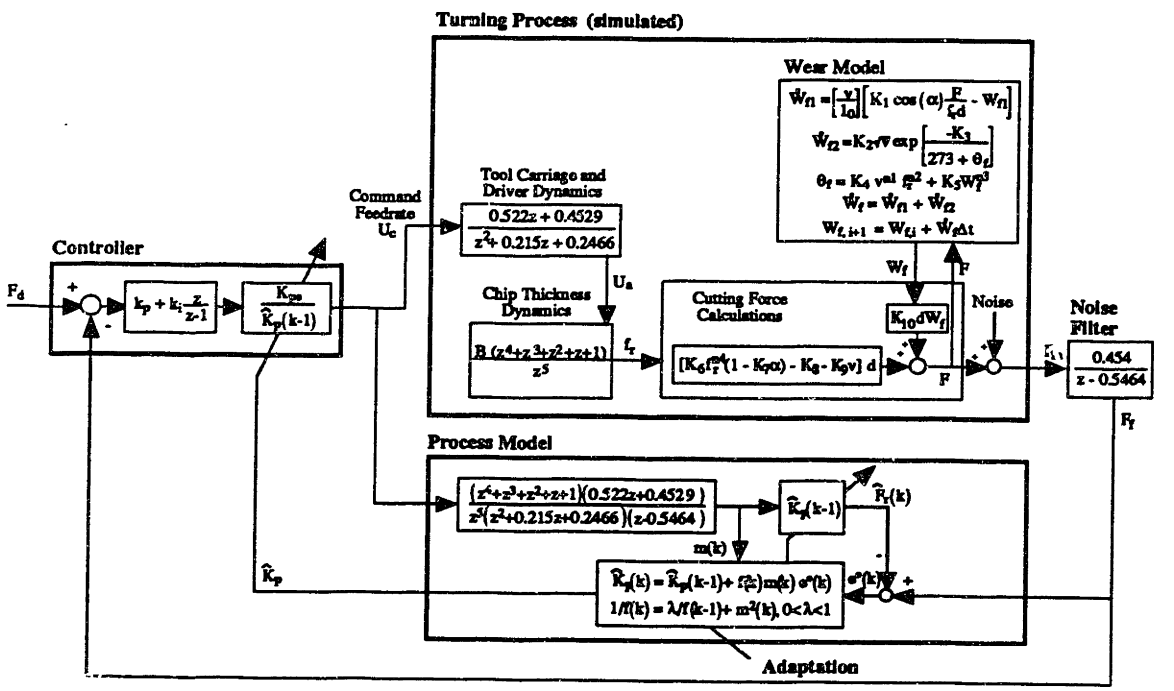

Figure 4.13 Adaptive Control Scheme Applied to a Turning Process

and sampling rate (equation 4-16), and d is the initial depth of cut. The controller gains k_p and k_i were selected to be $0.0294/K_{po}$ and $0.0235/K_{po}$, respectively [109]. $\hat{K}_p$ was initialized to K_{po} at the beginning of each turning process. The forgetting factor, λ, was set at 0.95.

Short sampling times are preferred in an ACC approach [5,6]. The ideal case is to have sampling intervals that approach a continuous system, but this is not possible because of computational limitations. The general tendency is to have about two to four samples per rise time. The simulations of the adaptive control approach were based on a 10 ms sampling interval.

4.3.2 RESULTS AND DISCUSSION

The ACC approach was simulated for a 1000 N value of the reference force, F_d (Figure 4.14). In the simulations of the decision-making approach, increasing the weight on the production rate criterion, p, (cases 2 and 5 in Figure 4.14) tended to increase the production rate, P, reduce the cost per part, C, and increase the surface roughness, R. Conversely, increasing the weight on the surface roughness criterion, r, (cases 3 and 6 in Figure 4.14) tended to increase the performance measure of cost per part, C, decrease the production rate, P, and decrease the surface roughness, R.

The decision criteria used in the decision-making approach are directly related to the performance measures used to evaluate the methods of operating the process over the period of eight hours. Thus the weight selected for a criterion directly influences the corresponding performance measure. For example, weighting only the surface roughness criterion, r, minimized the surface roughness performance measure, R, (Case 3 in Figure 4.14). This clear relationship does not exist between the performance measures and the

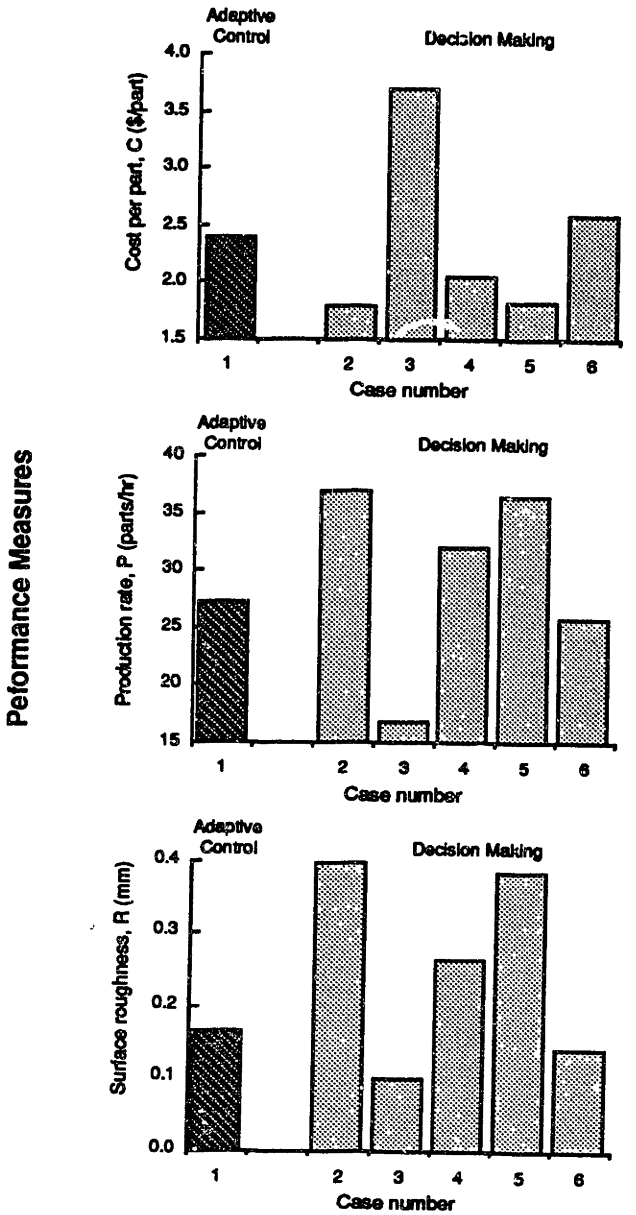

Case No.	Case details	Weight for Production rate criterion, p	Weight for Surface roughness criterion, r
1.	ACC at 1000 N	-	-
2.	Decision making	1.00	0.00
3.	Decision making	0.00	1.00
4.	Decision making	0.50	0.50
5.	Decision making	0.75	0.25
6.	Decision making	0.25	0.75

Figure 4.14 Comparative Performance of the AC and Decision-Making Approaches

reference value selected for the force in an adaptive control approach. Therefore the decision-making approach can be more easily interfaced with optimization and scheduling decisions made at higher levels in the manufacturing system hierarchy. In addition, the inherent tradeoffs between the values of the different performance measures, i.e.

production rate and surface roughness, are clearly evident in the decision-making approach during the selection of the relative weights on the decision criteria. Such performance tradeoffs are less easily identifiable in any ACC approach.

The speeds and feeds commanded by the ACC approach and by the decision-making approach during a turning process (Figure 4.15) reveals that the range of feeds utilized by the decision-making approach is greater than the range utilized by the ACC approach. The ACC approach attempted to maintain the cutting force at 1000 N and as the tool wear increased it was necessary to decrease the feed somewhat in order to maintain this force. The ACC approach controls only the feed; the speed of 200 m/min was selected a-priori and must remain constant during the process. For the simulation case shown in Figure 4.15, the decision-making approach attempted to optimize the process with respect to the production rate and the surface roughness. In the initial stages of the process the tool wear rate is high regardless of the speed selected (Figure 4.11). Consequently a high speed was selected at the beginning of the process in order to maximize the production rate. Later in the process the wear rate is more sensitive to the speed selected and a lower speed was selected in order to provide a reasonable tool wear rate. An excessively high tool wear rate requires frequent replacement of the tool which will tend to reduce the production rate. In the case of the feed, consideration of the surface roughness criterion will tend to reduce the feed selected while consideration of the production rate criterion will generally tend to increase the feed selected. Consequently it is more difficult to analyze the trends for the feeds selected. In the initial stage of the process the decision-making approach may have selected a low feed in order minimize the surface roughness while attempting to reduce the high wear rate provided by the high speed which was selected. Later in the process when a lower speed was selected the feed may have been increased in order to increase the production rate. During the rest of the process where the wear rate tends to gradually increase (Figure 4.11) the feed may have been decreased in order to reduce the wear rate.

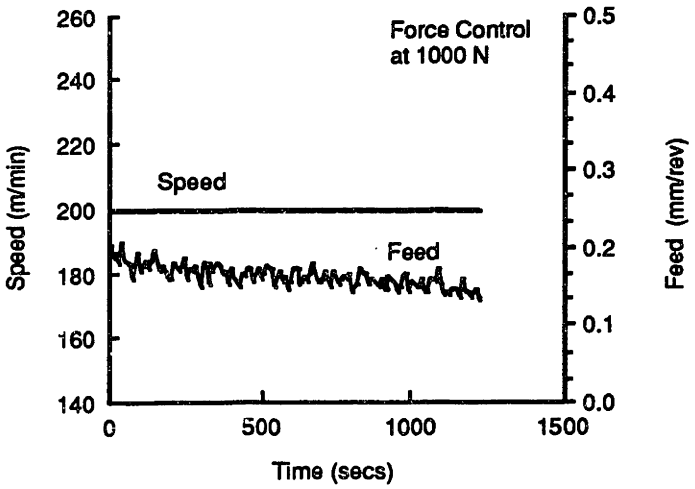

(a)

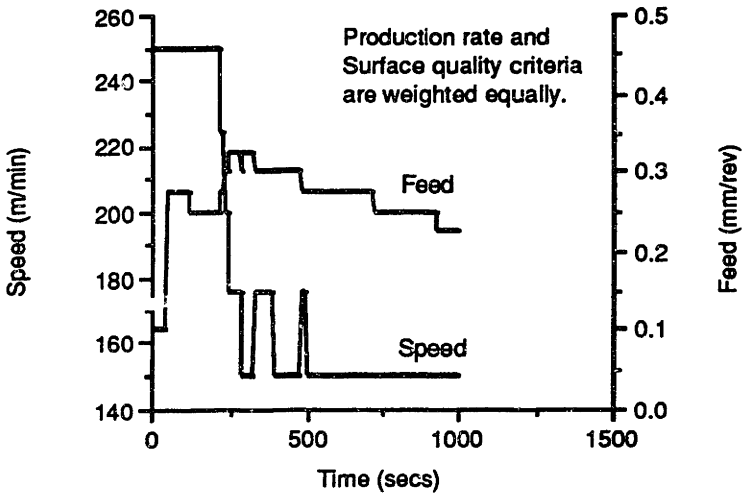

(b)

Figure 4.15 Speed and Feed vs. Time for the Turning Process
a) Adaptive Control (corresponds to case 1 in Figure 4.14)
b) Decision-Making (corresponds to case 4 in Figure 4.14)

It is conceivable that a different value for the reference force, F_d, or a different speed selected a-priori in the ACC approach would change the performance measures. However, this is a rather indirect approach; if one is interested in the performance of a turning process with respect to measures such as cost per part and production rate one might not be able to establish the influence of the reference force or the speed selected on the performance measures. One could also imagine that an ACC approach which controls both the feed and speed instead of only the feed may provide different values of the performance measures. However, the objective of this work was not to develop a more sophisticated ACC scheme for machining, but rather to compare the decision-making approach with what was currently available. The decision-making approach can consider multiple process inputs in a straight-forward manner without restructuring the basic framework of the approach. It may be more difficult to change the ACC approach to control multiple process inputs. The primary point of comparing the decision-making approach with the ACC approach is not to show that the decision-making approach will provide better values of the performance measures under all circumstances; the primary point is that the decision-making approach provides a clear relationship between the weights on the decision criteria and the resulting values of the corresponding performance measures.

4.4 CONCLUSIONS

As an alternative to adaptive control approaches to manufacturing process control, this chapter considered a decision-making approach. In the decision-making approach the optimal process input settings are selected by evaluating a set of feasible input settings with respect to one or more decision criteria. The decision criteria can be defined in a manner which will tend to optimize the process with respect to relevant performance measures.

This chapter investigated the feasibility and limitations of this decision-making approach.

Based on simulations of the turning process, it was found that the decision-making approach is capable of reducing the machining cost per part as compared with a typical ACO approach.

Simulations of a turning process also showed that the values of cost per part, production rate and surface roughness performance measures provided by the decision-making approach were directly influenced by selecting appropriate values of the relative weights on each of the corresponding decision criteria. Such clearly identifiable relationships did not exist when using a typical ACC approach.

The comparison of the decision making with a typical ACO scheme in Section 4.2 considered the performance of the decision-making approach when the wear rate estimates used by the decision-making approach contained random error. The simulations of the turning process in Section 4.3 used to compare the decision-making approach with a typical ACC scheme included a random signal to simulate sensor noise. Therefore, in both of these sets of simulations the outcome of each alternative was somewhat uncertain in the decision-making approach. In this chapter this uncertainty was not taken into account in the decision-making process. Use of a method for handling uncertainty may have improved the performance of the decision-making approach, and such an evaluation should be considered in future work.

5 CONCLUSIONS AND FUTURE WORK

As an alternative to adaptive control approaches to manufacturing process control this thesis has presented a decision-making approach to process operation. In this approach, the process input parameters are selected in-process in an attempt operate the process in accordance with a set of performance objectives. The selection of the input parameters is performed with the help of functions which relate the performance objectives with the input parameters and sensor signals used to monitor the process. The decision-making approach includes the synthesis of multiple sensor information for process monitoring in an effort to minimize the difficulties caused by the lack of reliable sensing devices for manufacturing processes and the lack of a single model which adequately reflects the complexity of the process.

In the decision-making approach, the process input settings are selected by evaluating a set of feasible input settings with respect to one or more decision criteria. This scheme can be concisely expressed in a decision matrix format where the matrix elements indicate the consequences of each feasible alternative with respect to a set of optimization criteria. The decision criteria can be defined in a manner which will tend to optimize the process with respect to relevant performance measures. This thesis presented a modular structure for implementing the decision-making approach. A modular structure allows each module to be constructed specifically to execute each decision-making step in the most systematic and efficient way. In addition, the modules can be easily modified or replaced in order to adapt the control approach to different sets of process conditions without changing the overall structure of the system.

In manufacturing literature, many attempts to model and control manufacturing processes are focused on machining processes. Machining operations are widely used throughout industry and improvements in the monitoring and operation of these processes would have great economical impact on the entire manufacturing industry. Consequently, this thesis focused on the development of three of the modules in the structure of the decision-making approach in the context of applying the approach to a turning process. These modules are:

- A module which contains a set of process models which provide independent estimates of the state variables necessary for determining the values of the decision-making criteria.

- A module which estimates the consequences of the decision alternatives via an intelligent synthesis of the information provided by the process models.

- A module in wnich a set of decision-making rules is applied to the information concerning the consequences of the decision alternatives in order to select the best alternative.

Chapter 2 considered the development of an acoustic emission-based model appropriate for in-process monitoring of tool wear within a scheme such as the decision-making approach to process operation. In order to be useful for wear monitoring during process operation this model was structured to account for changes in the AE signal due to changes in machine tool settings such as the speed and feed. After considering the methods which have been proposed for detecting the tool wear in machining based on measurements of the AE, it was concluded that a model based on fundamental cutting principles and parameters would be best for in-process tool wear monitoring. Such a model was

developed which more adequately relates the cutting forces and speed with the RMS signal than previously proposed models.

Chapter 3 considered the implementation and analysis of methods for synthesizing multiple sensor information for process monitoring. The synthesis of information from several sensors may provide estimates of state variables which are more accurate, more reliable and less sensitive to sensor noise than estimates based on information from a single sensor. This chapter considered synthesis methods requiring a training phase and methods which use a statistical criterion to determine the synthesized estimate based on information from multiple sensors. The methods requiring training included multiple least-squares regression, an inverse least-squares technique, the group method of data handling (GMDH), an interpolation neural network, and a muti-layer perceptron neural network.

Sensor synthesis was considered for providing estimates of the tool wear during a turning operation. Evaluating the synthesis methods in a simulated environment using test data composed of linear, sinusoidal and random signals indicated that synthesis of multiple sensor information will generally provide better estimates of tool wear than information from only one sensor. The multi-layer perceptron appeared to be more effective than the other methods based on training for learning a relationship for providing synthesized wear estimates, particularly when the relationship between the sensor-based information and the actual wear is nonlinear. The simulations indicated that when the sensors operate properly and the corresponding process models adequately reflect the complexity of the process, a method based on training will provide similar performance to a method based on a statistical criterion. When the process models do not adequately reflect the process or when the sensor-based information contains errors which may be caused by sensor drift or variations in material properties the simulations indicated that a method based on training will provide better synthesized estimates of the wear than a method based on a statistical

criterion. The simulations also indicated that a method based on training may be somewhat less sensitive to the failure of one of the sensors than a method based on a statistical criterion.

Evaluation of the synthesis approaches based on data from tool wear experiments during which force, temperature and acoustic emission signals were recorded indicated that synthesis of multiple sensor information will provide better estimates of the tool wear than using information from only a single sensor. In the experiments performed for this thesis, all of the synthesis methods implemented except for the interpolation network provided better estimates of the wear than using information from only one sensor.

Implementation of a sensor synthesis approach based on a statistical criterion requires probability density functions for the state variables as estimated by the process models. Chapter 3 presented a method of determining these density functions in-process by evaluating the uncertainty in the state variable estimates provided by the models due to parametric uncertainty in the models. If the probability density functions can be determined in-process, the statistical approach to sensor synthesis has a significant advantage over the methods requiring training since it can be implemented without using training data.

In Chapter 4 the feasibility and limitations of a decision-making approach to manufacturing process operation were discussed. The operation of the decision-making approach was compared with typical Adaptive Control Constraint (ACC) and an Adaptive Control Optimization (ACO) approaches using the simulation of a turning process. The values of cost per part, production rate and surface roughness performance measures provided by the decision-making approach were directly influenced by selecting appropriate values of the relative weights on each of the corresponding decision criteria. This clear relationship did not exist between the performance measures and the reference value

selected for the force in the ACC approach. Therefore, the decision-making approach can be more easily interfaced with the optimization and scheduling decisions made at higher levels in the manufacturing system hierarchy. Through simulation of a turning process it was also found that the decision-making approach can reduce the cost of machining each part as compared with a typical Adaptive Control Optimization (ACO) approach.

Some of the advantages of the multi-layer perceptron mentioned in the literature are fault tolerance and insensitivity to incomplete information. Yet in evaluating of performance of this type of neural network for sensor synthesis through simulation it was found that methods could be investigated in the future for making the network less sensitive to erroneous or incomplete sensor information. A possible solution to this problem is to include some erroneous values in the data used to train the network.

In the decision-making approach the outcome of each alternative is somewhat uncertain due to factors such as sensor noise and uncertainties in the structure or parameters of the models into which the sensors feed their signals. This thesis did not explicitly take this uncertainty into account in the implementation of the decision-making approach. Future efforts should focus on implementing a method for handling uncertainty in an attempt to improve the performance of the decision-making approach.

Given functions which relate the performance objectives with the process inputs and with the sensor signals used to monitor the process, approaches other than the use of a decision-matrix could be considered for the selection of the most appropriate input parameters. One would not necessarily have to consider the alternatives as being discrete as was done in the work presented in this thesis. Future work should include investigating alternative methods of searching the feasible input space for the optimal input settings. The speed, robustness and flexibility of these alternative approaches should be evaluated and

compared with the performance of the decision-matrix approach.

In this thesis, the feasibility of the decision-making approach was evaluated through computer simulation. In the future, the decision-making approach should be further evaluated and a comprehensive comparison of the decision-making approach with typical ACO and ACC approaches should be made based on machining experiments. This evaluation will require the development of the necessary equipment and computer software to experimentally implement these process operation approaches.

REFERENCES

[1] Abuelnaga, A.M. and M.A. El-Dardiry, "Optimization Methods for Metal Cutting," *Int. J. Mach. Tool Des. Res.* (Vol. 24, No. 1, 1984), pp. 11-18.

[2] Agogino, A., M.S. Srinivas and K.M. Schneider, "Multiple Sensor Expert System for Diagnostic Reasoning, Monitoring and Control of Mechanical Systems," *Mechanical Systems and Data Processing* (Vol. 2, No. 2, 1988), pp. 165-168.

[3] Albrecht, P., "New Development in the Theory of the Metal-Cutting Process. Part II: The Theory of Chip Formation," ASME Trans., *Journal of Engineering for Industry*, (Vol. 83, Nov. 1961).

[4] Allen, D.M., "The Relationship Between Variable Selection and Data Augmentation and a Method for Prediction," *Technometrics* (Vol. 16, No. 1, 1974), pp. 125-127.

[5] Astrom, K.J. and B. Wittenmark, *Adaptive Control*, Addision Wesley Publishing Company, 1989.

[6] Astrom, K.J. and B. Wittenmark, *Computer Controlled Systems: Theory and Design*, Prentice Hall International, 1984.

[7] Balakrishnan, P. and M.F. Devries, "Adaptive Enhancement of Machinability Data Base Systems in Automated Manufacturing," *Proceedings of the XII North American Manufacturing Research Conference* (1984), pp. 460-467.

[8] Bedini, R. and P.C. Pinotti, "Experiments on Adaptive Constrained Control of a CNC Lathe," ASME Trans., *Journal of Engineering for Industry* (Vol. 104, May 1982), pp. 139-150.

[9] Birla, S.K., "Sensors for Adaptive Control and Machine Diagnostics," *Machine Tool Task Force Study - Machine Tool Controls*, ed. Sutton, G., SME, Dearborn, Michigan (Vol. 4, October 1980), pp. 7.12.1-7.12.70.

[10] Blackman, S.S., "Theoretical Approaches to Data Association and Fusion," *Proc. of SPIE* (Vol. 931, 1988), pp. 50-55.

[11] Blelloch, G. and C. Rossenburg, "Network Learning on the Connection Machine," *Knowledge Acquisition and Learning Engineering Track*, Short Paper (Jan. 1987).

[12] Bogler, P.L., "Shafer-Dempster Reasoning with Applications to Multisensor Target Identification Systems," *IEEE Trans. on System, Man, and Cybernetics* (Vol. SMc-17, No. 6, Nov./Dec. 1987), pp. 968-977.

[13] Boothroyd, G., "Tool Life and Tool Wear," *Fundamentals of Metal Machining and Machine Tools*, McGraw-Hill, New York, 1975, pp. 108-124.

[14] Bowker, A.H. and G.J. Lieberman, *Engineering Statistics*, Prentice-Hall, Englewood Cliffs, NJ, 1972.

[15] Brummett, F.D., "Adaptive Control Systems," (SME Paper No. MM840307, 1984).

[16] Burke, L., "An Unsupervised Neural Network Approach to Tool Wear Identification," to appear in IIE Transactions.

[17] Chandrasekaran, H. and R. Nagarajan, "Influence of Flank Wear on the Stresses in a Cutting Tool," ASME Trans., *Journal of Engineering for Industry* (Vol.99, Aug.1977).

[18] Chen, B.S. and Y.F. Chang, "Constant Turning Force Adaptive Controller Design," ASME Trans., *Journal of Engineering for Industry* (Vol. 111, 1989), pp. 125-132.

[19] Choi, G.S., Z.X. Wang and D. Dornfeld, "Development of an Intelligent On-Line Tool Wear Monitoring System for Turning Operations," *Proc. USA-Japan Symposium on Flexible Automation* (1990), pp. 683-690.

[20] Chryssolouris, G. and M. Domroese, "An Experimental Study of Strategies for Integrating Sensor Information in Machining," *Annals of the CIRP* (Vol. 38/1, 1989), pp. 425-428.

[21] Chryssolouris, G. and M. Domroese, "Sensor Integration for Tool Wear Estimation in Machining," ASME Winter Annual Meeting, *Sensors and Controls for Manufacturing* (PED-Vol. 33, 1988), pp. 115-123.

[22] Chryssolouris, G. and M. Guillot, "A Comparison of Statistical and AI Approaches to the Selection of Process Parameters in Intelligent Machining," ASME Trans., *Journal of Engineering for Industry* (Vol. 112, May 1990), pp. 122-131.

[23] Chryssolouris, G. and S. Patel, "In-Process Control for Quality Assurance," in *Industrial High Technology for Manufacturing*, eds. K. McKee, and D. Tijunelis, Chapter 22, Marcel Dekker Inc., New York, 1987, pp. 609-643.

[24] Chryssolouris, G., M. Domroese and L. Zoldos, "A Decision Making Strategy for Machining Control," *Annals of the CIRP* (Vol. 39, No. 1, 1990), pp. 501-504.

[25] Chryssolouris, G., M. Domroese and P. Beaulieu, "A Statistical Approach to Sensor Synthesis," *Proceedings of the XIX North American Manufacturing Research Conference* (May 1991), pp. 333-337.

[26] Chryssolouris, G., M. Domroese and P. Beaulieu, "Sensor Synthesis for Control of Manufacturing Processes," ASME Winter Annual Meeting, *Proceedings of the Symposium on Control of Manufacturing Processes* (1990), pp. 67-76.

[27] Chryssolouris, G., M. Guillot and M. Domroese, "A Decision Making Approach to Machining Control," ASME Trans., *Journal of Engineering for Industry* (Vol. 110, No. 4, Nov. 1988), pp. 397-398.

[28] Chryssolouris, G., M. Guillot and M. Domroese, "An Approach to Intelligent Machining," *Proceedings of the American Control Conference* (June 10-12, 1987), Minneapolis, Minnesota, pp. 152-160.

[29] Chryssolouris, G., M. Guillot and M. Domroese, "Tool Wear Estimation for Intelligent Machining," ASME Winter Annual Meeting, *Proceedings of the Symposium on Intelligent Control* (December 1987), Boston, Massachusetts .

[30] Danai, K. and A.G. Ulsoy, "A Dynamic State Model for On-Line Wear Estimation in Turning," ASME Winter Annual Meeting, *Sensors and Controls for Manufacturing* (PED-Vol. 18, Nov. 1985), pp. 137-148.

[31] Dornfeld, D., "Acoustic Emission Monitoring for Untended Manufacturing," *Japan-USA Symposium on Flexible Automation* (July 1986), JAACE, Osaka, Japan.

[32] Dornfeld, D., "The Role of Acoustic Emission In Manufacturing Process Monitoring," *Proceedings of the XIII North American Manufacturing Research Conference* (1985), pp. 69-74.

[33] Durrant-Whyte, H.F., "Consistent Integration and Propagation of Disparate Sensor Observations," *Proc. IEEE Int. Journal of Robotics and Automation* (April 1986), San Francisco, CA, pp. 1464-1469.

[34] Emel, E. and E. Kannatey-Asibu, Jr., "Acoustic Emission and Force Sensor Fusion for Monitoring the Cutting Process," *International Journal of Mechanical Sciences* (Vol. 31, No. 11/12, 1989), pp. 795-809.

[35] Emel, E. and E. Kannatey-Asibu, Jr., "Tool Failure Monitoring in Turning by Pattern Recognition Analysis of AE signals," ASME Trans., *Journal of Engineering for Industry* (Vol. 110, May, 1988), pp. 137-145.

[36] Ermer, D.S. and S. Kromodihardjo, "Optimization of Multipass Turning with Constraints," ASME Trans., *Journal of Engineering for Industry* (Vol. 105, No. 4, Nov. 1981), p. 462.

[37] Fassois, S.D., K.F. Eman K.F. and S.M. Wu, "A Fast Algorithm for On-Line Machining Process Modelling and Adaptive Control," ASME Trans., *Journal of Engineering for Industry* (Vol. 111, 1989), pp. 133-139.

[38] Fu, K.S., "Learning Control Systems and Intelligent Control Systems: An Intersection of Artificial Intelligence and Automatic Control," *IEEE Transactions on Automatic Control* (Vol. AC-16, Feb. 1971), pp. 70-72.

[39] Fu, K.S., "Learning Control Systems - Review and Outlook," *IEEE Transactions on Automatic Control* (Vol. AC-15, April 1970), pp. 210-221.

[40] Fussell, B.K. and K. Srinivasan, "On Line Identification of End Milling Process Parameters," ASME Trans., *Journal of Engineering for Industry* (Vol. 111, 1989), pp. 322-330.

[41] Giusti, F., M. Santochi and G. Tantussi, "On-line Sensing of Flank and Crater Wear of Cutting Tools," *Annals of CIRP* (1987), pp. 41-44.

[42] Groover, M.P., et al, "Determination of Machining Conditions by a Self-Adaptive Procedure," *Proceedings of the IV North American Manufacturing Research Conference* (1976), pp. 267-271.

[43] Hadeby, H., "Increasing Availability and Efficiency by Monitoring the Cutting Process in a Lathe During Production with Limited Manpower," *Annals of CIRP* (1989), pp. 393-398.

[44] Ham, I. and D.G. McClenahan, "Computer Optimization of Machining Conditions for Shop Production using Performance Index," *Manufacturing Engineering* (Vol. 3, 1974), pp. 103-113.

[45] Haton, J.P., "Knowledge-Based and Expert Systems in Industrial Applications," *IFAC Artificial Intelligence* (1983), pp. 83-89.

[46] Hecht-Nielsen, R., *Neurocomputing*, Addison-Wesley, Reading, MA, 1991.

[47] Hitomi, K., "Analysis of Production Models, Part I: The Optimal Decision of Production Speeds," *AIIE Trans.* (Vol. 8, No.1, 1976), pg. 96.

[48] Horne, J.G., E.D. Doyle and D. Tabor, "Direct Observation of the Chip-Tool Interface in Metal Cutting," *Proceedings of the V North American Manufacturing Research Conference* (1977).

[49] Huber, J. and R. Centner, "Test Results with an Adaptively Controlled Milling Machine," (ASTME paper MS68-638, 1968).

[50] Inasaki, I. and S. Yonetsu, "In-Process Detection of Cutting Tool Damage by Acoustic Emission Measurement," *Proceedings of 22nd MTDR Conference* (1981), pp. 261-268.

[51] Ivakhnenko, A.G., "Heuristic Self-Organization in Problems of Engineering Cybernetics," *Automatica* (Vol. 6, 1970), Pergamon Press, pp. 207-219.

[52] Ivakhnenko, A.G., "The Group Method of Data Handling - A Rival of the Method of Stochastic Approximation," *Soviet Automatic Control* (Vol. 13, No. 3, 1968).

[53] Iwata, K. and T. Moriwaki, "An Application of Acoustic Emission Measurement to In-Process Sensing of Tool Wear," *Annals of the CIRP* (Vol. 26, No. 1, 1977), pp. 21-26.

[54] Jaeschke, J.R., R.D. Zimmerly and S. M. Wu, "Automatic Cutting Tool Temperature Control," *Int. J. MTDR* (Vol. 7, 1967), pp. 465-475.

[55] Jiang, C.Y. and Y.Z. Zhang, "In-process Monitoring of Tool Wear Stage by the Frequency Range-Energy Method," *Annals of CIRP* (1987), pp. 45-48.

[56] Jones, A.J., *Game Theory: Mathematical Models of Conflict*, Ellis Horwood Limited, 1980.

[57] Kannatey-Asibu, E., "The Metal Cutting Optimal Control Problem - A State Space Formulation," ASME Winter Annual Meeting, *Proceedings of the Symposium on Control of Manufacturing Processes and Robotic Systems* (1983).

[58] Kannatey-Asibu, E. and D. Dornfeld, "A Study of Tool Wear Using Statistical Analysis of Metal Cutting Acoustic Emission," *Wear* (Vol. 76, No. 2), pp. 247-261.

[59] Kannatey-Asibu, E. and D. Dornfeld, "Quantitative Relationships for Acoustic Emission from Orthogonal Metal Cutting," ASME Trans., *Journal of Engineering for Industry* (Vol. 103, No. 3, 1981), pp. 330-349.

[60] Koren, Y., "The Optimal locus Approach with Machining Applications," ASME Trans., *Journal of Dynamic Systems, Measurements and Control* (Vol. 111, 1989), pp. 260-267.

[61] Koren, Y. and O. Masory, "Adaptive Control with Process Estimations," *Annals of the CIRP* (Vol. 30, No.1, 1981), pp. 373-380.

[62] Koren, Y. and E. Lenz, "Mathematical Model for the Flank Wear While Turning Steel with Carbide Tools," *CIRP Seminar* (June 1970), Trondheim.

[63] Koren, Y. and O. Masory, "Adaptive Control System for Turning," *Annals of the CIRP* (Vol. 29, No. 1, 1980), pp. 281-284.

[64] Koren, Y., K. Danai, A.G. Ulsoy and T-R. Ko, "Monitoring Tool Wear Through Force Measurement," *Proceedings of the XV North American Manufacturing Research Conference* (May 1897), pp. 463-468.

[65] Korobko, A.V., M.I. Koval and E.N. Kim, "Adaptive Control of Milling with Microprocessor NC System," *Soviet Engineering Research (GB)* (Vol. 3, No. 12, Dec. 1985), pp. 76-79.

[66] Lan, M.S. and D.A. Dornfeld, "Acoustic Emission and Machining - Process Analysis and Control," *Advanced Manufacturing Processes* (Vol. 1, No. 1, 1986), pp. 1-21.

[67] Langhammer, K., "Cutting Forces as Parameters for Determining Wear on Carbide Lathe Tools and as Machinability Criterion for Steel," *Carbide J.* (Vol. 8, No. 3, May-June 1976), pp. 5-13.

[68] Lauderbaugh, L.K. and A.G. Ulsoy, "Model Reference Adaptive Force Control in Milling," ASME Trans., *Journal of Engineering for Industry* (Vol. 111, 1989), pp. 13-21.

[69] Lee, C.H. and J. Hoh, "Mini-computer Application on Adaptive Control System for Turning Process", *Proceedings of the VIII North American Manufacturing Research Conference* (1980), pp. 419-424.

[70] Lewis, A. and B.K. Nagpal, "Economic Considerations in Adaptive Control," *22th Int. MTDR Conference* (1981), Manchester, U.K., pp. 187-195.

[71] Liang, S.Y. and D.A. Dornfeld, "Detection of Cutting Tool Wear Using Adaptive Time Series Modeling of Acoustic Emission Signal," ASME Winter Annual Meeting, *Proceedings of the Symposium on Sensors for Manufacturing* (Dec. 12-13, 1987), Boston, MA.

[72] Lin, T.I. and S.M. Wu, "On-Line Drill Wear Monitoring", ASME Winter Annual Meeting, *Sensors and Controls for Manufacturing* (PED-Vol. 33, 1988), pp. 99-104.

[73] Lippmann, R.P., "An Introduction to Computing with Neural Nets," *IEEE ASSP Magazine* (April 1987).

[74] Liu, M.Y. and H.H. Yang, "An Adaptive Control for Machining Processes and a Digital Observer for Tool Wear Detection," *Annals of CIRP* (1988), pp. 469-472.

[75] Luce, R.D. and H. Raiffa, *Games and Decisions: Introduction and Critical Survey*, John Wiley and Sons, 1957.

[76] Lundholm, T., M. Yngen and B. Lindstrom, "Advanced Process Monitoring - A Major Step Towards Adaptive Control," *Robotics and Computer-Integrated Manufacturing* (Vol. 14, No. 3-4, 1988), pp. 413-421.

[77] Luo, R.C. and M.G. Kay, "Multisensor Integration and Fusion: Issues and Approaches," *Proc. of SPIE* (Vol. 931, 1988), pp. 42-49.

[78] Luo, R.C. and M.-H. Lin, "Robot Multi-Sensor Fusion and Integration: Optimum Estimation of Fused Sensor Data," *IEEE Journal of Robotics and Automation* (November 1988), pp. 1076-1081.

[79] Luo, R.C., M.-H. Lin and R.S. Scherp, "Dynamic Multi-Sensor Fusion for Intelligent Robots," *IEEE of Journal of Robotics and Automation* (Vol. 4, No. 4, August 1988), pp. 386-396.

[80] *Machining Data Handbook*, Metcut Research Associates Inc., Cincinnati, Ohio, 1966.

[81] Malkin, S. and Y. Koren, "Optimal Infeed Control for Accelerated Spark-Out in Plunge Grinding," ASME Trans., *Journal of Engineering for Industry* (Vol. 106, Feb. 1984), pp. 70-74.

[82] Mannan, M.A. and S. Broms, "Monitoring and Adaptive Control of Cutting Process by Means of Motor Power and Current Measurements," *Annals of CIRP* (1989), pp. 347-350.

[83] Masory, O. and Y. Koren, "Stability Analysis of a Constant Force Adaptive Control System for Turning," ASME Trans., *Journal of Engineering for Industry* (Vol. 107, No. 4, Nov. 1985), pp. 295-300.

[84] Matsushima, K. and T. Sata, "On-line Control of the Cutting State by the Pattern Recognition Technique," *Annals of the CIRP* (Vol. 23, Jan. 1974).

[85] Micheletti, G.F., W. Koenig and R.H. Victor, "In Process Tool Wear Sensor for Cutting Operation," *Annals of the CIRP* (Vol. 25, No. 2, 1976), pp. 483-496.

[86] Neter, J., W. Wasserman and G.A. Whitmore, *Applied Statistics*, 3rd ed., Allyn and Bacon, Newton, Massachusetts, 1988.

[87] Neter, J., W. Wasserman and M.H. Kutner, *Applied Linear Regression Models*, Irwin, Homewood, Illinois, 1983, pp. 78-81 and 172-174.

[88] Novak, A., "The Concept of Artificial Intelligence in Unmanned Production - Application of Adaptive Control," *Proceedings from Second International Conference of Flexible Manufacturing Systems* (1983), pp. 669-680.

[89] Pao, Y.-H., "Theory of Acoustic Emission," Winter Annual Meeting of ASME, *Elastic Waves and Non-Destructive Testing of Materials* (AMD, Vol. 29, 1978), pp. 107-128.

[90] Park, J.J. and A.G. Ulsoy, "On line Flank Wear Estimation Using Adaptive Observers," Winter Annual Meeting of ASME, *Automation of Manufacturing Processes* (Nov. 25-30, 1990), Dallas, Texas, pp. 11-20.

[91] Preiss, K. and E. Kaplansky, "Automated CNC Milling by Artificial Intelligence Methods," (SME Paper No. MS840718, 1984).

[92] Ramalingam, S., T. Shi, D.A. Frohrib and T. Moser, "Acoustic Emission Sensing with an Intelligent Insert and Tool Fracture Detection in Multi-Tooth Milling," *Proceedings of the XVI North American Manufacturing Research Conference* (1988), pp. 245-255.

[93] Rangwala, S. and D. Dornfeld, "Sensor Integration Using Neural Networks for Intelligent Tool Condition Monitoring," Trans. ASME, *Journal of Engineering for Industry* (Vol. 112, 1990), pp. 219-228.

[94] Rong, Y., J. Ni and S.M. Wu, "An Improved Model Structure for Forecasting Compensatory Control," ASME Winter Annual Meeting, *Sensors and Controls for Manufacturing* (PED-Vol. 33, 1988), pp. 175-181.

[95] Ross, P., *Taguchi Techniques for Quality Engineering: Loss Function, Orthogonal Experiments, Parameters and Tolerance Design*, McGraw-Hill, New York, 1988.

[96] Rumelhart, D.E., G.E. Hinton and R.J. William, "Learning Internal Representations by Error Propagation," In: Rumelhart, D.E. and J.L. McClelland, *Parallel Distribution Processing: Explorations in the Microstructure of Cognition. Vol. 1: Foundations*, M.I.T. Press, Cambridge, MA, 1986.

[97] *Self-Organizing Methods in Modelling - GMDH Type Algorithms*, Farlow, S.J., ed., Marcel Dekker Inc., New York, 1984.

[98] Shafer, G., *A Mathematical Theory of Evidence*, Princeton Univ. Press, Princeton, NJ, 1976.

[99] Shaw, M.C., *Metal Cutting Principles*, Clarendon Press, 1984.

[100] Schey, J.A., *Tribology in Metalworking, Friction, Lubrication and Wear*, American Society for Metals ed., 1983.

[101] Somlo, J., "Optimization Principles for Computer Integrated Manufacturing Systems," *Proc. Japan-U.S.A. Symposium on Flexible Automation.*

[102] Somlo, J. and M. Horvath, "On the Hierarchical Systems, Optimization and Adaptive Control of Machine Tools," *IFAC Control Sci. and Techn. (8th Triennual World Congress)* (1981), Kyoto, Japan, pp. 2011-2020.

[103] Stute, G., "Adaptive Control," *Proc. of the Machine Tool Task Force Conf.*, (Vol. 4, Chapter 14, Oct. 1980).

[104] Taguchi, G., *System of Experimental Design: Engineering Methods to Optimize Quality and Minimize Cost*, Unipub/Kraus International Publications, White Plains, N.Y., 1987.

[105] Takahashi, N. and C.H. Kahng, "Stochastic Optimization of Production Speed," *Proceedings of the XII North American Manufacturing Research Conference* (1983), pp. 461-465.

[106] Thomas, L.C., *Games Theory and Applications*, Ellis Horwood Limited, 1984.

[107] Thomsen, E.G., A.G. MacDonald and S. Kobayashi, "Flank Friction Studies With Carbide Tools Reveal Sublayer Plastic Flow," ASME Trans., *Journal of Engineering for Industry* (Vol. 84, Feb. 1962).

[108] Tlusty, J. and G. Andrews, "A Critical Review of Sensors for Unmanned Machining," *Annals of the CIRP* (Vol. 32/2, 1983), pp. 563-572.

[109] Tomizuka, M. and S. Zhang, "Modelling and Conventional Adaptive PI Control of a Lathe Cutting Process," ASME Trans., *Journal of Dynamic Systems, Measurements and Control* (Vol. 110, 1988), pp. 350-354.

[110] Tomizuka, M., J.H. Oh and D.A. Dornfeld, "Model Reference Adaptive Control of the Milling Process," ASME Winter Annual Meeting, *Control of Manufacturing Processes and Robotic Systems* (1983), pp. 55-63.

[111] Tsukiyama, M. and T. Fukuda, "An Application of Knowledge Base to Control Systems," *Proceedings from International Conference on Cybernetics and Society* (1981), pp. 341-346.

[112] Uehara, K. and Y. Kanda, "Identification of Chip Formation Mechanism through Acoustic Emission Measurements," *Annals of the CIRP* (Vol. 33/1, 1984), pp. 71-74.

[113] Ulsoy, A.G., Y. Koren and F. Rasmussen, "Principal Developments in the Adaptive Control of Machine Tools," ASME Trans., *Journal of Dynamic Systems, Measurement and Control* (Vol. 105, June 1983), pp. 107-112.

[114] Usui, E. and M.C. Shaw, "Free Machining Steel -- IV: Tools With Reduced Contact Length", ASME Trans., *Journal of Engineering for Industry* (Vol. 84, Feb. 1962).

[115] Usui, E., T. Shirakashi and T. Kitagawa, "Analytical Prediction of Cutting Tool Wear," *Wear* (Vol.100, 1984), pp. 129-151.

[116] Watanabe, T., "A Model Based Approach to Adaptive Control Optimization in Milling," ASME Trans., *Journal of Dynamic Systems, Measurements and Control* (Vol. 108, 1986), pp. 56-54.

[117] Watanabe, T. and M. Sakamoto, "On-line Scheduling for Adaptive Control Machine Tools in FMS," *Robotics and Computer-Integrated Manufacturing* (Vol. 2, No. 1, 1985), pp. 65-73.

[118] Winston, P.H., draft of "Learning by Training Approximation Nets," 1991.

[119] Wright, P., "Physical Models of Tool Wear for Adaptive Control in Flexible Machining Cells," ASME Winter Annual Meeting, *Computer Integrated Manufacturing* (PED-Vol. 8, November 1983).

[120] Wright, P.K. and D.A. Bourne, *Manufacturing Intelligence,* Addison-Wesley, Reading, MA, 1988.

[121] Wu, S.M. and J. Ni, "New Approaches to Achieve Better Machine Performance," *Proc. of the USA-Japan Symp. on Flexible Automation* (1988), pp. 1063-1068.

[122] Wu, S.M. and J. Ni, "Precision Machining Without Precise Machinery," *Annals of CIRP* (1989), pp. 533-536.

[123] Yen, D.W. and P.K. Wright, "Adaptive Control in Machining - A New Approach Based on the Physical Constraints of Tool Wear Mechanisms," ASME Trans., *Journal of Engineering for Industry* (Vol. 105, 1983), pp. 31-38.

[124] Yonetsu, S., I. Inasaki and T. Kijima, "Optimization of Turning Operations," *Proceedings of the VI North American Manufacturing Research Conference* (1978), pp. 17-23.

[125] Zorev, N.N., "Interrelationship Between Shear Processes Occurring along Tool Face and on Shear Plane in Metal Cutting," *International Research in Production Engineering*, ASME (1963), pp. 42-49.

[126] Zorev, N. N., *Metal Cutting Mechanics*, Pergamon Press, 1966.